HYDROLOGIC CHARACTERIZATION OF TWO FULL-SCALE WASTE ROCK PILES

By

PAMELA ELIZABETH FINES
B.Sc., The University of Saskatchewan, 2000

A THESIS SUBMITTED IN PARTIAL FULFILLMENT OF
THE REQUIREMENTS FOR THE DEGREE OF

MASTER OF APPLIED SCIENCE

in

THE FACULTY OF GRADUATE STUDIES

(Mining Engineering)

THE UNIVERSITY OF BRITISH COLUMBIA
March 2006

ABSTRACT

Waste stockpiles pose an environmental risk for leaching of metals and low pH water long after a mine has stopped operations. To determine the potential for acid generation in waste materials a clear understanding of flow through the waste rock piles is required. Based on field and laboratory investigations, this research focuses on developing an understanding of flow mechanisms through waste stockpiles. Two mine sites were selected for the fieldwork. The fieldwork was conducted while the waste rock material was being replaced in the open pit for closure. The relocation of the waste rock dump allowed for in-situ observation and testing of the materials stockpiled. The field investigations included excavation of test pits in each bench of the waste rock pile during relocation, logging of structure and materials present, and in-situ testing for density and matric suction. The laboratory investigations comprised the determination of grain size distribution, water content, paste pH, Soil Water Characteristic Curve, and saturated hydraulic conductivity. The field and laboratory data was used to develop conceptual models of flow for each waste rock pile. These models were based on the observed structure and material properties determined in the laboratory. The typical observed structure included inclined dense layers at the angle of repose, weathered waste rock, and traffic surfaces. The conceptual flow model at Site 1 was evaluated using a finite element seepage analysis program. The modeling clearly shows that preferential flow develops within the waste rock pile. Leaching of soluble minerals out of the dump will be governed by flow paths of infiltrating water and these paths can be estimated based on field observations and numerical modeling. The structure at Site 1 showed evidence of interbedded layers and this structure controls the flow paths developed within the dump. Predictions of which materials will be the dominant flow paths, and subsequently which minerals are most likely be to be mobilized can be estimated for any waste rock dump if there is knowledge of the hydraulic and geochemical properties of the waste rock and internal structure within the dump.

TABLE OF CONTENTS

PAGE

TABLE OF CONTENTS
(continued)

PAGE

TABLE OF CONTENTS
(continued)

PAGE

LIST OF TABLES

LIST OF FIGURES

DEDICATION

To my family, without your unending support all my achievements would not be possible.

CHAPTER ONE: INTRODUCTION

1.0 BACKGROUND

Mining is one of the largest global industries and is the economic backbone of many countries. The extraction of natural resources generates economic activity and production of goods. Environmental liabilities associated with mining include poor quality drainage from waste storage facilities such as tailings dams, waste rock and slag stockpiles. Elevated levels of metals and sulfates in the discharge water may exceed acceptable water quality standards. Acid rock drainage that results from the oxidation of sulfide minerals is the major source of poor quality drainage. As the pH of the seepage water drops, metals such as iron, copper and aluminum go into solution and are leached out from the waste rock dump. Although acidic drainage at mine sites is a well-known risk, neutral drainage of metals such as arsenic, which is mobile at neutral pH, is also a concern at some sites. Likewise, heavy metals such as selenium and mercury are also a concern for neutral drainage.

Predicting the quality of the leachate from waste rock piles is of interest to mining companies. However, to accurately predict leachate quality it is required to describe the water flow paths within the waste rock dump. These flow paths determine which particles within the dump the water will contact and this will directly influence the outflow geochemistry.

The economic pressure from the potential liability from ARD has resulted in an increased desire to understand the internal physical processes within tailings and waste rock

dumps. The goal of many mining operations is to reduce long term liability by designing better waste facilities. This study was initiated when two mine operations elected to move existing waste rock piles into their respective open pits for closure. This provided the opportunity to conduct detailed observation and analyses of two full-scale waste rock piles.

1.1 Research Objectives

This study examines the internal structure and hydrology of two waste rock dumps in order to develop an understanding of the relationships between host rock geology, weathering of particles and the resulting outflow geochemistry. The primary objective of this research program was to make in-situ field observations and measure material properties to describe seepage pathways within the waste rock dump. The primary objective of this thesis is to describe the results of the field and laboratory program that was implemented to evaluate two waste rock piles.

The first waste rock dump was located at the Ridgeway Gold Mine in South Carolina and the second waste rock pile was situated at the Whistle Mine near Sudbury, Ontario. The specific objectives of the thesis are outline below:

1. To excavate test pits in each bench of material that was exposed as the waste rock dumps were being relocated.
2. To inspect and classify the structures and materials present in each test pit.
3. To collect samples and conduct in-situ testing for density and matric suction following the visual inspection. Detailed laboratory analysis of the samples for measurement of particle size distribution, paste pH, and water content.
4. To measure the saturated hydraulic conductivity and Soil-Water Characteristic Curves for representative materials.

5. To develop a conceptual model of the flow paths within the waste rock piles based on the material properties evaluated in the laboratory and the structure that was observed in the field.

6. To conduct saturated/unsaturated seepage analyses based on the conceptual flow model and estimate flow rates based on infiltration rates and hydrologic properties of the materials.

Detailed geochemical analyses were completed within a separate study described by Tran (2003).

1.2 Thesis Organization

Chapter One outlines a brief introduction to the research program. Chapter Two provides a review of the literature relevant to the research objectives. Chapter Three describes the field and laboratory investigation that was carried out at site, as well as a detailed description of the in situ conditions at both mines. Chapter Four presents the results of the field and laboratory testing. Chapter Five contains discussion and analyses of the numerical modeling. A summary and conclusions as well as recommendations for future research, are provided in Chapter Six. Appendix A contains data collected in each test pit at Site 1 and Appendix B provides test pit records for Site 2.

CHAPTER TWO: LITERATURE REVIEW

2.0 INTRODUCTION

This chapter presents literature related to waste rock characterization, preferential flow, and contaminant transport. There are numerous mine sites located world wide with no apparent acidic drainage issues but are still required by the regulatory authority to treat the water for elevated levels of metals and dissolved solids. The end result is that water discharging from the mine site must meet certain standards for metals, total suspended solids, and ion composition. The concern is not only the water pH 2 and the metal loadings but also includes defining the quantity of water that will require treatment. Therefore, the extent of the current study extends beyond acid rock drainage to flow and transport of soluble ions present within waste rock systems.

Studies on in-situ testing in waste rock piles, deconstruction of waste rock lysimeters, and field scale experiments in waste rock have been conducted. One of the main issues highlighted by the previous studies is the applicability of results to site geology and climate. Hydrogeologic studies in waste rock have focused on both laboratory scale and field scale issues and as such do not truly represent full-scale waste rock dumps. Research on infiltration and flow in coarse media is essential in developing a conceptual model of flow within a waste rock dump. Understanding preferential flow mechanisms and the segregation of granular material during construction is also needed to describe how the flow systems are created.

2.1 Theory of Unsaturated Media

Structures that are constructed with rock or soil above the water table are unsaturated. Dams, road sub-grade, embankments and waste rock piles are generally all constructed in an unsaturated state. Waste rock piles remain unsaturated throughout their life. This requires an extensive understanding of unsaturated hydrologic properties in order to fully describe the behavior of the water flowing within the waste rock pile.

Water flowing through soil is driven by an energy gradient. The energy is referred to as hydraulic head. Hydraulic head comprises of elevation head, pressure head and velocity head. The velocity at which water moves through a soil is small and thus disregarded such that the equation shown to calculate hydraulic head in a soil contains only the elevation head and pressure head components. Water always moves in the direction of decreasing hydraulic head. Equation 2.1 shows the equation for hydraulic head in a soil

$$h = z + \frac{U_w}{p_w g} \qquad \textbf{(2.1)}$$

Where:
h = hydraulic head, m
z = elevation head, m
$\frac{U_w}{p_w g}$ = pressure head, m
u_w = pore-water pressure, kPa
p_w = density of water, kg/m^3
g = acceleration due to gravity, m/s^2

The energy gradient required for flow is the change in hydraulic head over a given distance. The gradient indicates the direction of flow. Darcy's Law, which was developed using experiments on saturated sand columns, states that the volume of flow through a porous media is proportional to the gradient applied to the column. The theory was formalized into a finite equation by including a constant of proportionality that is material dependent. Hydraulic conductivity was shown to be constant for saturated materials of a specific grain size. The formula used to calculate the total flow through saturated granular material is as follows:

$$Q = K_w \frac{\partial h}{\partial l} A \qquad (2.2)$$

Where K_w = hydraulic conductivity of water
$\delta h/\delta l$ = gradient
A = cross section area of material

The theory that describes unsaturated soil behavior has been explained in detail by Fredlund and Rahardjo (1993). Unsaturated media is a four-phase system containing soil, water, air and the contractile skin. Figure 2.1 shows an idealized section of an unsaturated soil. The contractile skin takes up an insignificant volume and is ignored when calculating flow volumes. However the physical effects of the contractile skin makes unsaturated soils complex to understand. The contractile skin is only a few molecules of water thick but has density similar to that of ice. The contractile skin allows water to form a convex dome over the top of a glass. The contractile skin does not behave strictly as a fluid and therefore contributes to some of the unusual properties of water.

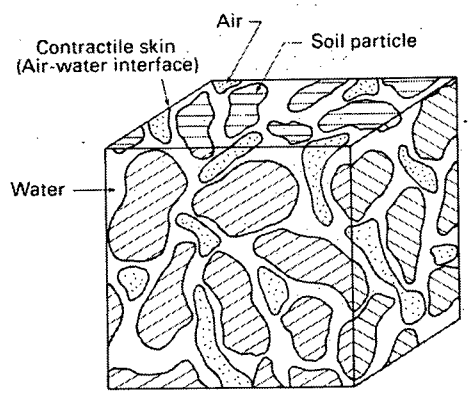

Figure 2.1 Section of Unsaturated Medium (Fredlund and Rahardjo, 1993)

Fredlund and Rahardjo showed that the saturated flow theory could be derived from basic principles to show that Darcy's law applies to unsaturated soils and that saturated flow is actually a special case of the general theory. The complete derivation of Darcy's law is

found in Fredlund and Rahardjo (1993). The theory starts from the second law of thermodynamics, which states that mass can neither be created nor destroyed. Therefore, inward flow minus outward flow equals a change in storage. For an unsaturated soil, the hydraulic conductivity becomes a function of water content and matric suction rather than a constant and Darcy's law is expressed as follows:

$$Q = Kf(U_a - U_w)\frac{\partial h}{\partial l}A \qquad (2.3)$$

The Soil-Water Characteristic Curve is a function that represents a material's ability to retain water under increasing values of matric suction. Matric suction is the pore air pressure minus the pore water pressure acting at a point. This can be expressed as (U_a-U_w) and since the water pressure above the water table is negative but the pore air pressure is atmospheric, matric suction is expressed as a positive value. The matric suction acting on the unsaturated media is a function of the elevation above the water table and atmospheric forcing evens such as wind, rain, or evapotranspiration. The curve can approach horizontal until the air-entry value of the soil is exceeded. The air-entry value of a soil is the matric suction that is required to drain the water out from the largest pore in a soil matrix. The Soil-Water Characteristic Curve is measured using a pressure plate apparatus (sometimes referred to as a Tempe Cell). This apparatus and testing procedure is described in Chapter 3. Figure 2.2 shows Soil-Water Characteristic Curves for typical soils (Newman, 1999).

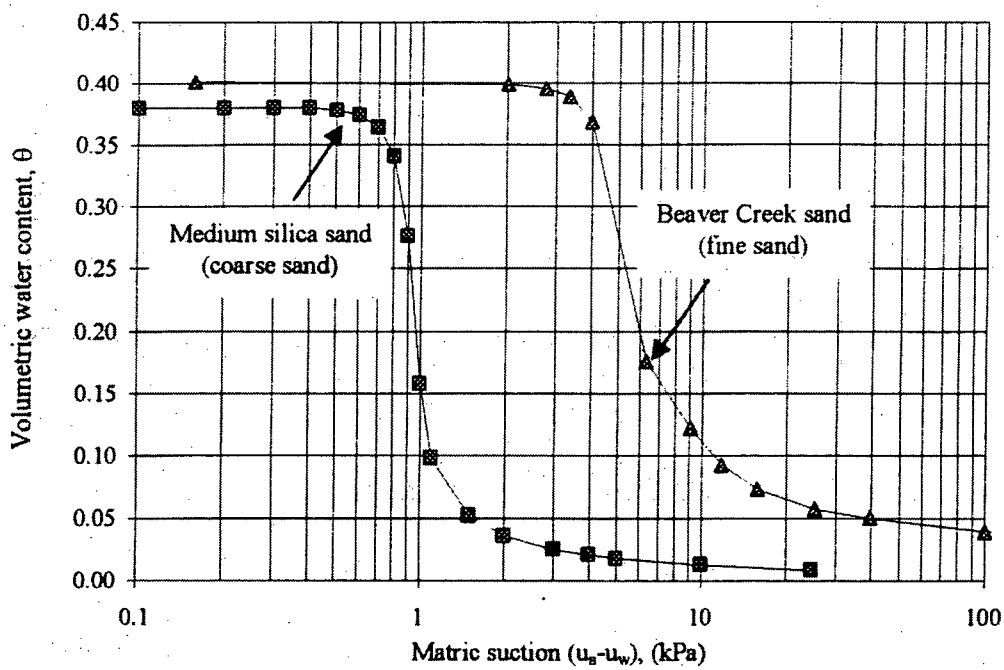

Figure 2.2 Soil-Water Characteristic Curves for Representative Soils

The shape of the Soil-Water Characteristic Curve influences the unsaturated hydraulic conductivity function. The steeper the Soil-Water Characteristic Curve from the air-entry values to the residual water content, the steeper the hydraulic conductivity function.

Hydraulic conductivity for any soil is a function of the degree of saturation (Fredlund and Rahardjo, 1993). The Soil-Water Characteristic Curve describes the saturation of a soil for a given matric suction. The hydraulic conductivity function provides the hydraulic conductivity of a soil for a given matric suction. The Soil-Water Characteristic Curve and the hydraulic conductivity functions are fundamentally linked for a given soil type.

There have been a number of theories to mathematically describe the unsaturated hydraulic conductivity function. Essentially, the hydraulic conductivity of a soil is constant until the air entry value is reached. Once this value is exceeded, the hydraulic conductivity decreases linearly on a log-log scale with increasing suction. Figure 2.3 shows a typical unsaturated hydraulic conductivity functions for the soils depicted in Figure 2.2.

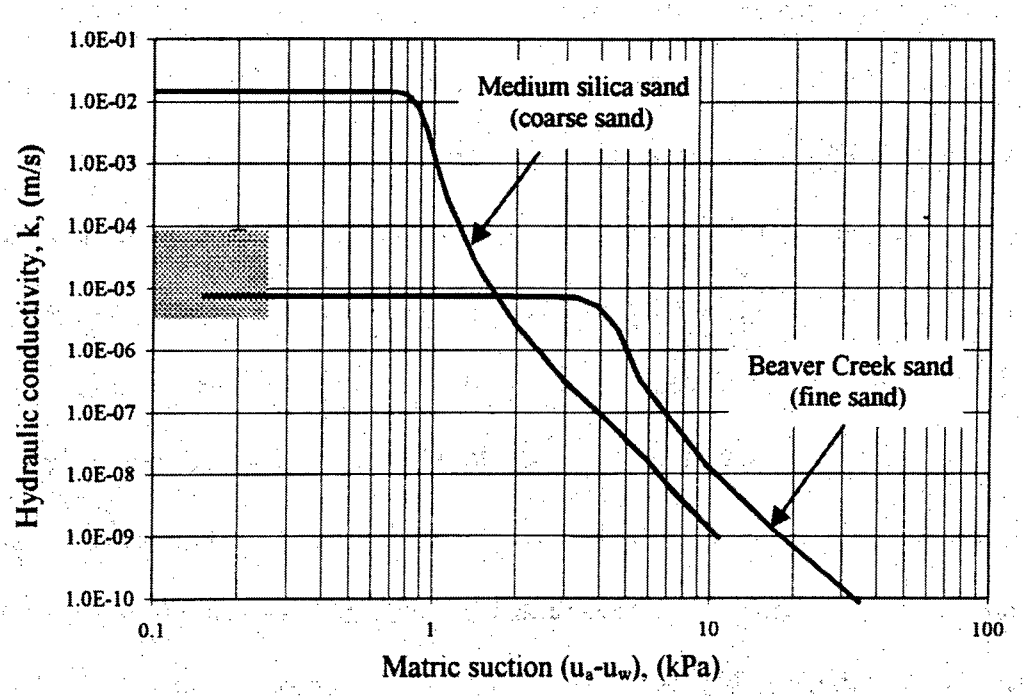

Figure 2.3 Typical Unsaturated Hydraulic Conductivity Functions (Newman, 1999)

2.1.1 Estimation of Unsaturated Soil Properties

Unsaturated soil properties are difficult to determine in the laboratory and the application of the properties into routine practice is slowed by the high cost and time involved in determining unsaturated soil properties. Research conducted by Fredlund (2001) showed that a mathematical curve could be fit to grain size data, based on either a bimodal or a unimodal function. The grain size distribution curve defines the pore size distribution in a material, which can be used to estimate the Soil-Water Characteristic Curve and hydraulic conductivity function. The determination of a grain size distribution is common laboratory practice, however for accurate estimations of hydraulic properties a mathematical expression must be generated to fit the laboratory data.

Also required for this analysis is an understanding of in-situ density, water content, and specific gravity of the soil so the porosity can be calculated and the pore size distribution

can be estimated. The size of the pores determines the matric suction required by the pores to desaturate. The program SoilVision (Fredlund, 2001) uses a statistical method to estimate pore size density and in turn calculates the Soil-Water Characteristic Curve for the material based on a Pedo Transfer Function (PTF). A number of PTF functions are used to define boundary limits and to estimate the Soil-Water Characteristic Curve. The program also includes methods of fitting mathematical equations to the estimated curves, such as those developed by Fredlund and Xing (1993) and van Genuchten (1980). The program includes eleven methods of estimating saturated hydraulic conductivity. Unsaturated hydraulic conductivity functions are estimated based on saturated hydraulic conductivity and a fitted Soil-Water Characteristic Curve.

2.2 Segregation of Granular Soils

Research on landslides and debris flows have studied granular material movement in a downward direction. The main observation of these studies was that the materials tend to sort or segregate during transport such that the coarse particles tend to flow further down the slope than fine particles. Nichol (1986) examined the segregation of material that was end-dumped or pushed dumped over a tip face. The objective was to create filter zones in rock dams by taking advantage of the natural segregation. The study looked at the difference in the resulting grain size distribution along the tip face between push dumping and end dumping. The length of the slope over which the material was tipped was also examined.

Nichol (1986) identified three distinct zones of particle size distribution. The upper zone of the tip face showed an elevated concentration of fines. The middle section of the slope showed a well-graded grain size distribution with the overall average particle size smaller than the non-segregated sample due to the loss of large particles to segregation at the toe. The toe of the slope had large particles extending well past the toe of the slope. The length of the slope is reported to have an impact on the grain size distribution of the material measured down the slope. The longer the slope, the greater the segregation and a greater difference in average particle size measured at each sampling location along the slope.

Nichol (1986) also showed that there is a significant difference in the particle distribution between push dumping and end dumping. When the material was push dumped the resulting material was generally well graded from the top of the tip face to the bottom. However, this method often resulted in over-steepened slopes that could become unstable at long slope lengths. There was still some particle segregation but the effects were greatly reduced compared to end dumping.

Herasymuik (1996) conducted observations at Golden Sunlight Mine and indicated a similar trend in the formation of a concentration of fines at the top of the slope with large rubble zones forming at the base of each tip face. The segregation appeared to be a function of the construction method, that is, end dumping of waste rock from haul trucks. Segregation of material and the resulting issues of hydrology are well documented in roadbed construction (Chapuis, et. al. 1996, 1992) and in the design and construction of filters (Silveria, 1965, Kenney, 1985, 1985). There are documented cases of road base and sub-base materials being placed and having zones develop within the earthen structure that retain water and result in lower strength of the pavement surface.

In most applications, such as dam construction, railway ballast construction, road sub-grade construction, the main objective of the construction method is to reduce segregation because historical analysis has shown that segregation of particles results in zones of material that retain water and this results in lower strength (Cedergren, 1974, Chapuis, 1992, 1996). The difference in the strength of the material can also be affected by the particle size distribution. When applying this knowledge to end dumped waste rock, significant segregation can be expected internally and the associated impact on the strength and hydrology within the waste rock structure.

2.3 Infiltration and Flow in Coarse Media

Reinson (2001) conducted detailed analysis of water-particle interaction in coarse materials. This work analyzed dye dispersion, infiltration rates and Soil-Water Characteristic Curves, and hydraulic conductivity functions for 12 mm marbles and uniform sand. Reinson

(2001) described the flow of a single droplet of water on the surface of a smooth marble. The rate of fall of the water droplet on the surface of the dry marble is quite slow compared to the rate of fall of a second drop of water along the wetted surface of the marble. The second water droplet tends to follow the path that has already been wetted. Similar behavior can be observed in many everyday locations, including raindrops sliding down a windowpane. The droplets tend to collect and run down one vertical path, and subsequent drops can move much faster down the surface of the window.

Experiments examining the vertical migration of wetting fronts were found to be influenced by whether or not the marbles were initially wet or dry. The wetted marbles show a lower contact angle than dry marbles and the upward motion of the wetting front was much faster when the marbles were wet. Part of the experiment conducted by Reinson (2001) also examined the dissipation of pore water pressure as the water level was allowed to drop. The analysis showed that the water phase never fully drained to the residual water content upon lowering of the water table. However, the maximum matric suction that was measured in the columns was approximately equal to that of the residual water content of the material. The excess residual can possibly be attributed to the discontinuous nature of the water phase or the remainder of pendular rings of water surrounding glass beads. This mechanism for water retention after free drainage may be extended to almost all materials of coarse texture. The conceptual model of the distribution of the water phase in coarse-grained materials described by Reinson (2001) is most applicable to sites with extremely coarse texture that are devoid of fine interstitial material.

A major portion of the experiments conducted by Reinson (2001) was focused to measure the Soil-Water Characteristic Curve for the glass beads using a Tempe Cell style pressure plate. The testing proved to be almost impossible due to the sensitivity of the water content to the thickness of the sample (that is. number of layers of marbles in the cell) being tested in the cell and showed the difficulty in measuring a Soil-Water Characteristic Curve for a coarse grained soil. The standard testing procedure for a small diameter Tempe cell is to analyze material passing the ASTM Sieve No. 4 (4.75 mm). Smaller diameter material

contain smaller pores and thus, this material will respond more evenly to applied matric suction at the base of the sample.

Research carried out at Cluff Lake Mine in Northern Saskatchewan by Belleheumer (2001) was a detailed infiltration study on the Claude waste rock pile. The field research program was conducted on two separate surfaces of the Claude Pile, the west side of the pile was trafficked and a hard pack surface was developed. On Claude East, the surface was free dumped and the apparent texture was a result of physical weathering in place of the material that had been dumped on the surface. The research showed that there were two main processes affecting the infiltration rate into the coarse waste rock. Those processes were infiltration into the fine matrix and funneling of water into the subsurface through the voids created by the coarse particles. The second process was related with a drain effect into the subsurface of the waste rock pile. The voids around coarse particles were most visible on Claude East where there had been little breakdown of material associated with trafficking.

When the upper surface of the waste rock pile was excavated to map the path of the tracer-laced flow, evidence of water flowing around the outer surface of the coarse particles was clearly visible. When the flow reached the underlying traffic surface, the tracer laced water pooled onto the traffic surface and then soaked into the matrix of the finer material.

The fraction of infiltration that was observed to be either matrix or coarse drain dominated infiltration was also influenced by the intensity of the rainfall event. The more intense the rainfall, the higher the fraction of water that infiltrated the upper surface through the rock drains due to runoff and ponding. The intensity dependent infiltration function can be applied at most sites when determining the number of high flow intensity events that would likely occur each year and the volume of flow that would be expected from these events.

2.4 Waste Rock Hydrology

Golden Sunlight Mine in Montana, USA experienced a lateral slide in 1993 caused by a failure of the foundation material underlying the waste rock dump. Approximately 15 millions tones of waste rock was excavated to stabilize the waste rock dump. While this material relocation was being carried out a detailed study of the internal structure of the dump was completed. The waste rock relocation allowed an ideal opportunity to examine the internal structure of the waste rock and to determine identifiable flow pathways within the waste rock pile.

Herasymuik (1996) observed a dipping bedding structure within each bench of material. The structure was created by end-dumping of waste rock, which was the standard disposal method at the site. This resulted in alternating coarse and fine layers. The coarse layers were drained and the fine layers were able to retain water in capillary tension. The water phase was discontinuous in the coarse layers and liquid flow was considered to be negligible. The fine layers, due to the higher degree of saturation, were considered to be the dominant flow pathways for liquid water. Herasymuik (1996) developed a conceptual model of the internal structure and flow paths within an end-dumped waste rock pile as shown in Figure 2.4.

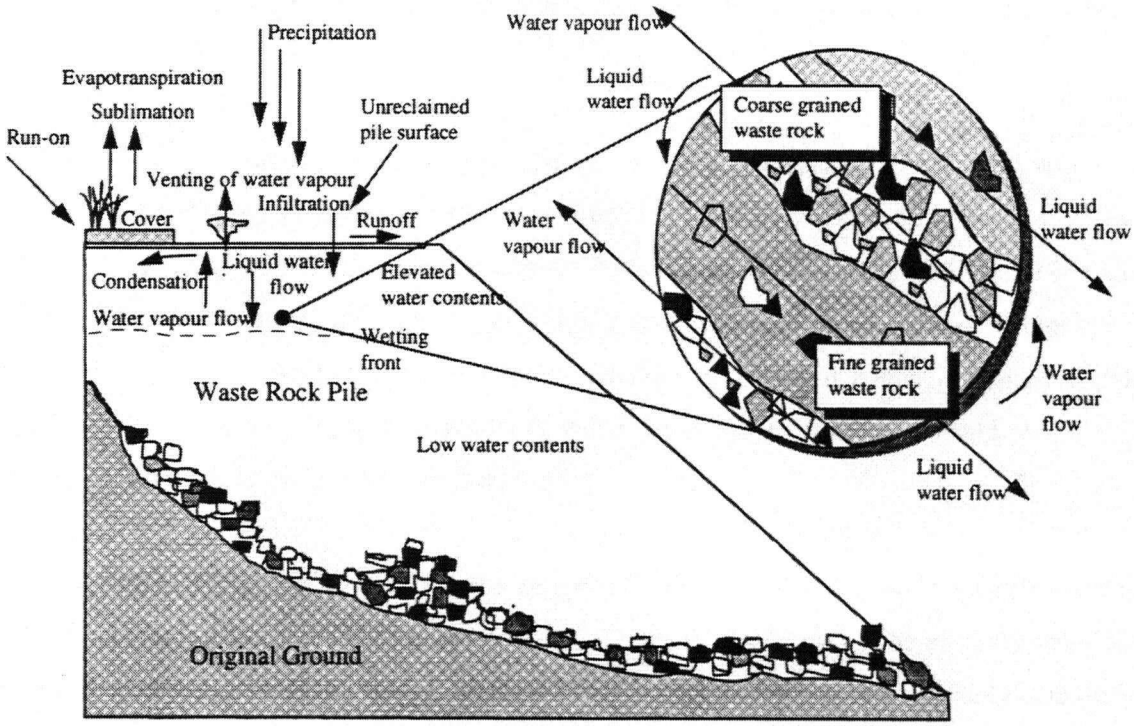

Figure 2.4 Conceptual Model of Flow within Waste Rock Proposed by Herasymuik (1996).

The conceptual model presented by Herasymuik (1996) is considered to be the first attempt at describing unsaturated flow associated with structure found in waste rock. There have been other theories to describe how waste rock transmitted water but the tendency is to try and use the "black box"-or "what goes in must come out" theory but ignored any potential influence from internal structure. This procedure essentially uses a weighted average for all of the material properties for the source waste rock (i.e. grain size, geochemical properties, weathering characteristics) and assumes that the waste material forms a homogeneous structure such that all the waste is contacted by infiltrating water equally. This eliminates the influence of segregation of flow and disparate material properties in the analysis. The primary challenge presented by Herasymuik (1996) relates to the linkage with the geochemistry specifically in that the water quality for the discharge cannot be predicted

unless the flow path of the water can be accurately described. In other words, it is not reasonable to use average material structure, grain size, material composition, and sulfide content to a system that is extremely heterogeneous. For example, the grain size distribution can vary from large boulders to clay size particles, which affects the reaction rates due to available surface area.

Newman (1999) conducted a laboratory study at the University of Saskatchewan following the field research conducted at Golden Sunlight Mines. The column study attempted to determine the parameters that would lead to preferential flow in a vertically layered column. A 2 meter high column was constructed with one side filled with sand sized material and the other side with silt sized material. Various infiltration rates were analyzed to determine the effect of infiltration rate with respect to the development of preferential flow.

Newman (1999) used two different infiltration rates that resulted in two distinctly different flow patterns. The first infiltration rate equal to 4.25×10^{-7} m/s was specified to be less than the saturated hydraulic conductivity of the silt material within the column. Figure 2.5 shows the resulting flow vectors. The bulk of the flow was found to occur within the fine material in the column. The second infiltration rate equal to 4.25×10^{-5} m/s, was specified to be greater than the saturated hydraulic conductivity of the silt. Figure 2.6 shows that the bulk of the flow occurs through the coarse fraction of the material within the column. Further analysis showed that in order to achieve an infiltration rate greater than the saturated hydraulic conductivity of the fine material, the rainfall rate would have to be greater than 1300 m/year of precipitation. In the case of high rainfall tropical locations, a much more realistic infiltration rate falls within the range of the infiltration rate used in the first example, (i.e. 4.25×10^{-7} m/s). In summary, flow within the coarse layers of a waste rock dump is not expected to occur under normal flow conditions, except for intense storms or where funneling of ponded water enters a coarse rock layer that intersects the surface of the dump.

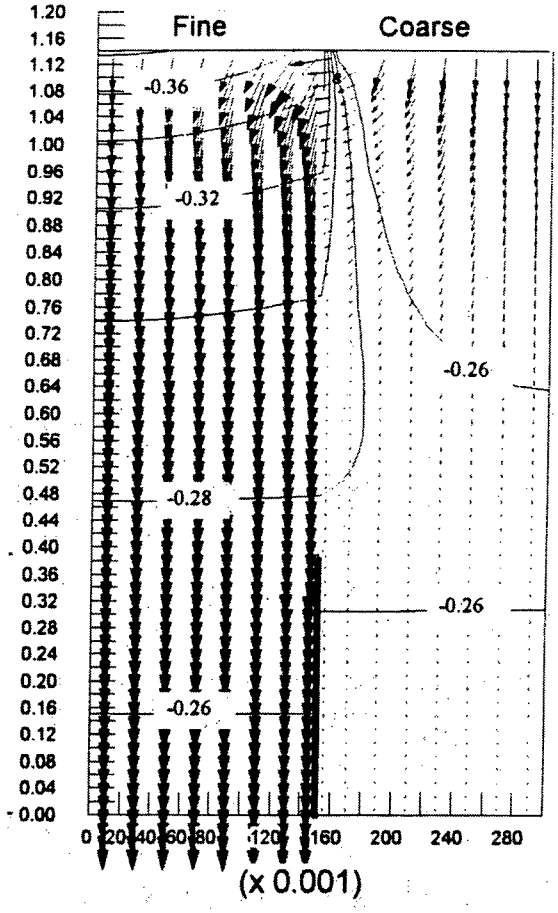

Figure 2.5 Flow Vectors Resulting from Low Infiltration Rate (Newman, 1999)

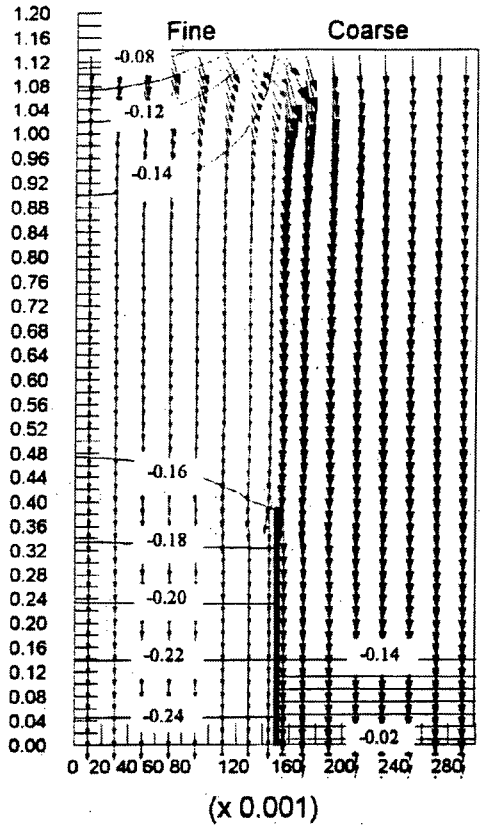

Figure 2.6 Flow Vectors Resulting from High Infiltration Rate (Newman, 1999)

The effect of dipping structure on the preferential flow was examined by Wilson (2003) who conducted extensive numerical analyses for preferential flow through waste rock. The modeled structure was that observed at Golden Sunlight Mine; dipping beds of alternating coarse and fine material. SEEP/W was used to analyze the seepage through a layered system at various angles of bedding. This study showed that the phenomenon of preferential flow occurs when the layers are dipping and that the angle of layers governs the total flow measured in each layer. The dipping structure modeled closely represented the type of structure observed for a waste rock pile constructed using end-dumping techniques.

Nichol (2002) constructed a test pile constructed at Cluff Lake Mine in Northern Saskatchewan that showed the extreme variability of waste rock outflow was obvious, even in a small, controlled experiment. The test pile was 8 m by 8 m and was 5 m in height. The

pile was lined with high-density polyethylene along the sides to eliminate the possibility of water flowing around the collection system at the base. The base of the pile was divided into 16 equal 2m by 2 m sections with pan lysimeters connected to tipping bucket rain gauges and ultimately to a collection system. The pile was constructed by hand in small lifts to allow for the installation of instruments. This construction technique minimized the development of internal structure. The test pile was designed to try and limit the number of possible variables within its confines thereby facilitation interpretation of the results.

The material used in the construction of the pile at Cluff Lake was fairly homogeneous in terms of geology and geochemistry. All of the waste rock was taken from a stockpile on site. The overall texture of the waste rock was of a coarse nature but contained a large fraction of fine material. The site at Cluff Lake is located in a semi-arid region that receives approximately 400 mm of rainfall each year and evaporation exceeds rainfall. It was necessary to add water to the pile to simulate rainfall events during the tracer test as summer rainfall events tended to be sporadic.

A tracer experiment conducted at the site showed that there were a number of distinct flow paths to the various 2 m by 2 m lysimeters underlying the 5 m waste rock profile. Following a rainfall event, some of the lysimeters showed a distinct peak flow before the arrival of the actual wetting front. This provided evidence of the fact that there is water flowing down the entire 5 meters of waste rock and not interacting with the bulk of the surrounding waste rock. It was considered likely that water was flowing along the surface of large boulders down through the waste rock under gravity and not flowing through the finer matrix material. Bellheumer (2001) also observed this type of flow, as discussed previously. It is worth noting that this first arrival of flow represented less than 5% of the total flow that would be observed in the lysimeter. Nichol (2002) also observed that the flow and geochemical measurements for the lysimeters could not be averaged to provide the overall flow and geochemistry. This means that even for a waste rock pile with 320 m^3 of material, 20 m3 is not enough material to be sure that a representative sample has been collected. Nichol (2002) concluded that quantitative determinations of behavior are difficult to make.

Stockwell (2002) completed a study of a waste rock lysimeter was deconstructed at Key Lake Mine in Northern Saskatchewan. Initially the lysimeter was constructed to study the waste rock and flow characteristics expected in larger piles. The objective was to deconstruct the lysimeters and examine the internal structure and geochemical characteristics of the rock contained within the lysimeters. The lysimeters were constructed in one lift approximately 6 m in height by end dumped using haul trucks. The study involved sampling and field sieving the samples to limit the particle size of materials collected for further analysis in the laboratory. The samples were sieved hydraulic conductivity and Soil-Water Characteristic Curves were determined. Stockwell (2002) concluded that these physical characteristics could not be linked in any conclusive way to the geochemical characteristics that were measured in the laboratory. The internal structure of the waste rock in the lysimeters was not analyzed in any specific manner. The sampling conducted was grid and bullet sampling along the trench excavation face and no record of any structure or variation in the waste rock types that were placed in the lysimeters was available. This structure, if it had been quantifiable, may have better assisted in linking the physical and geochemical characteristics of the materials sampled.

2.5 Summary

Much of the research on waste rock has been at the laboratory scale or at a limited number of mine sites. Applicability of the data to different geological and climatic conditions has not been demonstrated. The hydrologic behavior of coarse grained materials is not well understood and waste dump deconstruction completed for the present study presents a unique opportunity to evaluate flow processes in-situ. Laboratory scale research using coarse grained soils is difficult since representative samples need to be greater than 2 m3 to be truly representative. Further field scale trials and in-situ observations are required to confirm hydrologic properties and behaviors in full scale structures. The work presented in this thesis summarizes the field observations and material properties for two waste rock dumps in North America.

CHAPTER THREE: FIELD AND LABORATORY INVESTIGATION METHODS

3.0 INTRODUCTION

Site characterizations for both Site 1 and Sit 2 together with the details of the field and laboratory programs for the waste rock piles at each site are described in this chapter. The field and laboratory programs were designed to create an observationally based conceptual model of the internal structure and flow within waste rock piles. The first phase of the research was to complete a detailed description for each site. The second phase was to excavate test pits at selected locations and obtain to representative samples of the waste rock materials as they were removed for disposal in the open pits. The third phase of the program was to determine the physical properties of the materials sampled from the test pits in the laboratory.

3.1 Site Characterization

Relevant site details including geology and climate for the two sites, as well as details for dump construction and history of mine observations relevant to the waste rock material deposited at each mine site are described in the following sections.

3.1.1 Site 1, South Carolina, USA

Site 1 is located in South Carolina, USA. The mining operation began in 1989 with milling completed in 2000. There were two open pits excavated during the operation of the mine as well as the construction of one waste rock pile. Waste rock was excavated from the North Pit and stockpiled until the end of 1991 when the dump was sealed off after concerns were raised about the possibility of acidic drainage. Subsequent to closure of the waste rock

pile, all further waste rock was either replaced in South Pit or was used for construction of embankments with treatment to prevent generation of acidic drainage. Closure of the mine site resulted in the decision to move the material stockpiled in the North Dump into the North Pit. The North Pit was filling with water due to the cessation of pit dewatering and groundwater levels began returning to regional levels. Water within the two open pits was treated with lime to increase pH and decrease the solubility of metals, therefore limiting contaminant migration from the site. The elevation of the final water table ensured that all waste rock materials are in a subaqueous state in order to limit further chemical oxidation.

3.1.1.1 Climate

The climate in South Carolina is humid sub-tropical. The site is located at 35° North Latitude in an active hurricane zone. The average annual temperature at the site is approximately 20°C and the mean annual rainfall is 1.3 m/year. Figure 3.1 presents data obtained from the South Carolina Department of Natural Resources for average climatic data for the site and the surrounding area.

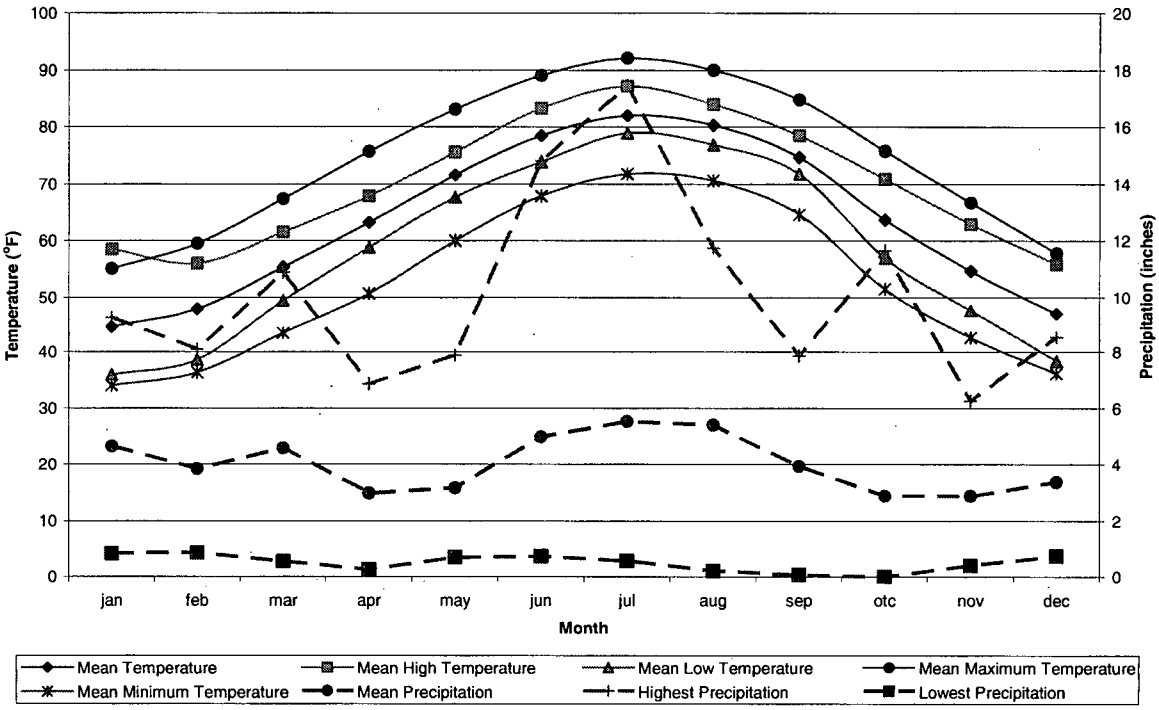

Figure 3.1 Average Climatic Data for Site1 and Surrounding Area (South Carolina DNR)

3.1.1.2 Geology

The near surface geology at the site consists of a surfical layer of saprolite overlying a volcanic intrusion that contained the mineralized ore. There are also zones of rock surrounding the volcanic intrusion that showed evidence of metamorphic alteration. Block modeling conducted on the open pit indicated the materials placed into North Dump, although it was not possible to determine where each material from the pit was deposited in the dump.

Humidity cell tests were performed before the waste rock pile was constructed and showed that there was below trace levels of sulfide present in the waste rock and that there was little to no risk of acid generation. Acid generation however did start to occur within the waste rock stockpiled in the North Dump resulting in the decision for permanent relocation of the waste rock to the North Pit.

3.1.1.3 Waste Rock Pile Configuration

The waste rock pile at Site 1 was constructed in a topographical low area adjacent to the North Pit. The material was end dumped in approximately 5 m lifts and was dozed smooth once each lift was completed. The dozing created a trafficable surface for the next lift of material to be placed and also generated horizontal internal layers within the waste rock that was being placed.

3.1.2 Site 2, Northern Ontario, Canada

Site 2 is located in Northern Ontario in a region of heavy mining activity. Site 2 was discovered in 1897 and exploratory drilling was completed by 1910. The site was abandoned in 1912 when a richer deposit was discovered in a nearby location. In 1987, mining started at the site and the rock developed during exploration was relocated and built over with waste rock being moved for the current mining operation. The Northwestern dump contained some waste rock that was segregated because on visual inspection it appeared to be "clean" waste rock. This waste rock was referred to as "pink granite" and was assumed to be non-acid forming and could be segregated from the rest of the waste rock.

All of the waste rock at Site 2, including the original rock developed during exploration was relocated to the open pit during 2001/2002 as part of closure operations. The current study was conducted during the final stages of material relocation. The total tonnage of waste rock moved was equaled approximately 7.5 million tons. The base of the waste rock dump was not cleared before construction of the dump began in 1987 and that resulted in trees and other organic material being mixed in with the waste rock. There were a number of locations where it was difficult to determine if the original ground surface had been reached due to the presence of trees and boggy material in the foundation of the dump.

3.1.2.1 Climate

The climate in Northern Ontario is described as a humid cool/cold continental with the average annual temperature heavily influenced by the cold arctic water in Hudson's Bay.

This large cool body of water leads to cold winters and heavy snowfall. The region receives an annual average precipitation of 900 mm and permits 920 mm of evaporation leaving the site with a slight water deficit. However, the spring freshet results in a significant recharge of water into the subsurface with the melting of the snow pack. Figure 3.2 presents a summary of the climate means for the region (Environment Canada).

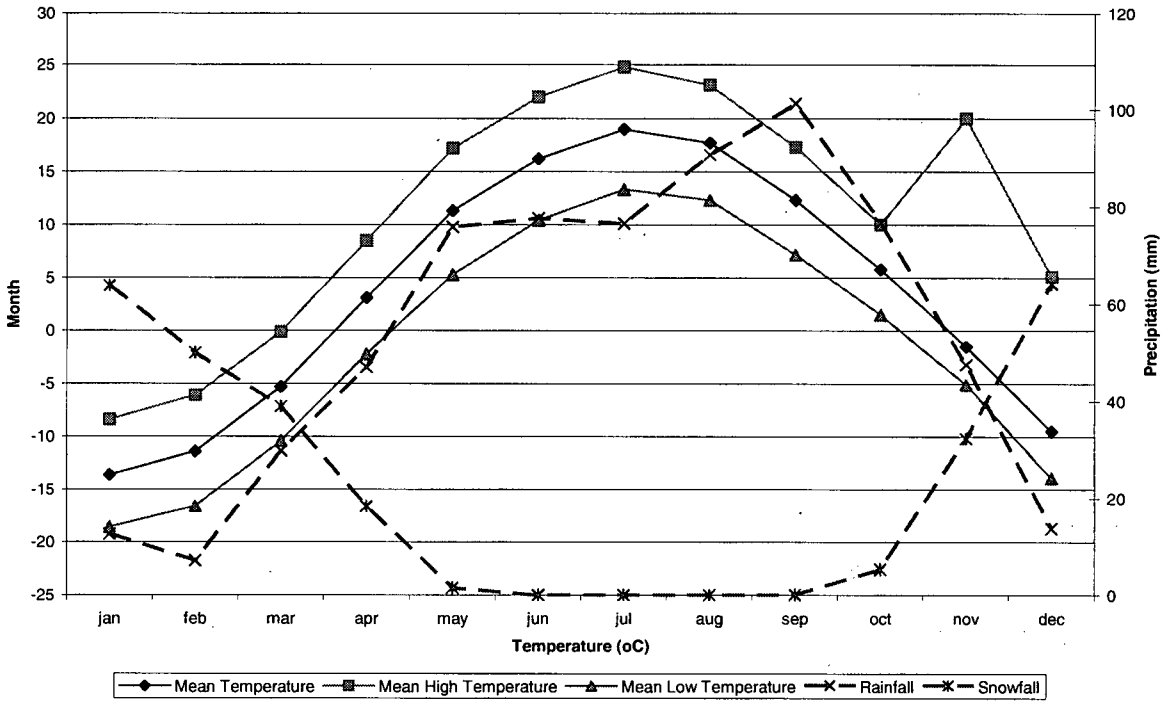

Figure 3.2 Average Climate Data from Site 2 (Environment Canada)

3.1.2.2 Geology

The geology of the region is well documented due to the fact that there have been hundreds of mine operations in the region over the last 100 years. The ore bodies that have been developed are well defined and the geology surrounding these ore zones has been thoroughly analyzed. The mine is located in the Canadian Shield, which is generally a large igneous bedrock deposit. The surficial material was scoured during the last ice age and thus left the bare bedrock exposed. The granite rock has undergone some metamorphic alteration, especially around other intrusions of igneous rock, which is common where ore zones are

located. Much of the regional geology shows significant mineralization, although not necessarily in grades high enough to be economical. This mineralization is the reason why so much of the waste rock is potentially acid generating.

Geochemical analysis of the waste rock at Site 2 reported in Tran, (2003) show that while there is carbonate material within the materials stockpiled in the dump there is also a significant amount of material that is potentially acid forming. The main sulfide minerals are pyrrhotite and chalcopyrite. Pyrrhotite is an extremely reactive form of iron sulfide and chalcopyrite oxidation mobilizes copper in the system.

3.1.2.3 Waste Rock Pile Configuration

The dump at Site 2 was constructed on a side hill using end-dumped construction techniques. The natural topography adjacent to the open pit is steep and the waste rock was end-dumped off the side hill. The dump was constructed in lifts of 5 m to 10 m throughout the life of the mine.

3.2 Field Program

The waste rock pile at Site 1 was excavated in 5 m high lifts. The sampling program was conducted from July, 2000 to October, 2000. The test pits were excavated with a DC Excavator provided by the mine operators. The test pits were excavated on the same day the sampling was conducted. A total of 19 test pits were excavated in the waste rock dump during the field sampling program. Test pits were excavated into each bench of the dump as it was exposed during the excavation process. Figure 3.3 the schematic plan of the surface waste rock pile along with the location of the test pits. Figure 3.4 shows a schematic cross-section of the dump with the location of the test pits and the location of the benches excavated from the waste rock pile.

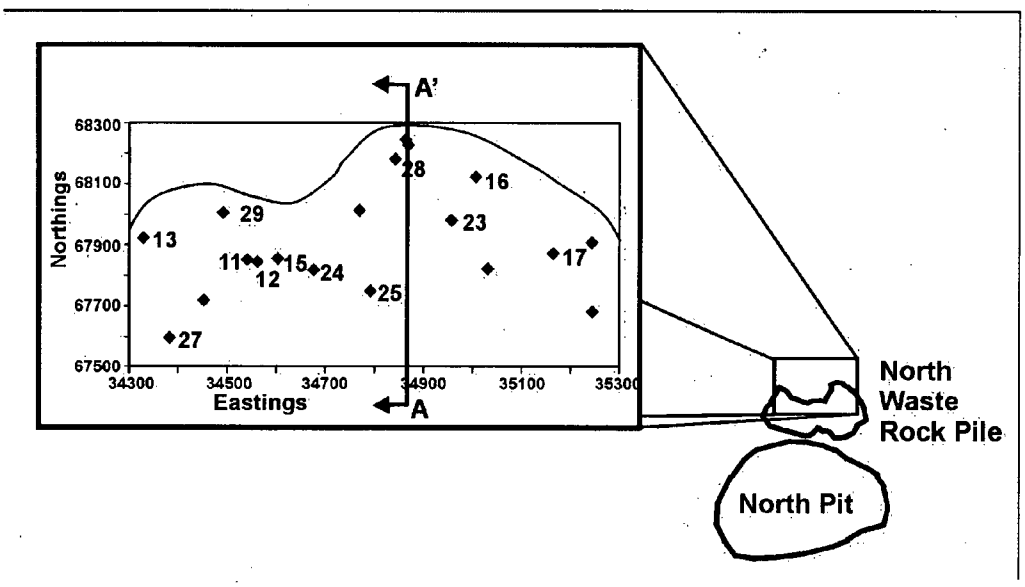

Figure 3.3 Plan Location of Test Pits

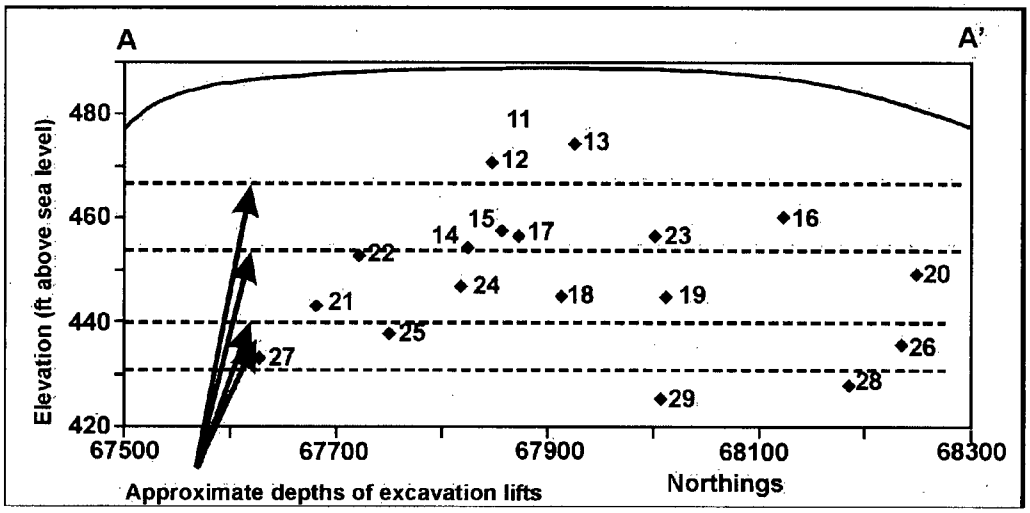

Figure 3.4 Section Location of Test Pits

The material at Site 1 was found to be soil-like in texture, which allowed for ease of sampling procedures. Most of the geotechnical sampling procedures used to characterize materials was developed for soil-like materials. The testing procedures outlined in the following sections were found to be most effective at Site 1. There were very few locations encountered where particles larger than gravel size dominated the matrix filling the void

spaces. The fine texture of the materials allowed for representative samples to be collected in the field for laboratory characterization.

The waste rock pile at Site 2 was excavated in 10 m lifts using a track mounted excavator and haul trucks. The field sampling program at Site 2 was conducted from November, 2000 to September, 2001. The test pits were excavated on the same day the test pit was sampled. The test pits were excavated using a track-mounted excavator provided by the contractor at the mine site. At Site 2 a total of 14 test pits were excavated in 6 different lifts as the waste rock was relocated. A test pit was located along the centerline of the dump as well as perimeter of the dump. The location of each test pit was selected on-site as the waste rock was being removed. The spatial distribution of the test pit locations was chosen to allow for a comparison of the materials that were sampled along the outer edges of the dump compared to the material sampled in the center of the dump. Figure 3.5 shows a plan view of the waste rock dump and the location of the test pits. Figure 3.6 shows a vertical section through the dump showing the vertical distribution of the test pit locations.

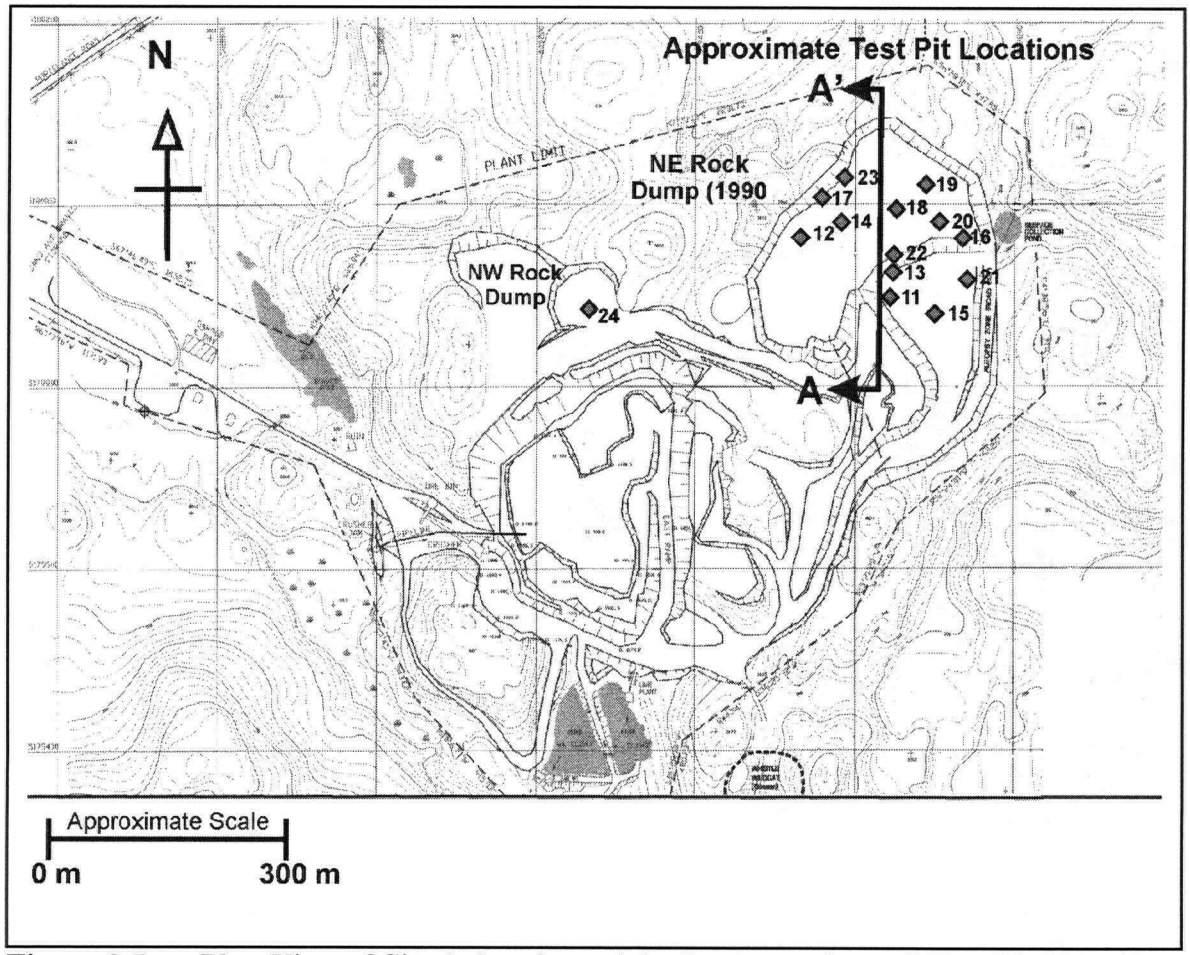

Figure 3.5 Plan View of Site 2 showing original topography and Test Pit Locations.

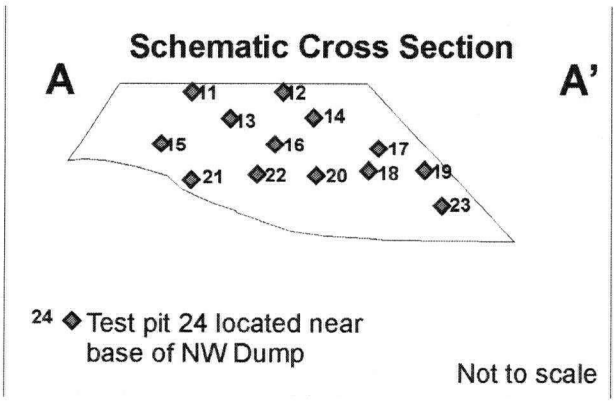

Figure 3.6 Section View of Waste Rock Pile showing Test Pit Locations at Site 2

Material in the waste rock dump at Site 2 was found to be very large grain sized. As a result, many procedures had to be modified. As the excavation progressed, each bench removed was reduced in thickness at the base of the dump and bedrock outcrops along the original ground surface. These layers were more difficult to sample due to the frozen conditions. The reduction in depth of material removed allowed for a greater frequency of test pit excavation in the lower benches of the dump. The large range in particle size lead to a difficulty in collecting representative samples, thus field screening at 100 mm was used to limit the size of particles selected for analysis in the laboratory.

At both sites, the first stage in the field program was to create a detailed test pit log of the materials present, record any apparent structure and photograph the test pit prior to any sample collection or in-situ testing. The second stage was to collect samples for analysis in the laboratory and the final stage was to conduct in-situ testing.

3.2.1 Bulk Sample Collection

Laboratory characterization of the waste rock samples required that large bulk samples be collected in the field. The samples ranged in weight from 5 to 15 kg. All of the samples collected in the field were mainly in a disturbed state.

The samples were collected by direct excavation from the side wall of the test pit using 20 l pails. The wall of the test pit was sampled using a geologist pick. Samples were collected from distinct layers visible on the face of the test pits. The samples were collected at or near the surface of the test pit walls. The samples were then placed in large polyethylene bags.

Site 2 provided a challenge when collecting large bulk samples. Samples collected in the field were sieved to a maximum particle size of 100 mm. To aid in determining the actual grain size distribution, the oversize particles that were removed from the bulk samples were recorded. The number and diameter of over-size particles not collected for laboratory

analysis was recorded. All of the laboratory test results presented in Chapter 4 are based on a material fraction sampled in the field (that is, material finer than 100 mm).

3.2.2 In-Situ Testing

The excavation of test pits allowed for the performance of in-situ testing. Testing consisted of measurements of matric suction and bulk in-situ density. The extremely coarse grained texture of the Site 2 waste rock pile made it necessary to modify some of the testing procedures adopted for Site 1. The following section describes the testing procedures for measuring matric suction and in-situ density used at both Site 1 and Site 2.

3.2.2.1 Matric Suction

The method used to measure matric suction at Site 1 involved the installation of tensiometers and recording the matric suction. The tensiometer consisted of a cylindrical ceramic tip that allowed water to flow into or out of the tensiometer and equilibrate with the surrounding soil. The tensiometers used at Site 1 were assembled at the University of Saskatchewan from parts provided by local suppliers. Figure 3.7 shows a typical tensiometer used at Site 1. To install the tensiometer, a hole was augured into the material at a slight downward angle. The tip of the tensiometer was coated with cuttings from the hole in order to achieve better contact between the tip and the soil. The tensiometer was then left overnight to allow the water phase in the tensiometer to come into equilibrium with the water phase in the soil before obtaining a final reading. The matric suction inside the tensiometer was measured using a digital meter (provided by the University of Saskatchewan) with a hypodermic needle to puncture the seal on the end of the tensiometer.

Figure 3.7 Typical Tensiometer used at Site 1.

Two major problems were encountered with this testing procedure at Site 1. First, the auger was significantly larger than the tip of the tensiometer. This resulted in relatively poor contact in many of the layers that were tested. Second, the holes for the tensiometer were bored by hand and the presence of gravel, cobble and rock sized material made installation of the tensiometers impossible at some locations. Coarse materials may also have limited contact of the waste rock with the tip of the tensiometer and thus resulted in poor quality readings.

The coarse grained nature of the material at Site 2 made measurement of matric suction very difficult at most test pit locations. There were only a few test pits where the voids created by the coarse particles (>100 mm) were filled with enough fine matrix material (<2 mm) to allow contact with a tensiometer and obtain an in-situ measurement of matric suction. A second type of tensiometer is available for matric suction measurements. The Quick Draw tensiometer is a commercially available product that has a quick response to soil moisture changes and is sensitive to low matric suction values. This was used at Site 2 for in-situ matric suction measurements. The Quick Draw tensiometer also has a small tip and can be used in small zone of matrix material. The tensiometer is supplied with a coring tool that is ideal for coring through rock-like materials.

3.2.2.2 In-Situ Density

The sand cone method was used to measure in-situ density following the ASTM standardized procedure D1556-90. The method involves the excavation of a 15 cm diameter hole approximately 15 cm deep. The apparatus includes a plastic bottle that contains dry sand and a cone that screws onto the top of the bottle. Once the excavation is completed the guide plate is placed over the hole and the cone is placed on the guide plate. The sand is then allowed to flow out of the bottle until the excavation and the cone have completely filled with sand. The remaining sand in the bottle is weighed, as is the material that was removed from the excavation. This allows for an estimation of the in-situ bulk density of a material. Figure 3.8 shows the sand cone and excavation plate used for the method described here.

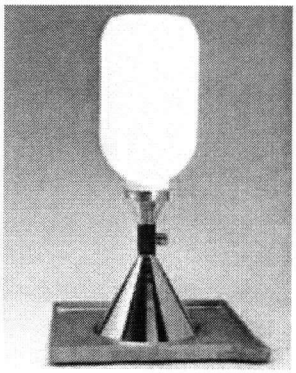

Figure 3.8 Sand Cone Apparatus for determining in-situ density.

There are three critical steps required to ensure that the measurement of density is successful for waste rock materials. First, the bottle must be filled the same way each time to ensure that the same volume of sand is used to fill the bottle. In this research, the sand was calibrated using a constant pouring rate with the bag 2.5 cm above the neck of the bottle. The sand was pluviated the same way each time to ensure that the density of the sand in the bottle was the same for each test. Second, a flat area of ground is needed where the material in question extends at least 15 cm below the ground. At Site 1 when two different materials were encountered in the excavation the measured density was a composite value of two materials rather than one material. At the base of each test pit excavated visible materials

were sampled from the side walls of the excavation. The orientation of the layers resulted in vertical sampling depths of less than 15 cm in several of the test pits, and this was not obvious until excavation of the sample hole was completed. If any visual changes in the material were noted, and if the excavation appeared to contain two layers, a new hole was made. The test also required that the matrix of the material being tested should be bounded by particles small enough to limit sand loss out of the excavation. At Site 2, the excavation was lined with plastic to minimize sand loss out of the excavation. This test was a modification of the rubber balloon method (ASTM D2167-94). At Site 2 a rubber balloon apparatus as described in ASTM D2167-94 was not available, thus a plastic lining was used instead of a rubber membrane.

3.3 Field and Laboratory Testing

Evaluation of the material properties was conducted after the samples had been collected in the field. Initial on-site testing at Site 1 included paste pH, water content, grain size distribution and visual inspection. This laboratory visual inspection is included in the material descriptions presented in Chapter Four. For Site 2, all samples were shipped to UBC for water content, paste pH, grain size distribution and visual inspection.

3.3.1 Water Content

At Site 1, additional samples were collected for the measurement of water content. The samples were collected in 500 ml glass jars. The samples collected for water content were dried in the oven at 105°C overnight. The values of water content were also used to back calculate the in-situ dry density for the sand cone tests. The sample excavated for the sand cone test was weighed at its in-situ moisture content and the measured water content was used to determine the dry weight of the sample that was excavated.

At Site 2, the gravimetric water content was determined on the sealed bag samples that were sent to UBC from the site. The samples were opened at UBC and placed in a

105°C oven overnight. The measured water contents were approximate as the samples can either dry or absorb moisture through the polyethylene bags during shipping.

3.3.2 Grain Size Distribution

A grain size distribution analysis was determined for each sample collected at Site 1 following ASTM D-422. The samples were washed over a 0.85mm sieve (ASTM No.20). The material that was retained on the 0.85 mm mesh was sieved using the following nest of sieves: 38 mm, 25 mm 16 mm 9 mm, 4.75 mm, 2 mm, and 0.85 mm. The excess water washed through with the fines was oven dried. The fine fraction was then sieved through the following nest of sieves: 0.6 mm, 0.425 mm, 0.250 mm, 0.150 mm, 0.106 mm, and 0.075 mm.

The material from Site 2 was sieved using a different set of sieves due to the coarse nature of the samples collected. The set of sieves included 75 mm, 50 mm, 38 mm, 16 mm, 9.5 mm, 4.75 mm, 2 mm, 0.85 mm, 0.425, 0.106 mm, and 0.075 mm. The samples from Site 2 were not wet sieved due to the lack of fines in the samples. The ASTM standard for determination of particle size distribution states that if the percent passing the 0.075 mm sieve is less than 2% of the sample being analyzed, a wash sieve is not required (ASTM D-422). Washing samples usually ensures that fines are not being retained on the surfaces of larger particles, however for samples containing a small fraction of silt and clay sized particles this error is small. The samples at Site 2 were field sieved to passing 100 mm, previous studies had estimated that the fraction of material less than 100 mm in size accounts for only 10% of the total material stockpiled in the dump. The samples being analyzed in the laboratory contained a small fraction of silt and clay sized particles. This lack of fines allowed for dry sieving only on the Site 2 samples.

3.3.3 Paste pH

Paste pH measurements were made to assess of the weathering of the materials. The paste pH testing method was based on the ASTM standard D4972-98a. Samples were sieved through the 2 mm sieve to separate the fines of the sample for testing. 10 grams of sample was mixed with 10 ml of distilled water for a 1:1 test and 50 ml of water for a 5:1 test. The samples were agitated for 1 hour and then allowed to rest for 1 hour before the pH of the slurry was measured using a commercially available Fisher pH meter.

3.4 Laboratory Testing for Hydraulic Properties

The testing of hydraulic properties included a number of tests to describe the soil water interactions of the materials sampled. The testing included the Soil-Water Characteristic Curve, the saturated hydraulic conductivity and one dimensional consolidation. All of these tests were conducted on the disturbed samples that were collected in the field.

3.4.1 Soil Water Characteristic Curves

The Soil-Water Characteristic Curve was measured using a pressure plate apparatus known as a Tempe Cell. Small diameter (10 cm) Tempe Cells were used to evaluate the Soil-Water Characteristic Curve for particles passing the 4 mm mesh. Large diameter (15.5 cm) cells were able to be used to evaluate samples containing particle sizes up to 2.5 cm. Figure 3.9 shows a typical Tempe Cell used to evaluate the hydraulic properties of the waste rock samples.

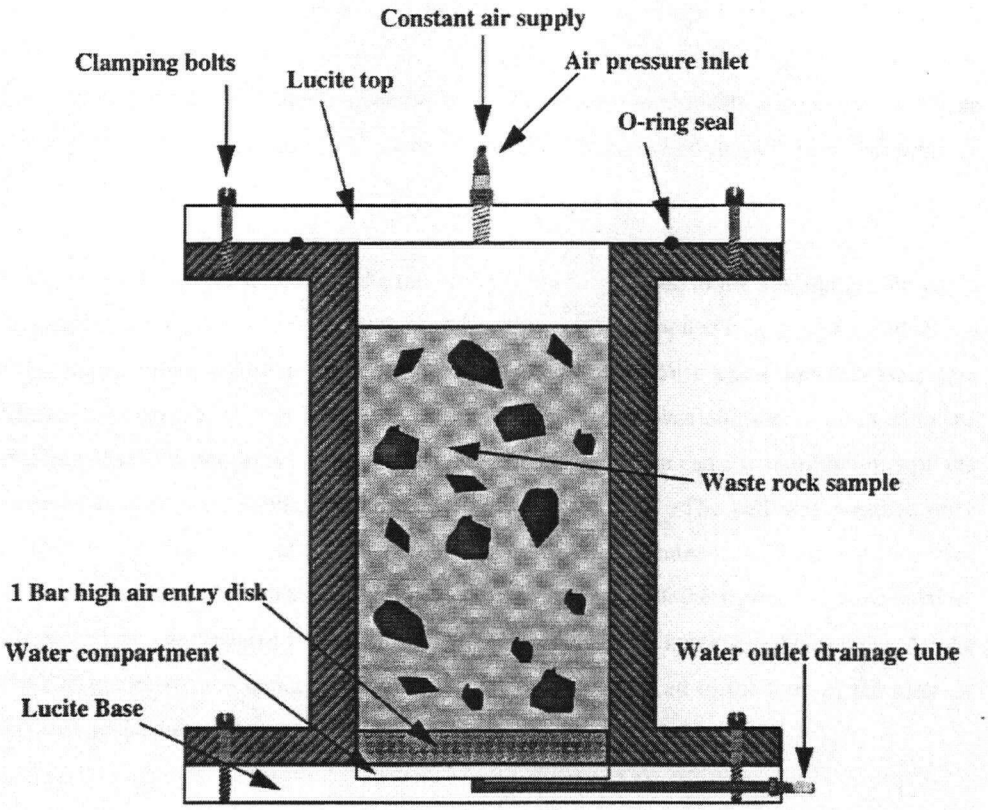

Figure 3.9 Typical Tempe Cell Apparatus (Herasymuik, 1996)

The procedure to determine a Soil-Water Characteristic Curve is described in detail in Fredlund and Rharhjo (1993). The test involves isolating a sample on a ceramic stone with a high air-entry value that undergoes no volume change. The soil sample is then subjected to a pressure gradient across the cell. This gradient is either achieved by lowering the water table, effectively placing matric suction on the base of the stone to pull water out of the sample or a standing air pressure can be applied at the top of the cell, forcing water out the base of the cell. To ensure that all water is flowing out of the base of the sample is only from the sample contained within the cell, the porous stone at the base of the cell must remain saturated at all times. The pressure applied at the porous stone does not exceed the air entry value of the stone to ensure that the stone will remain saturated.

For Site 1 the samples were prepared by sieving waste rock through the 4 mm sieve. A total of 500 g of sieved sample was used in the test. The waste rock was slurried and poured into a small diameter cell. The weight of the cell and the weight of the cell containing the sample were recorded. The cell was sealed and the sample was allowed to equilibrate at 0 kPa ensuring that the sample was fully saturated, but without any excess water. The sample was subjected to effective stresses of 0.1 kPa, 5 kPa, 10 kPa, 30 kPa, 50 kPa, 80 kPa and 100 kPa.

All of the samples evaluated were first tested using a 100 kPa stone. The "high flow" stones were used to allow for a faster test and the lower air entry value of the stone also increased the speed at which the testing can be conducted. One of the samples that was tested had an air entry value close to 100 kPa so a 500 kPa stone was installed in the cell.

The samples from Site 2 were sieved through a 4 mm sieve for testing in the small Tempe cells. A sample was also evaluated in a large Tempe cell. This sample was sieved through the 25 mm sieve and then placed in the large cell. The large cell is identical to the small cells and the same series of pressures were used to evaluate the material.

3.4.2 Saturated Hydraulic Conductivity

The saturated hydraulic conductivity of the samples from Site 1 was evaluated by two methods. The first method was to slurry the samples in a solid wall permeameter and to place the material at a density similar to that in the field. This test was performed according the ASTM standard D887. There are two potential drawbacks in this type of test. The first is that it is difficult to place the material at a density that is representative of field conditions. For the testing conducted at UBC the samples were placed in the cells at water content close to optimum water content and packed by hand. The second potential problem with the test is the sidewall leakage around larger particles. If preferential pathways develop within the sample then the hydraulic conductivity measured can greatly overestimate the actual value. As the samples were placed in the cells, an attempt was made to limit the large particles close

the side of the cell. However, the sides of the cells are solid and it is difficult to ascertain if the material was uniformly placed along the walls of the cell. Figure 3.10 shows a typical setup for a falling head hydraulic conductivity test in a solid wall permeameter. The inflow reservoir allowed for the rate of water drop across the sample to be calculated thereby estimating hydraulic conductivity.

The materials at Site 2 were too coarse to measure using either a solid wall permeameter or an odeometer; the measure of hydraulic conductivity would be approximate regardless of the testing procedure. The large particle size and free drained nature of the material means that the water flowing through the dump would be flowing as film around the surfaces of the particles. A field test was conducted at Klohn Crippen using a 50 gallon tank directly on the surface of the waste rock pile. The results of this test was also inconclusive because the tank could not supply water at a fast enough rate to create a standing water condition that is needed to get an accurate indication of the saturated hydraulic conductivity. However the test does give an indication of the minimum hydraulic conductivity of the material due to the rate at which water could flow out of the tank during the test.

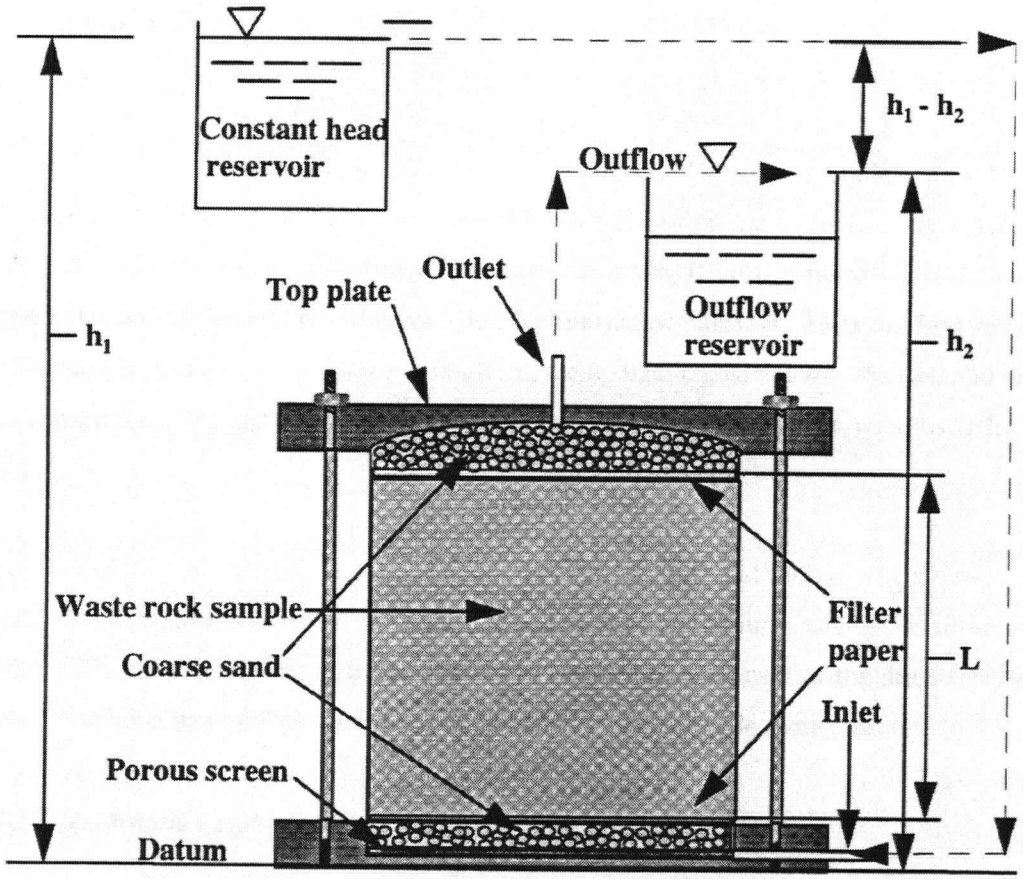

Figure 3.10 Typical Solid Wall Permeameter for Hydraulic Conductivity Analysis (Herasymuik, 1996)

To improve the accuracy of the hydraulic conductivity test, three samples from Site 1 were subjected to a standardized one-dimensional consolidation test in an oedometer ring. The procedure for the oedometer test can be found in Craig (1987). The test involves one-dimensional loading of a sample within a solid ring, which eliminate lateral expansion of the sample. The sample is placed in a solid metal cell and saturated. Loads are placed on the top of the cell via a loading frame and the vertical deflection of the sample is measured as each load is applied to the top of the cell. The test determines the consolidation properties of a material, which are related to the hydraulic conductivity. The test allows for the hydraulic conductivity of the sample to be back calculated at each loading stage of the test. The three

samples that were tested were selected materials that were considered to be the most representative.

3.5 Numerical Modeling

Numerical models were used to evaluate seepage for the waste rock pile at Site 1 using SEEP/W (Geo-Slope, 2001). The program uses the finite element method to compute the flow paths within defined material zones and hydraulic boundary conditions. The materials are defined with saturated/unsaturated material properties to allow for evaluation of preferential flow pathways within a defined boundary. Details of the model used to evaluate the waste rock dump at Site 1 are described in Chapter 5.

CHAPTER FOUR: RESULTS OF FIELD AND LABORATORY INVESTIGATIONS

4.0 INTRODUCTION

Chapter Four is a detailed description of the results of the field and laboratory investigation that was outlined in Chapter Three. Material properties and test results are presented in the following sections.

4.1 Site 1

The waste rock pile at Site 1 was excavated in lifts and the test pits were excavated in each bench of waste rock as it was removed. Each test pit was visually logged and photographed following excavation. Figure 4.1 shows the typical structure observed in the bench. The materials observed in the waste rock dump at Site 1 were highly weathered, fine grained in texture and had a low paste pH. Dipping layers of interbedded materials were observed throughout the profile of the dump. Oxidation products, extremely fine matrix material and traffic surfaces were the dominant features of the dump at Site 1.

Figure 4.1 Typical Structure Observed in Site 1 Test Pits

4.1.1 Physical Descriptions Materials Observed in Test Pits

This section presents the visual description and laboratory test results for each material that was sampled. Table 4.1 summarizes the material properties such as color and texture for materials at Site 1. The table is organized according to bench, test pit and sample identification of each test pit and material sampled. Table 4.2 provides a summary of the gravimetric water content, dry density, matric suction and material classifications. The material classifications (1 – 7) listed are a grouping of representative materials based on color, texture and paste pH and are summarized in Table 4.3. These characteristics were sometimes contradictory in terms of which group materials belong, but paste pH and color tended to be the most indicative characteristics for classification. The use of "soil-like" and "rock-like" was used as a qualitative description of the absence or presence of significant quantities of gravel and cobble sized particles, respectively.

Table 4.1 Description of Materials Sampled at Site 1

bench	test pit	sample #	Description	colour	texture	Classification
1	11	TP11GS1	soil with soft rock particles	light brown to pink	clay silt with large rock fragments	1
1	11	TP11GS2	soil like	light yellowish brown	clay silt gravel with 2" soft rock	1
1	11	TP11GS3	soil like	light brown	clayey silt with gravel	1
1	11	TP11GS4	soil like	red	medium plasticity clay	2
1	11	TP11GS5	soil like	olive yellow	silty plastic clay	2
1	11	TP11GS6	soil like	red	well graded clayey silt matrix	2
1	11	TP11GS7	soil like	brown	clay sand silt as gravel sized nuggets	5
1	12	TP12GS1	soil like	pale yellow	clayey silt matrix with gravel	3
1	12	TP12GS2	soft rock	red	soft rock fragments with gravel	2
1	12	TP12GS3	soft rock	red	sandy clay gravel with soft rock fragments	2
1	12	TP12GS4	soil like	light brown	well graded clay and sandy silt gravel	1
1	13	TP13GS1	soil like with soft rock particles	light grey	well graded gravel with silt and clay	1
1	13	TP13GS2	soil like	red	clayey silt with no rock	2
1	13	TP13GS4	soil like with hard rock particles	dark brown	silty clay matrix with hard rock particles up to 12"	5
1	13	TP13GS5	soil like	green grey	clay with silty sand particles	1
1	13	TP13GS6	soil like	pale yellow	organic/topsoil with presence of tree roots. Gravel to cobble sized particles also present	1

Table 4.1 Summary of Material Descriptions (continued)

bench	test pit	sample #	Description	colour	texture	Classification
2	14	TP14GS1	soil like	pale yellow	clayey silt	4
2	14	TP14GS2	soil like	light olive grey to reddish brown	clayey silt with gravel	2
2	14	TP14GS3	soil like	red	clayey silt with soft rock fragments	2
2	14	TP14GS4	soil like	light olive brown	clayey silt with gravel	1
2	14	TP14GS5	soil like	brownish yellow	silty gravel with rock particles	1
2	14	TP14GS6	soil like	red	silty clay	2
2	14	TP14GS7	soft rock	pale yellow	well graded gravel with silt	1
2	15	TP15GS1	soil like	dark red	medium plasticity clay	2
2	15	TP15GS2	soft rock	yellow to red	rock layer with silty clay matrix	1
2	15	TP15GS3	soil like	pink	well graded clayey silt to gravel	1
2	15	TP15GS4	soil like	pale yellow	silt	4
2	15	TP15GS5	soil like	red	medium plasticity clay	2
2	15	TP15GS6	soil like	pale yellow	sandy clay with silt and gravel	1
2	15	TP15GS7	soil like	brown	silty clay with gravel	6
2	15	TP15GS8	soil like	red	silty clay	2
2	15	TP15GS9	soil like	strong brown	clay and silty gravel	6
2	15	TP15GS10	soil	red	medium plasticity clay	2
2	16	TP16GS1	soil like	pale yellow	clayey silt with sand	4
2	16	TP16GS2	soil like	light olive grey	gravel with silt and clay	1
2	16	TP16GS3	highly weathered rock	brownish yellow	gravel with silty clayey sand	7
2	16	TP16GS4	soil like	brown	silty sand gravel	6
2	17	TP17GS1	soil like	yellowish brown	gravelly clayey silt	7
2	17	TP17GS2	rock like	grey	clean unoxidized waste rock	1
2	23	TP23GS1	soil like	yellowish brown	silty sandy clay	6
2	23	TP23GS2	soil like	red	silty sandy clay	2
2	23	TP23GS3	soil like	light olive grey	well graded gravel with high content of clay, silt and sand	1
2	23	TP23GS4	soil like	red	silty sandy clay	2
2	23	TP23GS5	rock	olive yellow	angular gravel with silt and sand	7
2	23	TP23GS5x	rock	greenish yellow jarosite and brown iron staining	large angular platey particles (1-6")	7

Table 4.1 Summary of Material Descriptions (continued)

bench	test pit	sample #	Description	colour	texture	Classification
3	18	TP18GS1	soil like	pinkish grey with white chalk	clayey silt	4
3	18	TP18GS2	soil like	pinkish grey with white chalk	clayey silt	4
3	18	TP18GS3	soil like	same as above containing dark red saprolite particle	clayey silt	4
3	18	TP18GS4	soil like	pale yellow	clayey silt	4
3	18	TP18GS5	soil like	light grey	silty clay matrix	4
3	18	TP18GS6	soil like	dark yellow brown	clayey silty sand with gravel	6
3	18	TP18GS7	soil like	dark red	clayey sandy silt	2
3	19	TP19GS1	rock like	grey	boulders with silty fines	7
3	19	TP19GS2	soil	light brown	clayey sandy silt	6
3	19	TP19GS3	soil	olive grey	silty clay	1
3	19	TP19GS4	soil like	dark red	clayey silt	2
3	20	TP20GS1	soil like	light olive grey	gravelly sandy clayey silt	1
3	20	TP20GS2	soil like	light grey	silty sandy gravel	4
3	20	TP20GS3	soil like	dark red	silty clay	2
3	20	TP20GS4	soil	browish yellow	clay	7
3	20	TP20GS5	soil like	brownish yellow	clayey silt	7
3	21	TP21GS1	soil like	reddish brown	clayey silt	6
3	21	TP21GS2	soil like	pale yellow	clayey silt	4
3	21	TP21GS3	soil like	brownish yellow	sandy clayey silt	7
3	22	TP22GS2	saprolitic rock like	light grey	gap graded with soil and rock	1
3	22	TP22GS3	rock	brownish yellow	gap graded with soil and rock	7
3	22	TP22GS4	soil like	red	silty clay	2
3	24	TP24GS2	soil like	olive green	silty clayey sand	1
3	24	TP24GS3	soil like	mottled red green yellow colour	low plasticity hardened clay	1
3	24	TP24GS4	soil like	red	medium plasticity clay	2
3	24	TP24GS5	soil like with hard rock particles	pale yellow	silty sand with rock particles	4
3	24	TP24GS6	soil like	dark green	silty clay with friable soil particles	1

Table 4.1 Summary of Material Descriptions (continued)

bench	test pit	sample #	Description	colour	texture	Classification
4	25	TP25GS1	soil like	pale yellow	silty clay	4
4	25	TP25GS2	soil like	red	silty clay	2
4	25	TP25GS3	soil like	pale yellow	silty clay	4
4	25	TP25GS4	soil like	light brown	silty clay with gravel	1
4	26	TP26GS1	rock	light grey	silty clay matrix with 0.5 to 3" rock particles	7
4	26	TP26GS2	rock	light grey over red and yellow rock particles	silty sand matirx with larger hard rock particles	7
4	27	TP27GS1	soil like with soft rock particles	grey	silty clay matrix with soft and hard rock particles (3")	1
4	27	TP27GS2	soil like	pink	silty clay with small rock particles	1
4	27	TP27GS3	rock	brown	large angular particles in a silty sand matrix	6
4	27	TP27GS4	soil like	red-orange	silty clay matrix that contains large sand and gravel particles	7
5	28	TP28GS1	soil like with small rock particles	brown	silty sand matrix with 1 to 2" hard rock particles	6
5	28	TP28GS2	soil like	greyish green	silty gravel matrix containing significant clay content	1
5	28	TP28GS3	soil like	brown	silty sand matrix with clay present and 1 to 2" rock particles	6
5	28	TP28GS4	rock	greyish green	gravel to cobble particles containing a sand silt matrix	7
5	28	TP28GS5	soil like with rock particles	reddish brown	silty sand matrix with clay present and 1 to 2" rock particles	6
5	29	TP29GS1	soil like with soft rock particles	red	silty clay matrix containing rock particles	2
5	29	TP29GS2	soil like	greenish grey	silty gravel with rock particles	1
5	29	TP29GS3	soil like	brown	silty sand with gravel sized particles	6

Table 4.2 Summary of Test Results for Site 1

bench	test pit	sample #	pH	Dry Density g/cm^3	Matric Suction kPa	grav. w.c. (%)	Volumetric Water Content	Degree of Saturation (%)	Classification
1	11	TP11GS1	2.71	1.6	60	11.8	19	47	1
1	11	TP11GS2	3.08	1.536	15	9.5	15	34	1
1	11	TP11GS3	4.01	1.775	15	18.5	30	73	1
1	11	TP11GS4	5.62	n/a	242	17.9	26	55	2
1	11	TP11GS5	5.38	n/a	23	17.6	24	52	2
1	11	TP11GS6	5.11	n/a	n/a	14.8	22	48	2
1	11	TP11GS7	4.94	1.193	n/a	22.3	24	39	5
1	12	TP12GS1	2.95	n/a	255	23.4	28	52	3
1	12	TP12GS2	2.68	n/a	n/a	9.7	13	27	2
1	12	TP12GS3	2.42	1.592	11	15.4	22	47	2
1	12	TP12GS4	2.78	1.437	6	13.5	18	37	1
1	13	TP13GS1	3.71	2.259	58	n/a	12	40	1
1	13	TP13GS2	4.93	1.687	58	22.1	32	67	2
1	13	TP13GS4	n/a	n/a	9	10.3	14	30	5
1	13	TP13GS5	n/a	n/a	68	13.3	18	37	1
1	13	TP13GS6	n/a	n/a	10	10.2	14	30	1

Table 4.2 Summary of Test Results (continued)

bench	test pit	sample #	pH	Dry Density g/cm^3	Matric Suction kPa	grav. w.c. (%)	Volumetric Water Content	Degree of Saturation (%)	Classification
2	14	TP14GS1	3.26	n/a	822	5.3	8	17	4
2	14	TP14GS2	5.51	n/a	14	14	19	38	2
2	14	TP14GS3	6.19	n/a	42	19.9	26	49	2
2	14	TP14GS4	6.68	n/a	2	11.6	16	33	1
2	14	TP14GS5	6.14	n/a	6	12.4	17	35	1
2	14	TP14GS6	5.28	n/a	4	18.2	24	46	2
2	14	TP14GS7	5.81	1.718	14	6.5	11	32	1
2	15	TP15GS1	3.82	1.592	231	16.68	24	49	2
2	15	TP15GS2	n/a	n/a	n/a	13.3	18	37	1
2	15	TP15GS3	2.62	n/a	414	10.1	14	30	1
2	15	TP15GS4	2.95	n/a	228	15.5	21	41	4
2	15	TP15GS5	n/a	n/a	85	11.1	16	32	2
2	15	TP15GS6	3.56	0.643	n/a	4.5	6	9	1
2	15	TP15GS7	3.87	1.73	224	13.5	21	48	6
2	15	TP15GS8	3.66	n/a	9	18.6	24	47	2
2	15	TP15GS9	3.86	1.803	n/a	8.9	15	41	6
2	15	TP15GS10	6.65	1.64	26	19.6	30	71	2
2	16	TP16GS1	2.4	n/a	10	27.25	40	85	4
2	16	TP16GS2	2.46	n/a	30	12.68	17	36	1
2	16	TP16GS3	2.41	n/a	n/a	3.91	5	8	7
2	16	TP16GS4	2.8	1.577	195	6.91	10	23	6
2	17	TP17GS1	2.32	n/a	n/a	10.6	16	33	7
2	17	TP17GS2	n/a	n/a	n/a	4.94	8	17	1
2	23	TP23GS1	3.77	n/a	n/a	13.6	19	40	6
2	23	TP23GS2	3.73	n/a	lost to rain	17.2	23	48	2
2	23	TP23GS3	3	1.887	n/a	6.3	11	33	1
2	23	TP23GS4	n/a	n/a	21	n/a			2
2	23	TP23GS5	2.36	n/a	n/a	1.8	3	6	7
2	23	TP23GS5x	2.48	n/a	n/a	n/a			7

Table 4.2 Summary of Test Results (continued)

bench	test pit	sample #	pH	Dry Density g/cm^3	Matric Suction kPa	grav. w.c. (%)	Volumetric Water Content	Degree of Saturation (%)	Classification
3	18	TP18GS1	4.1	1.593	17	21.5	28	55	4
3	18	TP18GS2	3.99	1.643	115	21.5	32	71	4
3	18	TP18GS3	4.03	n/a	225	12.8	18	38	4
3	18	TP18GS4	4.13	n/a	447	16	22	45	4
3	18	TP18GS5	4.89	1.651	7	16.1	24	52	4
3	18	TP18GS6	6.19	1.46	456	14.1	17	32	6
3	18	TP18GS7	5.99	2.045	546	16.8	29	78	2
3	19	TP19GS1	2.9	n/a	n/a	8.5	13	28	7
3	19	TP19GS2	2.6	1.28	200	8.5	11	21	6
3	19	TP19GS3	3.2	1.19	77	18.1	22	38	1
3	19	TP19GS4	2.5	1.26	120	16.4	21	40	2
3	20	TP20GS1	3.7	1.57	150	13.8	19	41	1
3	20	TP20GS2	3.4	n/a	n/a	7.6	11	25	4
3	20	TP20GS3	3.4	1.74	150	19.6	30	71	2
3	20	TP20GS4	3.6	n/a	n/a	13.8	19	41	7
3	20	TP20GS5	3.8	1.45	160	20.8	28	54	7
3	21	TP21GS1	4.1	1.71	130	10.9	18	48	6
3	21	TP21GS2	3.9	n/a	80	13.7	22	56	4
3	21	TP21GS3	4	1.37	n/a	10.9	15	29	7
3	22	TP22GS2	2.37	n/a	n/a	7.56	11	22	1
3	22	TP22GS3	2.72	n/a	n/a	13.2	18	34	7
3	22	TP22GS4	2.43	n/a	n/a	19.29	24	45	2
3	24	TP24GS2	n/a	n/a	n/a	24.1	29	53	1
3	24	TP24GS3	6.38	1.359	n/a	16.2	22	45	1
3	24	TP24GS4	5.18	n/a	n/a	18.8	25	50	2
3	24	TP24GS5	4.16	2.399	n/a	3.68	6	13	4
3	24	TP24GS6	6.19	n/a	n/a	21.9	29	56	1

Table 4.2 Summary of Test Results (continued)

bench	test pit	sample #	pH	Dry Density g/cm^3	Matric Suction kPa	grav. w.c. (%)	Volumetric Water Content	Degree of Saturation (%)	Classification
4	25	TP25GS1	5	1.446	29	18.5	27	57	4
4	25	TP25GS2	4.83	2.004	410	13.3	21	51	2
4	25	TP25GS3	5.02	n/a	n/a	16.1	22	45	4
4	25	TP25GS4	4.53	n/a	n/a	13.3	19	39	1
4	26	TP26GS1	3.76	1.64	n/a	12.1	17	37	7
4	26	TP26GS2	4.02	n/a	n/a	13.3	19	39	7
4	27	TP27GS1	2.87	n/a	10	8.5	12	28	1
4	27	TP27GS2	3.08	n/a	n/a	14.3	20	42	1
4	27	TP27GS3	3.7	n/a	n/a	5.86	9	20	6
4	27	TP27GS4	3.51	2	n/a	12.6	21	49	7
5	28	TP28GS1	4.39	1.938	n/a	6.7	10	23	6
5	28	TP28GS2	4.38	n/a	n/a	11.6	17	35	1
5	28	TP28GS3	n/a	n/a	n/a	9.8	14	31	6
5	28	TP28GS4	4.93	n/a	n/a	6.7	10	23	7
5	28	TP28GS5	n/a	n/a	n/a	8	12	26	6
5	29	TP29GS1	4.73	n/a	n/a	8.5	12	28	2
5	29	TP29GS2	4.79	1.797	20	10.4	15	32	1
5	29	TP29GS3	4.45	n/a	n/a	8.3	12	27	6

Inspection of each of the materials in the laboratory showed that there were similar rock types present across various layers with different levels of oxidation. This indicates that some materials that are distinguished based on color and pH may originate from the same geological material and only differ on a basis of oxidation. For example, Material 1 and Material 4 were identical only at slightly different states of weathering. Material 1 and Material 4 have similar color and paste pH but Material 1 contained a higher percentage of gravel to cobble sized materials of a more competent texture.

Figure 4.2 shows the grain size distribution for selected representative materials sampled at Site 1. The grain size distributions for all materials sampled are presented in Appendix A. The grain size distributions analyses show the fine texture of the materials at Site 1. Material 1 and Material 2 represented the majority of the samples obtained from the waste rock pile at Site 1. Material 1 did not have a large fraction of fine material, with less than 50% passing the 75μm size. However, Material 4, which appeared to be similar to Material 1, had a high fraction of fines with 80% passing the 75μm size. Material 4 was

likely at a high degree of weathering compared to Material 1 and represented what the material would appear once there is greater particle breakdown.

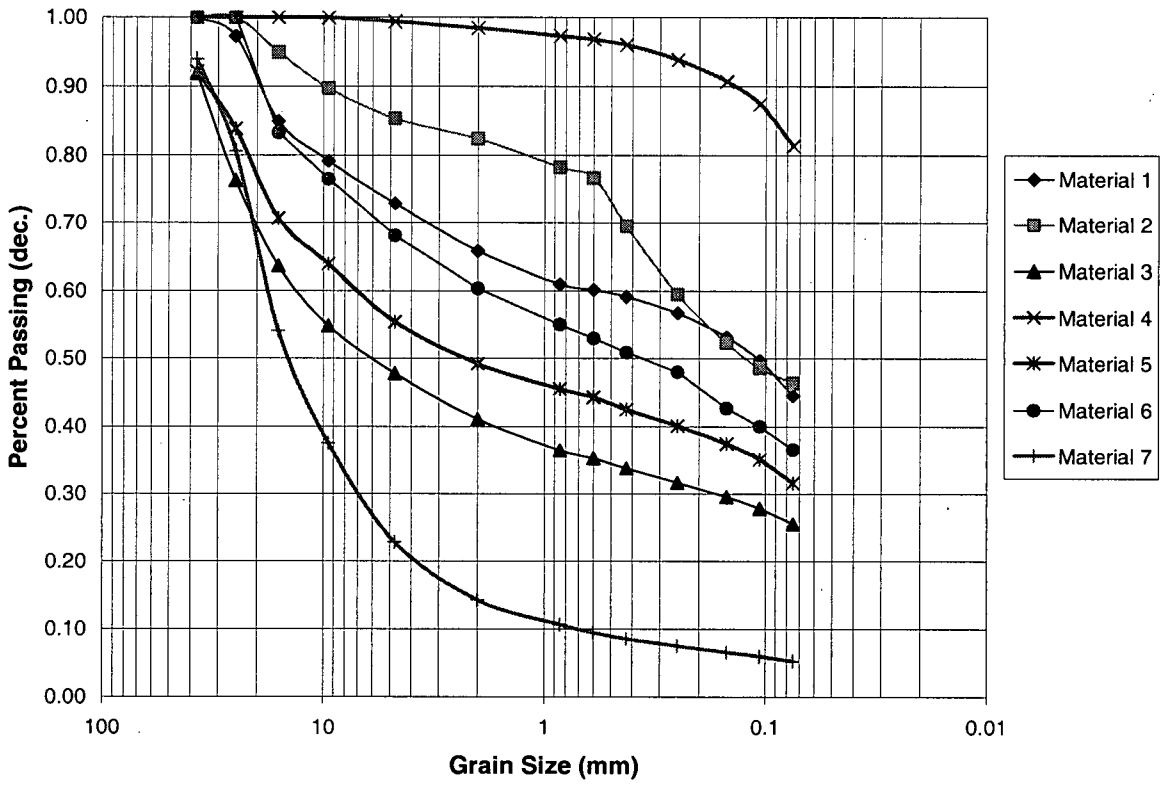

Figure 4.2 Grain Size Distribution of Representative Materials Selected from Site 1

Analysis for the test pits during excavation included measurement of width and orientation of each layer within the test pit, defining materials to be sampled. The samples were then separated into representative materials based on laboratory classification, paste pH and grain size. A qualitative estimate of the percentage of each material present within the waste rock pile was then determined based on the quantities of materials sampled during the excavation process. Table 4.3 provides a summary of the materials including visual description, water content, paste pH and in-situ density. Table 4.4 shows the percentage of

the materials present for each bench in the dump at Site 1. Material 1 was the most common in the waste rock pile and Material 1 and Material 4 accounted for over 50% of the total waste rock encountered during the field program.

Table 4.3 Summary of Materials Sampled at Site 1

Material Description		Paste pH	Water Content (%)	Density (g/cm^3)	USCS Classification
Material 1	yellow to brown with a clay silt matrix containing rock particles.	3.0	14.0	1.6	SM
Material 2	red, soil-like material with some small gravel and rock particles	5.0	22.0	1.7	SM
Material 3	pale yellow, soil-like material with a silt and clay matrix	3.0	23.0	1.5	GM
Material 4	yellow to grey soil-like clayey matrix material with few coarse particles	4.0	20.0	1.4	ML
Material 5	brown soil-like matrix with competent rock particles	5.0	15.0	1.2	SM
Material 6	yellowish brown silty sandy gravel	2.5	8.0	1.7	SM
Material 7	rock-like material with a silty to clayey matrix material	2.0	4.0	1.8	GP

Table 4.4 Percentage of Materials Present at Site 1

	Material Present by Bench (%)				
	Bench 1	Bench 2	Bench 3	Bench 4	Bench 5
Material 1	63	43	21	61	32
Material 2	31	27	12	17	17
Material 3	2	0	0	0	0
Material 4	0	14	28	5.6	0
Material 5	4	0	0	0	0
Material 6	0	10	21	13	51
Material 7	0	7	19	3.3	0

4.1.2 Hydraulic Properties for the Materials Encountered in the Test Pits at Site 1

This section presents the results of the hydraulic testing performed for selected representative samples from Site 1. Figure 4.3 shows the Soil-Water Characteristic Curves measured in the pressure plate apparatus. The Air Entry Values measured for the samples at

Site 1 ranged from 20 to 100 kPa. The samples analyzed were remolded from slurried samples and likely resulted in a lower Air Entry Value than would be expected for the intact samples. This reduction in Air Entry Value is attributed to a reduction in density for the slurried samples. Densities in the pressure plates were usually in the range of 1.3 g/cm^3 versus 1.5g/cm^3 to 2.0 g/cm^3 measured in the field. The Air Entry Values of greater than 10 kPa were indicative of the fine grained texture of the waste rock at Site 1. Yazdani, (2000) showed that the Soil-Water Characteristic Curve could be adjusted to account for the fraction of material greater than 4 mm. However, it was determined that the samples tested from Site 1 did not require this adjustment due to the lack of coarse material in most of the materials encountered in the waste rock pile.

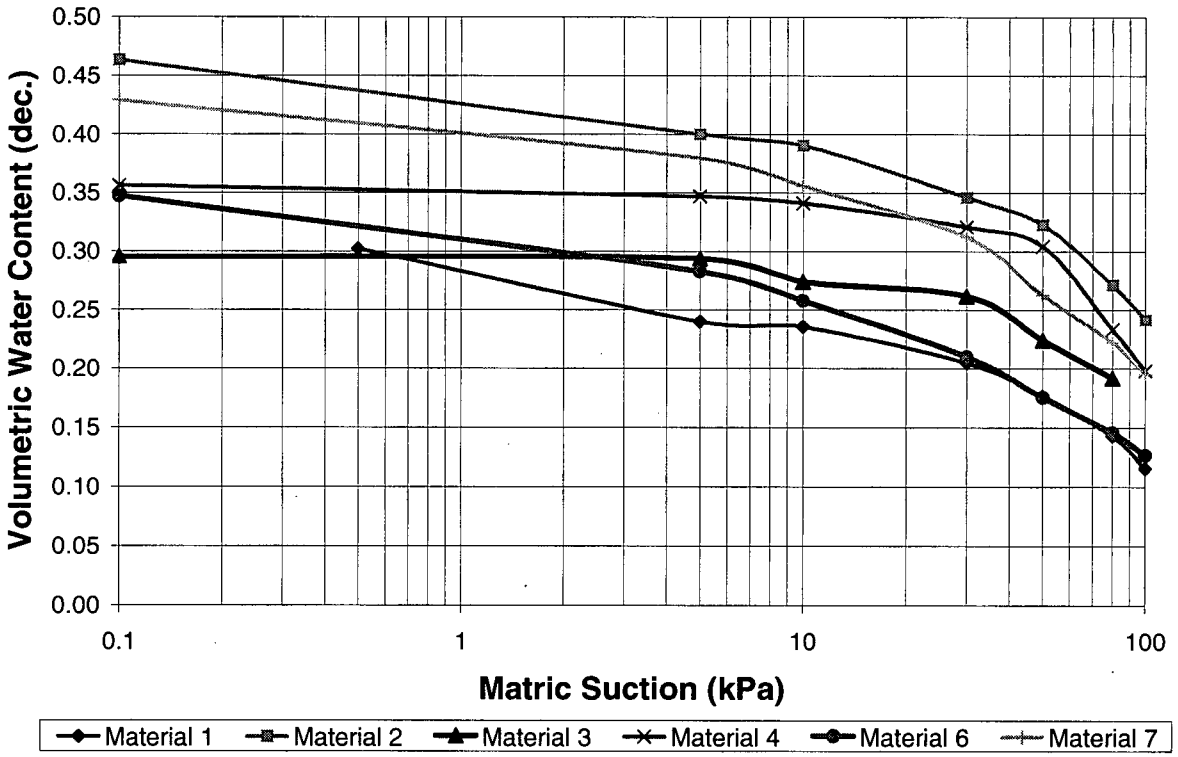

Figure 4.3 Soil-Water Characteristic Curves for Site 1 Representative Materials.

Saturated hydraulic conductivity tests were conducted for each sample selected for measurement of the Soil-Water Characteristic Curve. As was discussed in Chapter 3 this value was determined using a solid wall permeameter as well as estimated from the consolidation test data. Table 4.5 gives a summary of the hydraulic conductivity for the Site 1 samples.

Table 4.5 Measured Saturated Hydraulic Conductivity for Selected Samples at Site 1

Material	MEASURED SATURATED HYDRAULIC CONDUCTIVITY (m/s)	
	SOLID WALL PERMEAMETER	CONSOLIDATION TEST
1	$2x10^{-6}$	
2	$3x10^{-7}$	
3	$1x10^{-6}$	
4	$2x10^{-7}$	$2x10^{-9}$
6	$1x10^{-6}$	$1x10^{-8}$
7	$7x10^{-6}$	

The hydraulic conductivity determined by the consolidation test was found to be one to two orders of magnitude lower than the values measured in the solid wall permeameter. This is likely a result of the failure to achieve in-situ density in the permeameter.

The program SoilVision estimates hydraulic properties for granular materials based on grain size distribution and in-situ density and packing arrangements. SoilVision uses the mathematical equation for the grain size distribution curve (a fitted numerical equation to the laboratory determined distribution), the porosity, and packing arrangement within the soil to estimate a Soil-Water Characteristic Curve. The program was used to estimate saturated hydraulic conductivity and Soil-Water Characteristic Curves for each material. The estimated Soil-Water Characteristic Curves and the estimated values of saturated hydraulic conductivity (K_{sat}) for each material are included in the test pits logs presented in Appendix A.

4.2 Site 2

The waste rock pile at Site 2 contained many large cobble sized and gravel sized particles with very little matrix material observed throughout the profile of the dump. There

was evidence of layering within some of the test pits that were excavated however, traffic surfaces were not observed. During the excavation of the waste rock dump, gravel had to be added to the surface of the waste rock to limit tire damage to the trucks moving the waste rock. Oxidation was evident on a large fraction of the waste rock and there were indications of fine surface particles on the larger boulders. The waste rock dump was dry until the base of the dump was reached where a large frozen zone was encountered. Figure 4.4 shows the typical structure observed in the waste rock dump at Site 2.

Figure 4.4 Typical Structure Observed at Site 2

4.2.1 Physical Descriptions of Materials Observed in Test Pits

The materials sampled at Site 2 were characterized using the same methods as at Site 1. The detailed description of the materials observed in the field was also very important since only finer than 75 mm materials were sampled for laboratory testing. Table 4.6 presents the material descriptions such as color and texture of the waste rock pile at Site 2.

Table 4.6 Summary of Material Description for Waste Rock Samples Collected at Site 2

bench	test pit	sample #	Description	colour	texture	Classification
1	11	TP11GS1	rock	olive brown	gap graded 2-6" rock with silt and clay matrix	volcanic
1	11	TP11GS2	rock	olive grey	coarse angular rock with gravel	granitic
1	11	TP11GS3	rock	dark grey	angular gravel with high silt content and no plasticity	volcanic
2	12	TP12GS1	rock	dark grey to purple	angular gravel with 4" max particle size	volcanic
2	12	TP12GS2	rock	dark yellowish brown	angular gravel and rock and 5 to 10% clay sized particles	volcanic
2	12	TP12GS3	rock	olive grey	angular rock 2-6"	granitic
4	13	TP13GS1	rock	yellowish brown	hard rock with sandy silt matrix material	volcanic
4	13	TP13GS2	soil like	brown	clayey silt with small rock particles	granitic
4	13	TP13GS3	rock	olive grey	unoxidized rock, few fines	granitic
4	13	TP13GS4	rock	yellowish brown	clay silt with gravel	volcanic
4	13	TP13GS5	rock	olive grey	unoxidized rock with fine matrix material	granitic
4	13	TP13GS6	rock with soil matirx	yellowish brown	large rock and 50% sand and silt sized material	volcanic
4	14	TP14GS1	rock	yellowish brown	large rock and cobbles with silt and sand sized material	volcanic
4	14	TP14GS2	rock	olive grey	large rock, few fines edge of layer shows migration of oxidation products	granitic

Table 4.6 Summary of Material Descriptions for Waste Rock Samples Collected at Site 2(continued)

bench	test pit	sample #	Description	colour	texture	Classification
5	15	TP15GS1	soil like	brown	silty sand with gravel and cobbles	volcanic
5	15	TP15GS2	soil like	dark brown	sandy silt with gravel and cobbles	volcanic
5	15	TP15GS3	rock	yellowish brown	large cobbles and boulders	volcanic
5	15	TP15GS4	soil like	brown	sandy with small gravel and silt fraction	granitic
5	16	TP16GS1	soil like	brown	silty sand with clay and gravel	granitic
5	16	TP16GS2	rock	yellowish brown	gravel and cobble with silty clay matrix	volcanic
5	16	TP16GS3	soil like	dark brown	silty clay and tree roots	organic
5	16	TP16GS4	rock	yellowish brown	gravel and cobble with silty clay matrix	volcanic
5	17	TP17GS1	rock	yellowish brown	silt, sand, gravel, cobble angular and dry	volcanic
5	17	TP17GS2	rock	olive grey	sandy silt matrix around gravel to boulder sized particles	granitic
6	18	TP18GS1	rock with soil matirx	yellowish brown	coarse rubble with maximum 2" particle size gypsum and iron staining present	volcanic
6	18	TP18GS2	rock	brown	coarse rock with 8" max particle size and 1" traffic surface with fragmented particles present	volcanic
6	18	TP18GS3	rock with soil matirx	yellowish brown	fine grained silty sand matrix in coarse gravel to cobble sized particles	volcanic
6	18	TP18GS4	rock	grey to brown	cobble sized matrix in boulder sized material and contains both unoxidized and oxidized material	mix of granitic and volcanic material
6	18	TP18GS5a	coarse rock	yellowish brown	fine rock and sand with 2" max particle size	volcanic
6	18	TP18GS5b	fine rock	grey to brown	coarse rock (1' max particle size) with gravel matrix material	mix of granitic and volcanic material
6	18	TP18GS6	coarse rock with fine matrix material	olive grey	coarse rock with 2' max particle size and fragmented gravel and sand matrix material	granitic
6	18	TP18GS7	coarse rock	olive grey	1-4" cobble interbedded with 6"-2' boulders	granitic

Table 4.6 Summary of Material Descriptions for Waste Rock Samples Collected at Site 2 (continued)

bench	test pit	sample #	Description	colour	texture	Classification
6	19	TP19GS1	coarse rock with sandy matrix material	grey to brown	boulders (3') with gravel and sandy silt matrix material. Oxidation products present	granitic
6	19	TP19GS2	rock	yellowish brown	cobbles and boulders (4' max particle size) gravel to clay sized matrix material. Oxidation and dipping structure evident	volcanic
6	19	TP19GS3	rock	olive grey	cobble to gravel sized matrix material in boulder sized (7' max particle size)	granitic
6	20	TP20GS1	rock	reddish brown	coarse, angular sandy sitly gravel matrix in cobble and boulder sized material. 5' max particle size	volcanic
6	20	TP20GS2	rock	pink to brown	cobbles and boulders with angular gravel matrix material. Both pink granite and andesite rock present	granite and volcanic mix
6	20	TP20GS3	rock	yellowish brown	cobbles and boulders with silty sand gravel matrix, interbedding of fine and coarse material and heavy iron staining	volcanic
6	21	TP21GS1	rock	grey to brown	silty sandy gravel matrix with cobbles and boulders (6' max particle size) interbedded coarse and fine material dipping at angle of repose	volcanic
6	21	TP21GS2	rock	grey to brown	very coarse cobbles and boulders with limited fine material present	granitic
6	22	TP22GS1	rock	grey to brown	sandy silt with gravel matrix in cobbles and boulders. Granite and andesite present in an almost homogeneous mixture. Small zone of low grade ore also present	volcanic

Table 4.6 Summary of Material Descriptions for Waste Rock Samples Collected at Site 2(continued)

bench	test pit	sample #	Description	colour	texture	Classification
7	23	TP23GS1	rock	grey to brown	gravel with few cobbles and very little fines (silty sand)	granitic
7	23	TP23GS2	rock	dark brown	large cobbles and boulders with some gravel to silt sized matrix material. Some evidence of intebedding of coarse and fine material	volcanic
7	23	TP23GS3	rock	yellowish brown	gravelly silty sand with cobbles and boulders. Similar to layer 2 but with a greater fraction of fine material	volcanic
7	24	TP24GS1	rock	yellowish brown	cobbles and boulders to fine silt and sand. Material appeared damp in-situ and evidence of oxidation products	volcanic
7	24	TP24GS2	rock	pink to brown	angular cobbles to fine shards interbedded with GS1 and evidence of oxidation at interfaces between the layers	pink granite

All testing of the samples from Site 2 was conducted following shipping to the laboratory at the University of British Columbia. The paste pH for all samples was measured and samples that contained any apparent moisture were oven-dried to determine the gravimetric water content. The majority of the samples however, contained almost no apparent water and the water content could be assumed to be in the range of 3% to 7% representing the residual water content for these materials. Table 4.7 summaries the test results both in the field and in the laboratory.

Table 4.7 Summary of Test Results for Materials Sampled at Site 2.

bench	test pit	sample #	Description	WC (%)	Paste pH	Classification
1	11	TP11GS1	rock	5		volcanic
1	11	TP11GS2	rock	2	6.283	granitic
1	11	TP11GS3	rock	4	5.43	volcanic
2	12	TP12GS1	rock	0	5.832	volcanic
2	12	TP12GS2	rock	6		volcanic
2	12	TP12GS3	rock	2	6.345	granitic
4	13	TP13GS1	rock	3	2.493	volcanic
4	13	TP13GS2	soil like	3		granitic
4	13	TP13GS3	rock	n/a	6.873	granitic
4	13	TP13GS4	rock	2		volcanic
4	13	TP13GS5	rock	n/a	7.07	granitic
4	13	TP13GS6	rock with soil matirx	7	4.96	volcanic
4	14	TP14GS1	rock	28	3.174	volcanic
4	14	TP14GS2	rock	0	7.093	granitic
5	15	TP15GS1	soil like	n/a	3.428	volcanic
5	15	TP15GS2	soil like	n/a	3.648	volcanic
5	15	TP15GS3	rock	n/a	3.636	volcanic
5	15	TP15GS4	soil like	n/a	4.066	granitic
5	16	TP16GS1	soil like	n/a	4.1	granitic
5	16	TP16GS2	rock	n/a	3.818	volcanic
5	16	TP16GS3	soil like	n/a	4.415	organic
5	16	TP16GS4	rock	n/a	n/a	volcanic
5	17	TP17GS1	rock	n/a	3.202	volcanic
5	17	TP17GS2	rock	n/a	6.96	granitic

Table 4.7 Summary of Test Results for Materials Sampled at Site 2 (continued)

bench	test pit	sample #	Description	WC (%)	Paste pH	Classification
6	18	TP18GS1	rock with soil matirx	10.5	4.245	volcanic
6	18	TP18GS2	rock	1	3.925	volcanic
6	18	TP18GS3	rock with soil matirx	5.2	3.073	volcanic
6	18	TP18GS4	rock		4.939	mix of granitic and volcanic material
6	18	TP18GS5a	coarse rock		3.978	volcanic
6	18	TP18GS5b	fine rock	4.7	4.444	mix of granitic and volcanic material
6	18	TP18GS6	coarse rock with fine matrix material			granitic
6	18	TP18GS7	coarse rock	1.5	7.05	granitic
6	19	TP19GS1	coarse rock with sandy matrix material	1.4	7.1	granitic
6	19	TP19GS2	rock	2.3		volcanic
6	19	TP19GS3	rock	3.2	6.15	granitic
6	20	TP20GS1	rock	6.5	3.742	volcanic
6	20	TP20GS2	rock	8.2	4.976	granite and volcanic mix
6	20	TP20GS3	rock	19.9	3.955	volcanic
6	21	TP21GS1	rock	n/a	5.23	volcanic
6	21	TP21GS2	rock	n/a	7.1	granitic
6	22	TP22GS1	rock	0.1	3.631	volcanic
7	23	TP23GS1	rock	n/a	n/a	granitic
7	23	TP23GS2	rock	n/a	n/a	volcanic
7	23	TP23GS3	rock	n/a	n/a	volcanic
7	24	TP24GS1	rock	n/a	n/a	volcanic
7	24	TP24GS2	rock	n/a	n/a	pink granite

Figure 4.5 presents typical grain size distribution data for selected materials at Site 2. Grain size distributions were determined for about half of the samples that were collected. The lack of significant variation in the grain size distribution for the selected samples confirmed that there was little benefit in analyzing all samples. All the samples fall under the coarse gravel or boulder classification under the USCS classification system for soils. The data depicted in Figure 4.5 show only the material passing 100 mm. The fraction of the overall material within the dump passing the 100 mm particle size was reported to be approximately 10% (Devos et. al, 1997). Therefore, these grain size curves represent the matrix material within the cobble and boulder sized particles. The low silt and clay size

fraction present in the 100 mm passing material showed the low percentage of fine particles in the waste rock dump at Site 2.

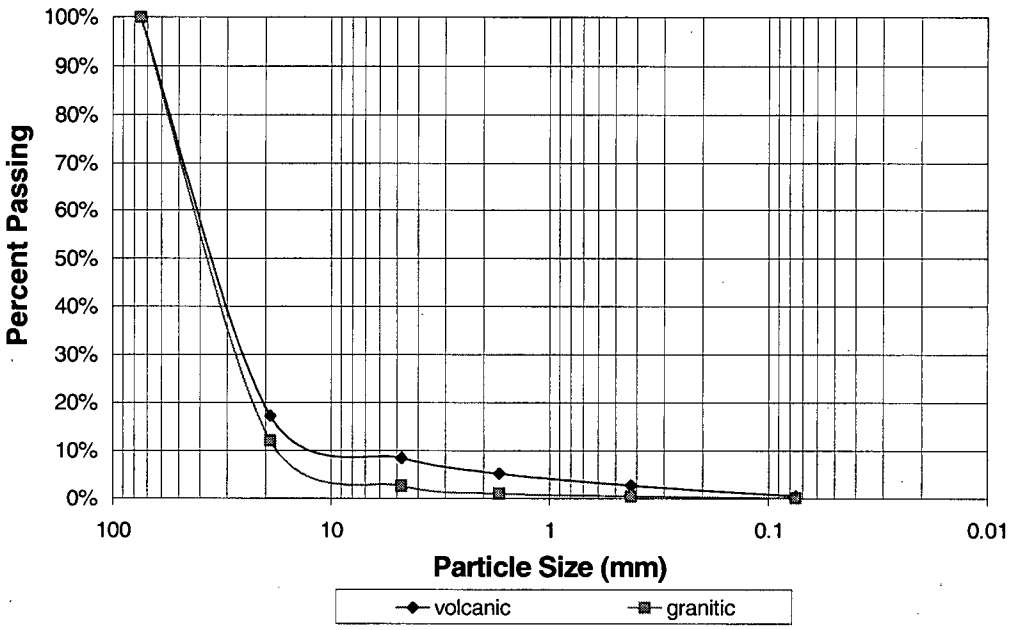

Figure 4.5 Grain Size Distribution Curves for Materials at Site 2.

4.2.2 Description of Waste Rock at Site 2

The classification and description of the waste rock at Site 2 was more difficult to establish compared to the Site 1 dump. The apparent surface oxidation gave an immediate indication of the paste pH and the surface chemistry. The deeper into the core of the waste rock dump, the more it became difficult to tell if the particles coating the surface of larger cobbles was chemical oxidation products or fine particles that were the product of physical weathering. Classification of material based on apparent surface oxidation was easily completed in the upper layers of the dump. The results of the geochemical analyses for the materials provided by Tran (2003) show that many of the materials had a high paste pH but contain a large fraction of unoxidized sulfide particles. This suggests that there were some materials that might have shown little or no visible evidence of chemical oxidation (such as

iron staining) and yet still be potentially acid forming materials. The relative percentages of material that are present in the dump at Site 2 are therefore an estimate.

4.2.3 Determination of Hydraulic Properties at Site 2

Hydraulic testing for the representative materials from Site 2 was more difficult than for the samples at Site 1. The first tests that were completed were Soil-Water Characteristic Curves. The complete testing procedure and apparatus were described in Chapter 3.

Particles larger than 4 mm without material filling the void space cannot support water under tension. This means that most of the materials within the Site 2 dump were not retaining water under matric suction and all water was being held in a film surrounding particles rather than filling void spaces. This limited the number of samples that could be evaluated using the pressure plate cell. The size of the standard pressure plate apparatus requires that the maximum particle size placed in the cell be less than 5 mm. For this test to be representative the material passing 5 mm must fill the void spaces created by larger particles for the entire sample. If the voids are not filled with finer than 5 mm material this test becomes irrelevant. The larger size pressure plate apparatus can have particle sizes up to 25 mm but care must be taken to ensure that the sample does not segregate while being placed in the cell. The sample analyzed from Site 2 was sieved through the 25 mm sieve and then placed in an unsaturated state in small lifts to limit segregation and to recreate the structure observed in the field.

The restriction on particle size meant identifying the samples collected within the dump at Site 2 that contained sufficient matrix material to fill the void spaces created by the gravel and cobble sized particles. The matrix material from Site 2 was not nearly as fine as the bulk of the material sampled at Site 1. However, to estimate the water retention capacity of this material tests were carried out. Figure 4.6 shows the Soil-Water Characteristic Curves measured for the materials from Site 2. The three curves in the graph represent three different materials sampled from Site 2. Two of the samples were tested using standard sized

pressure plate apparatus (9 cm diameter cell). The third sample was tested using a large pressure plate apparatus (15.5 cm diameter cell) containing a greater fraction of coarse material (25 mm minus) within the cell. These curves are only representative for the materials that had the large void spaces filled with finer than 5 mm material. The overall percentage of the waste rock dump that could be represented by these soil water characteristic curves is likely less than 10%.

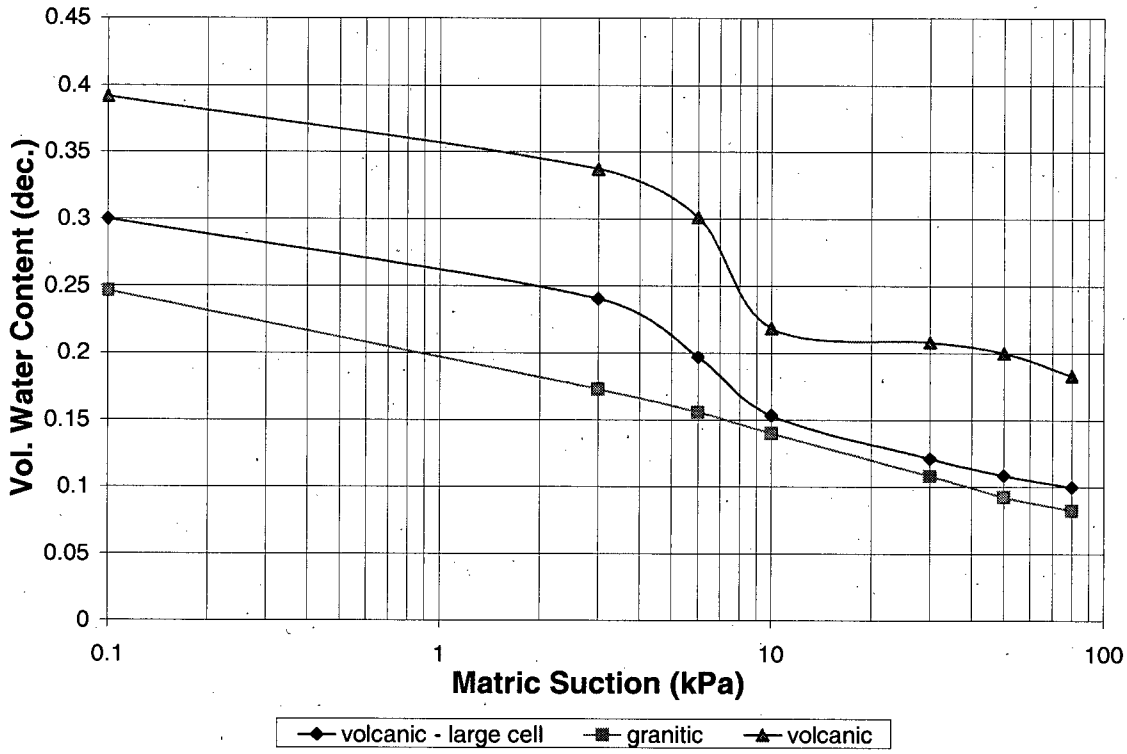

Figure 4.6 Soil-Water Characteristic Curves Measured on Materials from Site 2:

The second phase of the hydraulic property was the determination of saturated hydraulic conductivity. It was determined that the methods for measuring the saturated hydraulic conductivity described in Chapter 3 would not be useful for the coarse materials sampled at Site 2. The size of a cell required to place a representative material and to place the material at in-situ density is impractical for material sizes observed at Site 2. A sample

cell in the lab should be 6 to 10 times the D_{50} of the sample being analyzed. This means that for Site 2 a 3 m to 10 m cell should be used. Field testing of hydraulic conductivity was conducted in 2001 (Personal Communication, 2002) using a water truck with a 200 l tank. The tank could not release water fast enough to create a ponded condition on the surface of the waste rock pile. The calculations then showed that the minimum hydraulic conductivity of the material was in the order of 10^{-2}m/s and the actual value could be much higher.

CHAPTER FIVE CONCEPTUAL AND NUMERICAL MODELS

5.0 INTRODUCTION

This chapter presents conceptual models of flow and structure for Site 1 and Site 2. The results of the numerical modeling are also presented in this chapter.

5.1 Site 1 Conceptual Model

The structure and materials that were observed at Site 1 and used to develop the conceptual model of the waste rock dump at Site 1 are described in the following sections.

5.1.1 Structure and General Observations

Based on detailed observations of in-situ material properties and structure as well as visual classification of the materials in the laboratory, seven representative materials were selected from within the Site 1 waste rock pile. These materials were grouped based on similarities in grain size distribution, paste pH, density and color. The materials were generally fine grained in texture and compacted to a dense structure in-situ. The classification of each material sampled at Site 1 was given in Chapter 4. Material 1 and material 2 were found to be the most abundant materials encountered within the dump.

There was a marked contrast between the materials within the waste rock dump at Site 1 and what would be found in the majority of waste rock piles at other mine sites. The median particle size for materials present in the dump at Site 1 was coarse gravel, with an abundance of fine sand to silt size particles. The fine particle size leads to a relatively low

average hydraulic conductivity (1 x 10^{-7} m/s). In general, the low infiltration rate, high porosity, and low hydraulic conductivity of the materials within the dump result in low seepage rates at the base of the dump. According to mine personnel, no poor quality seepage had been observed in the groundwater. Impact to surface water was reported only in a creek downstream of the dump after high rainfall events.

The variation in texture between the layers can be expected to affect the flow of the liquid water phase throughout the waste rock dump as described by Herasymuik (1996). Layers that maintain a higher degree of saturation tend to have a greater saturated hydraulic conductivity than unsaturated materials. The hydraulic conductivity could differ by orders of magnitude over a short distance (less than 1 meter) and the variation in hydraulic conductivity may lead to concentration of flow in the more saturated layers. The impact of this structure and hydraulic conductivity will be further examined in Section 5.2.

5.1.2 Development of Model for Site 1

Previous analyses of waste rock piles have led to the development of a conceptual model of flow within waste rock piles. Herasymuik (1996) conducted an in depth field evaluation of a waste rock dump at Golden Sunlight Mine on the basis of the field and laboratory investigation developed a conceptual model for flow. Wilson, et. al. (2000) completed a detailed numerical analysis of the site based on this conceptual model. As discussed in Chapter 2, this conceptual model has shown that the interbedded coarse and fine layers lead to a preferential flow system where most of the flow occurs within the fine, more saturated layers and the coarse layers are dry and desaturated. Laboratory and numerical analysis by Newman, (1997) and Wilson et. al., (2000) have further refined this conceptual model. However, this work was all based on data from one site and had not been applied at other sites.

The field investigations at Site 1 showed a system that appeared to be similar to the waste rock dump investigated by Herasymuik (1996). Dipping, alternating fine and coarse layers appeared similar to observed structure at Golden Sunlight Mine. It was therefore

reasonable to assume that a similar conceptual model would be applicable for the Site 1 waste rock dump. The conceptual model proposed by Herasymuik (1996) was combined with the field and laboratory results for Site 1 to construct a numerical model to develop a seepage model for Site 1.

5.2 Site 1 Numerical Model

One of the objectives of the present study was to perform seepage modeling for idealized sections of waste rock to determine flow pathways through the waste rock profile. The results of these simulations could be used to estimate seepage rates based on the annual infiltration rate into the dump. The purpose of the analysis was to show, on a comparative basis, what the potential seepage rates would be given a range of infiltration rates and assumed structure for waste rock profiles. Geochemical analysis of the samples has shown a mutual relationship between median particle size and storage and flushing of oxidation products. (Tran, et. al., 2003, INAP, 2004). The seepage modeling presented herein is intended to help illustrate the seepage mechanism that could result in the storage and flushing of oxidation products.

The waste rock cross sections developed for the SEEP/W analyses were based on the observed angle of repose and relative cross sectional area of each material sampled in a given bench. Three representative sections were developed.

The numerical analysis of the waste rock pile involved two main assumptions. First, the simulations are for steady state conditions. The system is not truly at steady state due to the fact that the dumps are reacting to continuously variable climatic events. The quasi-steady state system could be reasonably modeled under a steady state analysis condition. Second, is was assumed is that the soil properties are constant within material types throughout the entire profile of the waste rock dump. This is also not strictly correct since the materials were defined at a relatively small scale. However, the nature of the field work meant that only a small fraction of the total volume of waste rock was actually sampled and tested. The samples were assumed to be representative of the materials within each bench.

Furthermore, the use of measured properties over the length of the bench should provide an indication of the general material behavior in each bench.

The Soil-Water Characteristic Curve (SWCC) for selected materials was measured in the laboratory (Figure 4.3). Furthermore, the SWCC was also predicted using the program SoilVision (SoilVision, 2001). The predicted and measured SWCC were used to develop representative soil property functions that were used in the numerical modeling. SoilVision was also used to generate unsaturated hydraulic conductivity functions to allow for a fully saturated-unsaturated seepage analysis to be conducted. A summary of soil properties for Site 1 is included in Table 5.1. Figure 5.1 and 5.2 shows the Soil-Water Characteristic Curves and hydraulic conductivity functions used for the representative materials modeled in each waste rock profile.

Table 5.1 Site 1 Material Properties

Material	Physical Description	USCS	% Passing 4.75 mm	D_{50} (mm)
1	Sandy silt containing some rock particles, yellow and brown staining.	SM	85	0.1
2	Sandy silt with some small gravel, red.	SM	72	0.15
3	Gravelly silt, pale yellow with some sand.	GM	45	6
4	Silt, low plasticity, yellow to gray in color.	ML	98	less than 0.075
5	Sandy silt, with hard gravel particles, brown	SM	55	2
6	Silty sand, with some gravel, yellowish brown.	SM	68	0.4
7	Poorly graded gravel, with some sand and silt.	GP	22	9.5

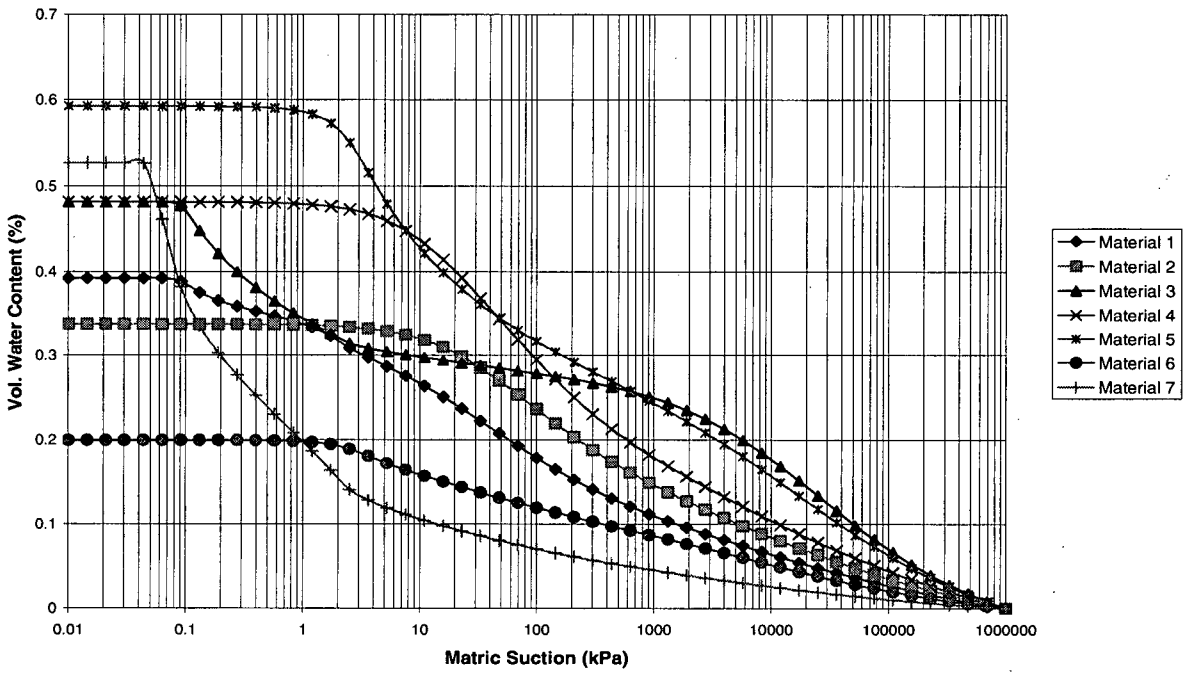

Figure 5.1 Soil-Water Characteristic Curves used in Seepage Model at Site 1

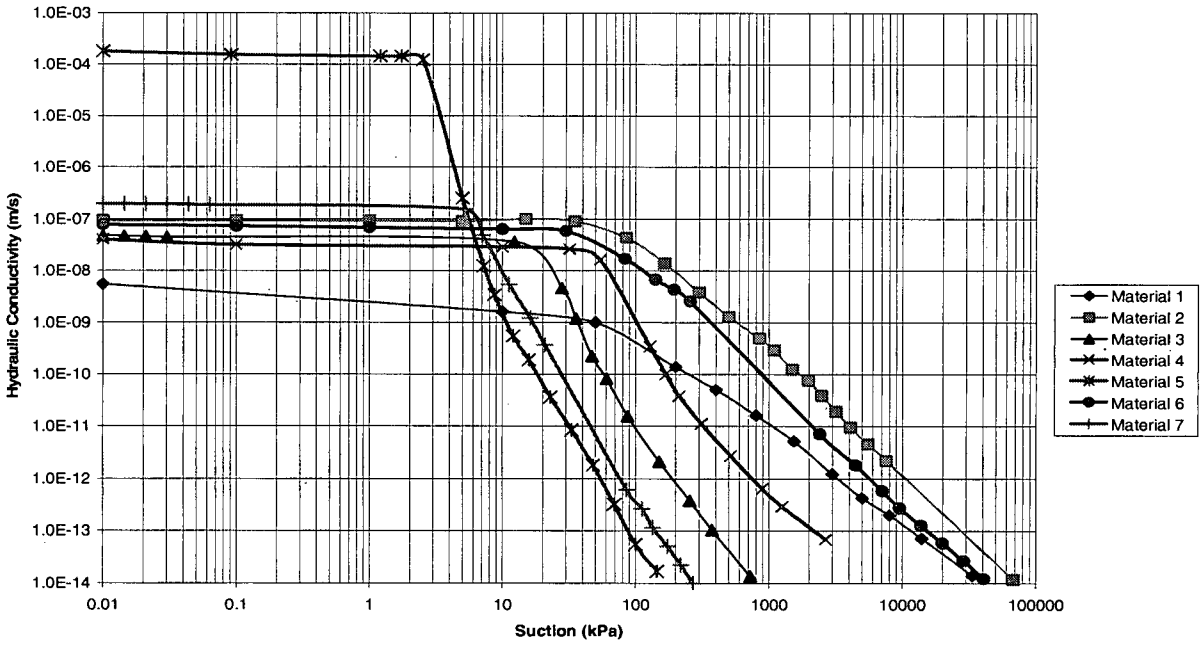

Figure 5.2 Unsaturated Hydraulic Conductivity Functions used in Seepage Model at Site 1

5.2.1 Representative Cross Section 1.

Figure 5.3 shows a test pit containing the structure that was modeled for the first representative section. The section was based on the top lift of the waste rock dump at Site 1.

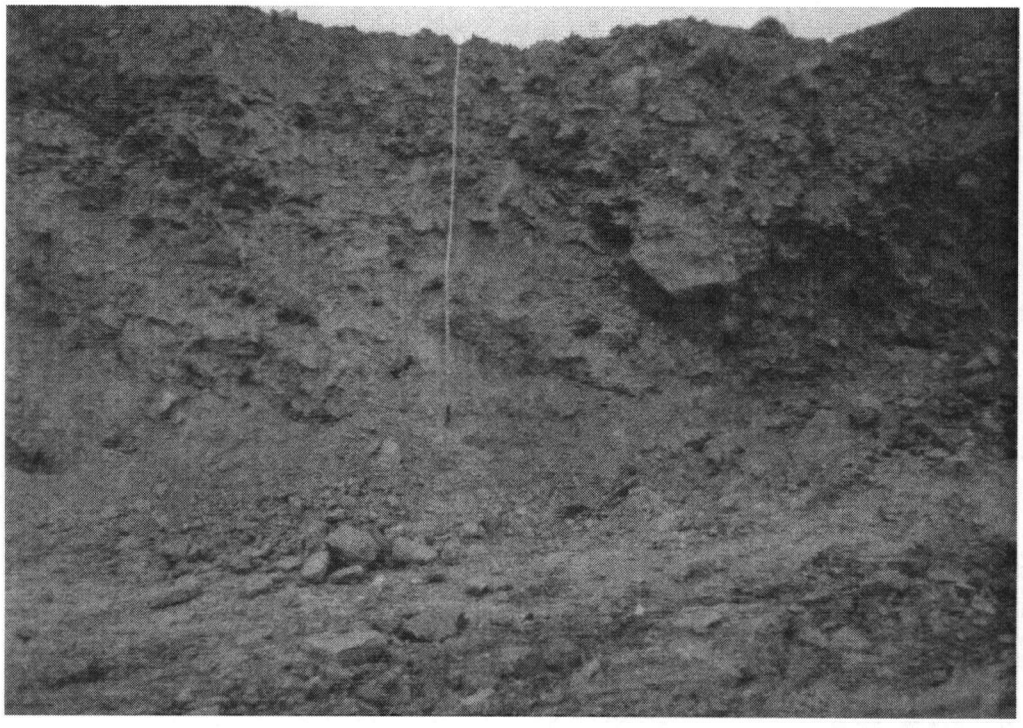

Figure 5.3 Test Pit 13 Representing SEEP/W Section1 for Waste Rock Bench 1

Based on physical observations, layer thickness was less than 1.0 m throughout the upper profile of the waste rock pile. Table 5.2 shows the materials sampled in the upper bench of waste rock at Site 1 and their relative cross sectional areas as well as the relevant hydraulic properties used in the seepage model. The overall percentage of each material sampled in the field was used to construct a seepage section representative to field conditions.

Table 5.2 Material Properties of Materials in Representative Section 1

MATERIAL	RELATIVE CROSS SECTIONAL AREA OF BENCH	% PASSING 4.75 mm	AIR ENTRY VALUE (kPa)	SATURATED HYDRAULIC CONDUCTIVITY (m/s)
Material 1	63	85	50	8×10^{-9}
Material 2	31	72	35	9.5×10^{-8}
Material 3	2	45	15	5.0×10^{-8}
Material 5	4	55	2.5	2.0×10^{-4}

Figure 5.4 shows the SEEP/W section constructed to represent the observed cross section in the upper profile of the waste rock dump at Site 1.

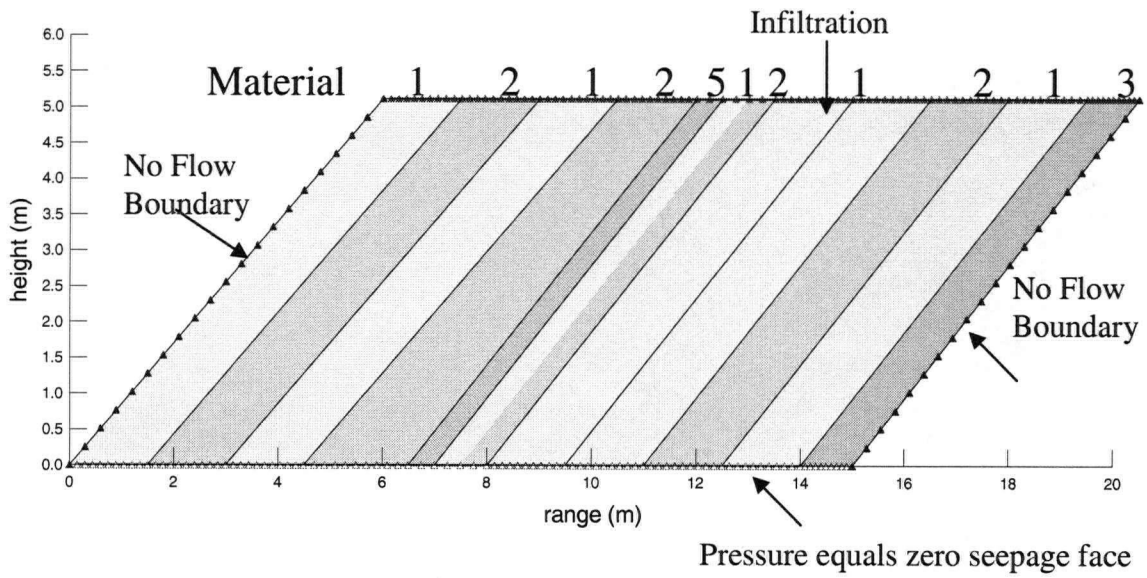

Figure 5.4 Representative Section 1 for SEEP/W Analyses

The seepage model showed little sensitivity to the sequence of materials within the cross section. However, layer thickness greater than 2.0 m was found to have a significant influence on the development of preferential flow in the cross section. When layers thicker than 5.0 m were used there was little horizontal migration of flow to adjacent layers. When the layer thickness was reduced to less than 2.0 m there was a significant change in the flow

paths within the cross section. As field observations showed, layer thickness was typically in the range of 1.0 m so the layer thickness in the cross section was limited in order not to unduly influence the predicted seepage paths with model construction.

The boundary conditions for the model are an infiltration boundary on the top, no flow boundaries on the side slopes and a pressure equals zero seepage review boundary was specified for the base of the section to allow emergent seepage.

The cross section shown in Figure 5.4 was analyzed under five different infiltration rates. The average infiltration rate at Site 1 was estimated to be approximately 50 mm/year. However, increased seepage rates were evaluated to determine the impact of high rainfall events that are sometimes experienced in the region. Flux rates of 50 mm/y, 100 mm/year, 200 mm/y, 500 mm/y, and 1000 mm/year were simulated. Table 5.3 presents a summary of the resulting flow rates discharging at the base of each material. The number in parentheses is the percentage of total flow from the section that was predicted in each material.

Table 5.3 Summary of Results of Seepage Analysis for SEEP/W Section 1

FLUX RATE (m/y)	FLOW FROM BASE OF THE SECTION (m^3/y/m) (PERCENTAGE TOTAL FLOW THROUGH SECTION)			
	MATERIAL 1	MATERIAL 2	MATERIAL 3	MATERIAL 5
0.05	0.13 (17)	0.43 (60)	0.11 (15)	0.05 (11)
0.1	0.13 (9)	0.93 (65)	0.23 (16)	0.14 (10)
0.2	0.14 (5)	1.84 (66)	0.47 (16)	0.37 (13)
0.5	0.83 (12)	3.78 (55)	0.94 (13)	1.35 (20)
1	1.64 (12)	7.11 (52)	1.59 (12)	3.38 (25)

Figure 5.5 shows the resulting seepage vectors generated under an applied flux rate of 100 mm/year. The concentration of flow in specific materials is evident.

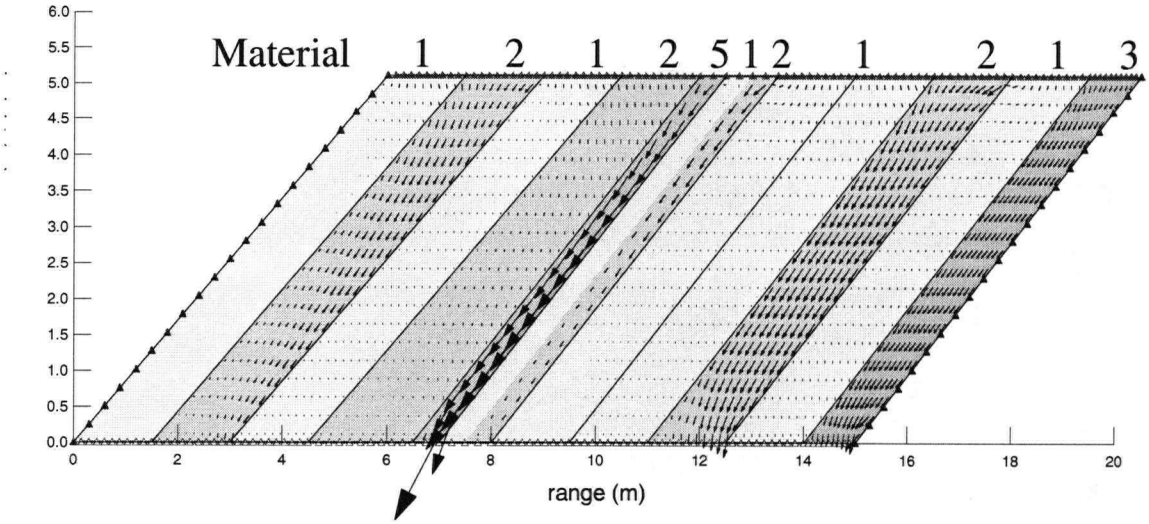

Figure 5.5 Seepage Vectors Under 100 mm/yr Flux Rate for SEEP/W Section 1

It can be seen that there is a concentration of flow through Material 5, which in Bench 1, had the highest hydraulic conductivity. However, based on the total cross sectional area of each material, Material 2 actually represents the greatest volume of water leaving the section. The air entry value for Material 2 is sufficiently high to maintain a high degree of saturation and thus becomes a preferential flow pathway. It is important to recognize that the cross section shown in Figure 5.5 is an idealization of the actual structure and material properties that are present in the waste rock profile. The cross sections however, do illustrate the mechanism of flow for the unsaturated waste rock profile. Material 5 could represent a rubble zone forming due to construction or a more competent material that has weathered less than adjacent materials. Material 5 could also have been represented as a material that did not extend the full thickness of the layer but was twice the thickness and half the height. This type of configuration would better represent a rubble zone forming near the base of a lift but could unduly influence the seepage analysis results by not allowing direct infiltration into the material. Figure 5.6 shows a plot of the total volume of flow for Section 1 (assuming a unit thickness of 1.0 m) for each material under a given applied surface flux rate.

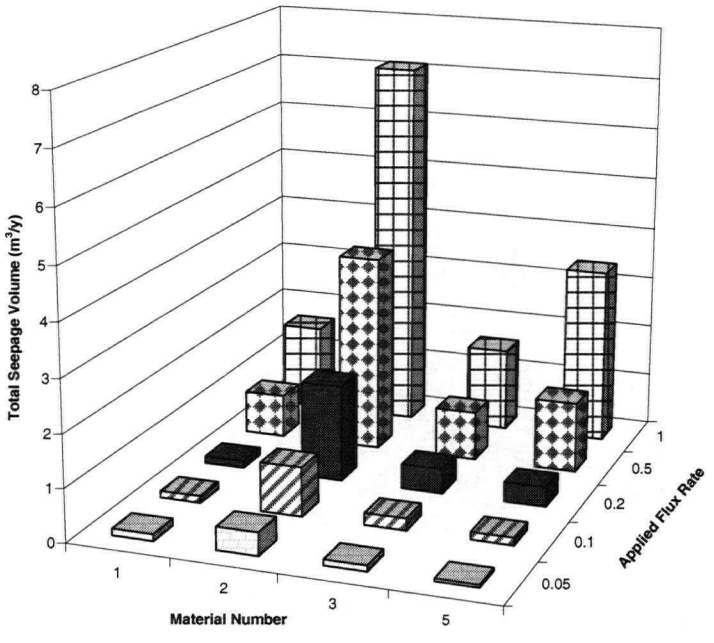

Figure 5.6 Total Seepage Volume Summary for Section 1

Figure 5.7 shows a normalized plot of flux out of Section 1. This section looks at flux or flow rate rather than flow volume. It can be seen that Material 3 has the highest flux velocity until the highest applied flux rate is applied to the section. Material 5, which is the coarsest material, carries a higher flux volume at the highest seepage rate. At lower applied flux rates the material remains at a lower degree of saturation and carries less flow.

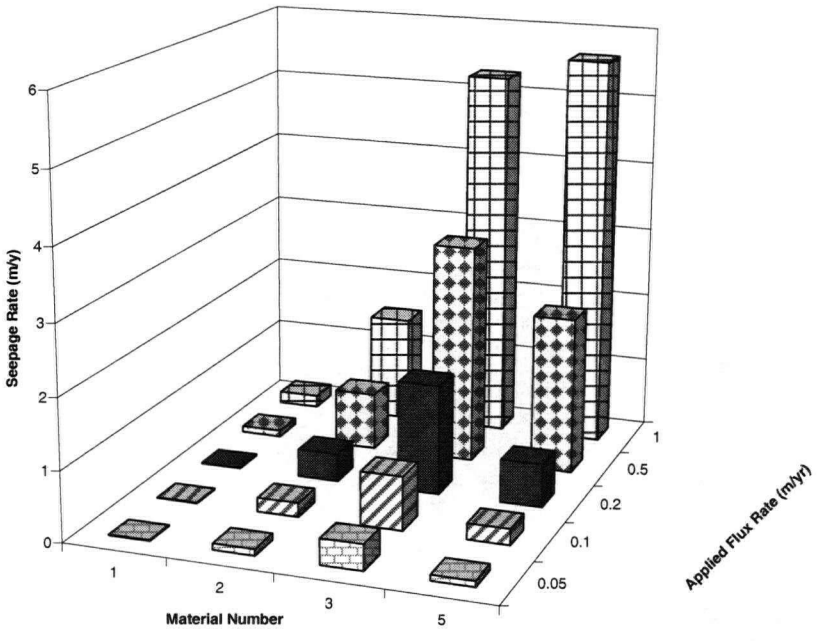

Figure 5.7 Seepage Rate Summary for Section 1

The results of the seepage analyses are summarized in Table 5.3 and illustrated in Figures 5.6 and 5.7 show expected trends in preferential flow. Material 1 is the finest material in the cross section, with the lowest hydraulic conductivity of the materials modeled, and thus, transports the smallest volume of water at the lowest flux rate regardless of applied flux to the section. Material 5 is the coarsest material and does not begin to transport large volumes of water until the applied surface flux rate increases significantly. The flow in Material 5 is expected as percentage of flow that passes through the coarse layers increases as the infiltration rate exceeds the hydraulic conductivity of the fine grained materials. Materials 2 and 3 represent materials with enough silt and sand sized particles to maintain saturation under tension but still have sufficiently high hydraulic conductivity to transport the bulk of the flow within the section. Material 1 represents 63% of the cross sectional area of the section but carries less than 15% of the total flow.

When examining the materials based on D_{50} and percent passing 4.75 mm. It can be clearly seen that Material 1, which has a D_{50} of 0.1 mm and is 85% passing 4.75 mm should be expected to have a low flux rate and total volume of flow transported. Material 5, which has a D_{50} of 2 mm and is 55 percent passing 4.75 mm should have a much higher flux rate. The total volume of flow through Material 5 is only limited by the fact that it accounts for only 4% of the total material present in Section 1.

5.2.2 Representative Cross Section 2

The second seepage cross section was developed to represent the second and third benches that were removed from the waste rock pile. Five different materials were used to represent the waste rock profile as shown in Figure 5.8. Table 5.4 summarizes the material properties used for each layer.

Figure 5.8 Test Pit 21 Representing the 2nd and 3rd Benches at Site 1

The relative abundance of materials in Benches 2 and 3 is summarized in Table 5.4. The table also presents the material properties used in the numerical model. Based on the relative abundance of materials the representative cross section was constructed and is shown in Figure 5.9

Table 5.4 Material Properties Selected for SEEP/W Analysis of Section 2

MATERIAL	RELATIVE CROSS SECTIONAL AREA OF BENCH	% PASSING 4.75 mm	AIR ENTRY VALUE (kPa)	SATURATED HYDRAULIC CONDUCTIVITY (m/s)
Material 1	21	85	50	8.0×10^{-9}
Material 2	12	72	35	9.5×10^{-8}
Material 4	28	98	40	5.0×10^{-8}
Material 6	21	68	30	9.0×10^{-8}
Material 7	19	22	5	2.0×10^{-7}

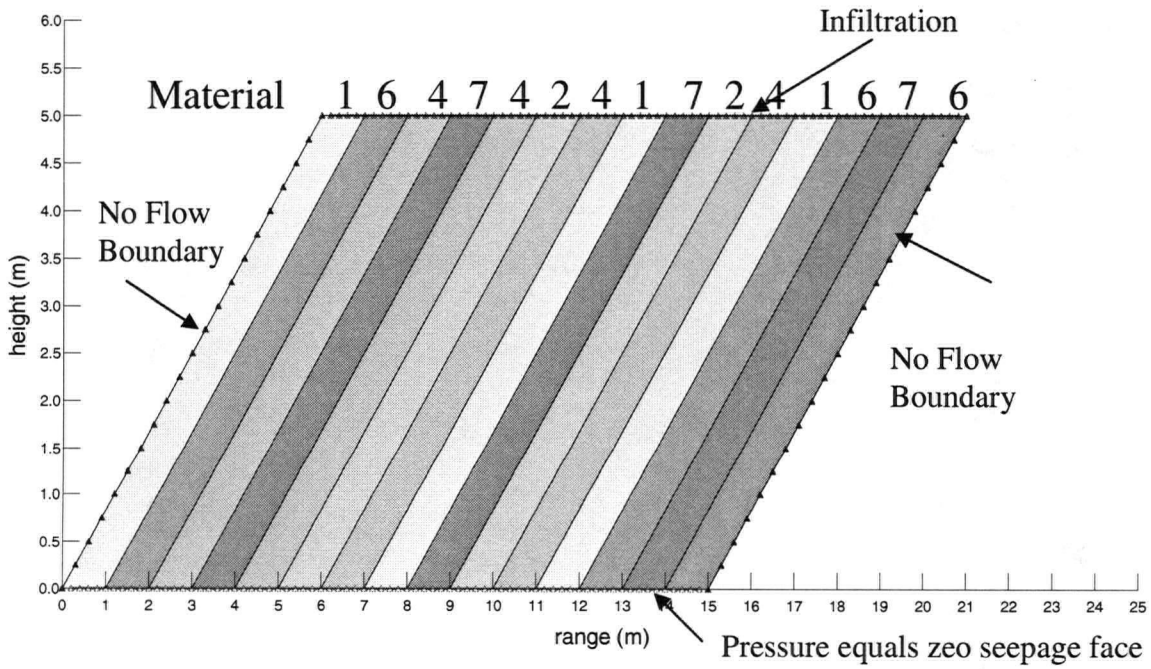

Figure 5.9 SEEP/W Section 2 to Represent the 2nd and 3rd Benches at Site 1

The same set of infiltration rates and boundary conditions were applied to SEEP/W Section 2 as was applied to SEEP/W Section 1. Figure 5.10 shows the resulting seepage vectors that were developed under an applied flux rate of 100 mm/year. Table 5.5 presents a summary of the flux rates leaving the base of the section through each of the materials.

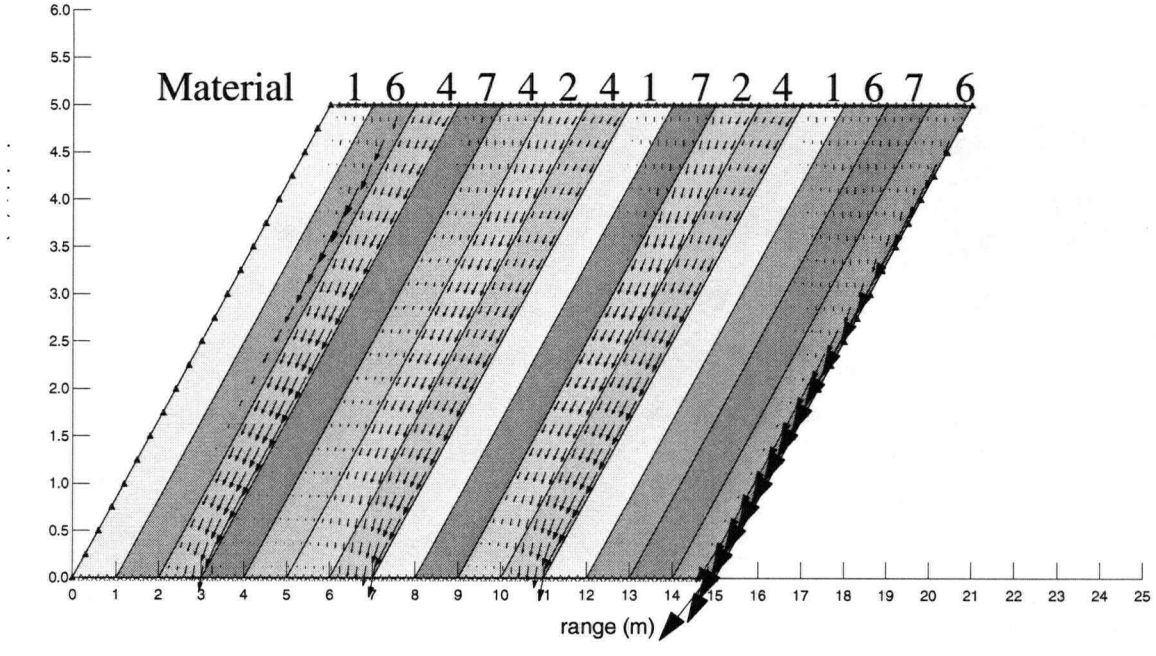

Figure 5.10 Seepage Vectors from Base of Seepage Section under Flux Rate of 100 mm/y

Table 5.5 Seepage Flux Rates from the Second Representative Section

FLUX RATE (m/y)	FLOW FROM BASE OF THE SECTION (m^3/y/m) (PERCENTAGE OF TOTAL FLOW THROUGH SECTION)				
	MATERIAL 1	MATERIAL 2	MATERIAL 4	MATERIAL 6	MATERIAL 7
0.05	2.62E-04 (0)	2.05E-01 (29)	2.32E-01 (33)	1.57E-01 (22)	1.18E-01 (17)
0.1	3.47E-03 (0)	3.72E-01 (26)	5.17E-01 (36)	3.85E-01 (27)	1.70E-01 (12)
0.2	4.73E-03 (0)	6.02E-01 (21)	1.30 (45)	7.13E-01 (25)	2.82E-01 (10)
0.5	0.46 (6)	1.08 (15)	3.07 (43)	1.37 (19)	1.18 (16)
1.0	1.04 (7)	3.01 (21)	4.89 (34)	2.90 (20)	2.57 (18)

Figure 5.11 shows the total volume of flow per unit thickness in Section 2 for each material and applied flux rates. Figure 5.12 shows a summary of the flux velocities out of the section.

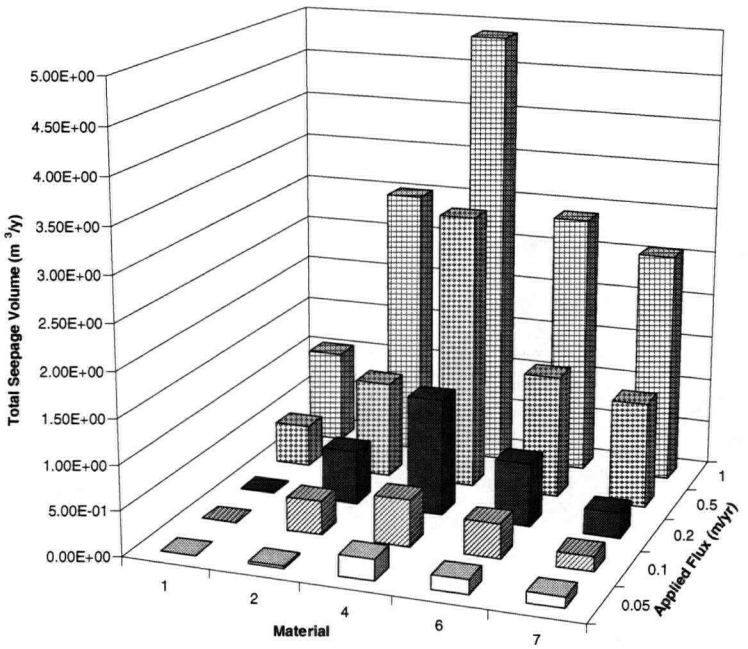

Figure 5.11 Flux Summary for SEEP/W Section 2 at Site 1

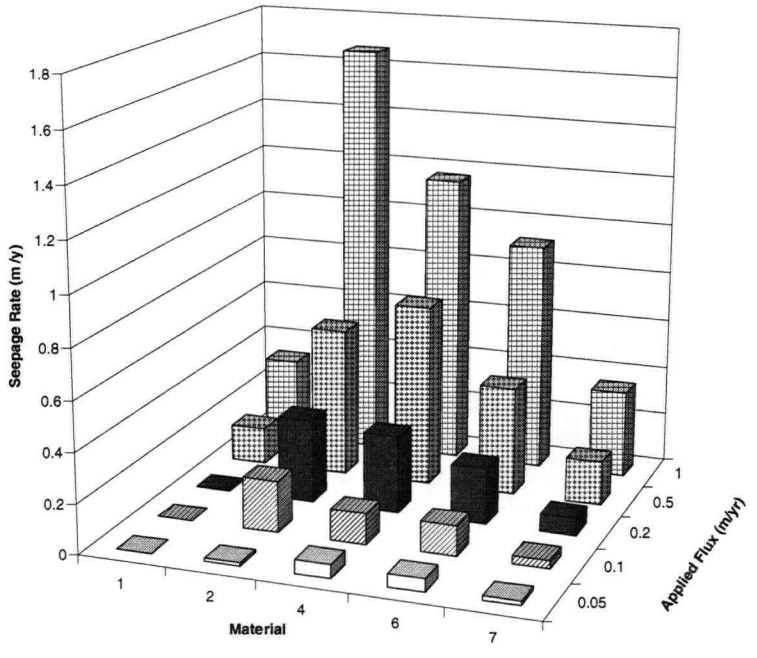

Figure 5.12 Seepage Rate Summary for SEEP/W Section 2 at Site 1

The plots above show that Material 3 carries the highest total volume of flow through the section, however it is also the most abundant material in the section. Material 2, which has a D_{50} of 0.15 mm and an AEV of 35 kPa develops the highest seepage rates under almost all of the applied flux rates. Material 7, which as a low AEV never develop significant, flow due to the presence of preferential layers adjacent to it. Material 6 and Material 4 become preferential pathways and Figure 5.10 shows the flux leaving Material 7 and flowing into the adjacent layers. This is the reason there is little flux developed in this material.

5.2.3 Representative Cross Section 3

The third representative SEEP/W section represents the relative cross sectional areas that were observed and sampled in the 4th bench and near the base of the dump. Figure 5.13 shows Test Pit 26 illustrating the structure that was observed at the base of the dump. Table

5.6 describes the percentage of each material that was present, and summarizes the hydraulic properties for each material.

Figure 5.13 Test Pit 26 Selected to Represent SEEP/W Section 3.

Table 5.6 Summary of Materials Present in Representative Section 3

MATERIAL	RELATIVE CROSS SECTIONAL AREA OF BENCH	PERCENT PASSING 4.75 mm	AIR ENTRY VALUE (kPa)	SATURATED HYDRAULIC CONDUCTIVITY (m/s)
Material 1	19	85	50	8.0×10^{-9}
Material 2	17	72	35	9.5×10^{-8}
Material 6	51	68	30	9.0×10^{-8}
Material 7	13	22	5	2.0×10^{-7}

SEEP/W Section 3 is considered to be most representative of the deeper profile of the waste rock dump. Materials 6 and 7 were observed to be the two most dominant materials present. The extent of weathering and the apparent high degree of consolidation due to self-weight loading produced a region of the dump that contained materials with homogeneous

properties. The materials at the base of the dump also largely control the rate at which water interacts with the surrounding geology.

Figure 5.14 shows SEEP/W Section 3 developed for the analyses. Note that the horizontal scale is different than for Sections 1 and 2. The angle of repose is the same as was used for the previous sections. Figure 5.15 shows the resulting flow vectors under an applied flux of 100 mm/year. Similar behavior was observed for Section 3 as was observed for Sections 1 and 2. The total amount of flow computed to discharge from each material was found to increase with the applied flux rate.

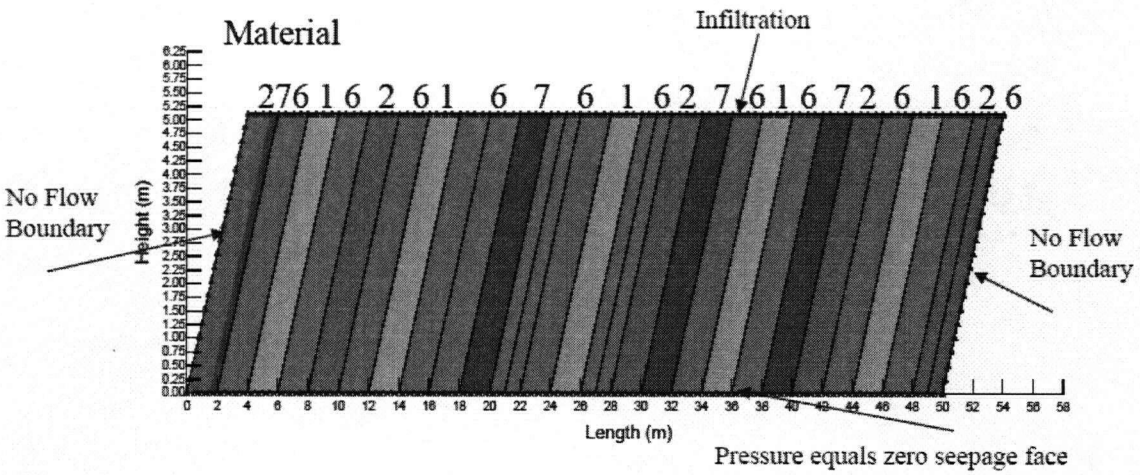

Figure 5.14 Representative SEEP/W Section for Section 3

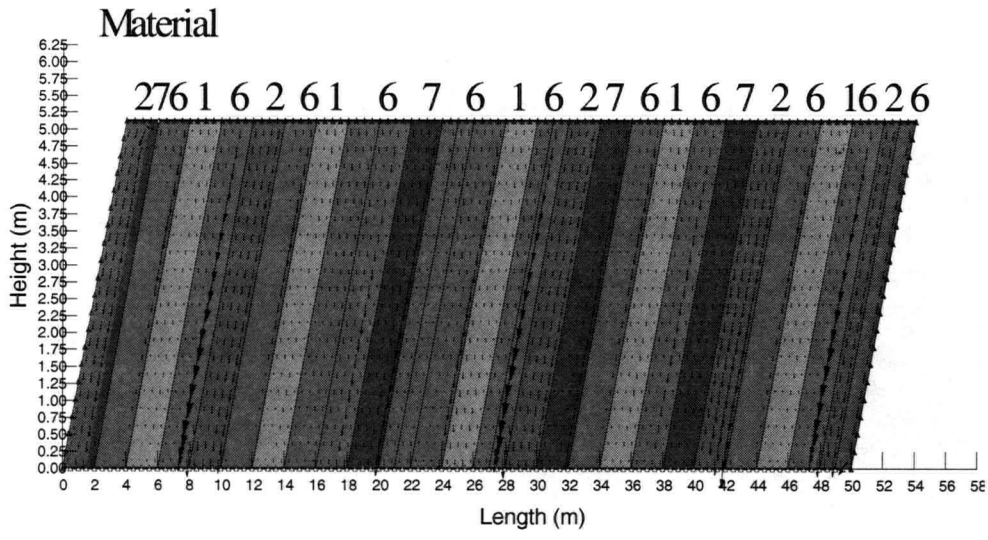

Figure 5.15 Seepage Vectors Developed under 100 mm/year Applied Flux Rate.

The total flow from each material in SEEP/W Section 3 for each of the applied surface flux rates has been summarized in Table 5.7 and the three-dimensional plot shown in Figure 5.16 similar to Section 1 and Section 2 described previously. The actual seepage rate from each material has been summarized in Figure 5.17.

Table 5.7 Summary of Total Seepage from Representative Section 3

FLUX RATE (M/YEAR)	FLOW FROM BASE OF THE SECTION (m^3/y/m) (PERCENTAGE OF FLOW)			
	MATERIAL 1	MATERIAL 2	MATERIAL 6	MATERIAL 7
0.05	0.29 (13)	0.59 (26)	1.09 (48)	0.31 (14)
0.10	0.53 (12)	1.20 (26)	2.23 (49)	0.57 (13)
0.20	1.24 (14)	2.34 (26)	4.35 (48)	1.04 (12)
0.50	2.24 (10)	5.92 (25)	12.26 (52)	3.03 (13)
1.00	2.22 (5)	9.03 (20)	27.84 (62)	6.07 (13)

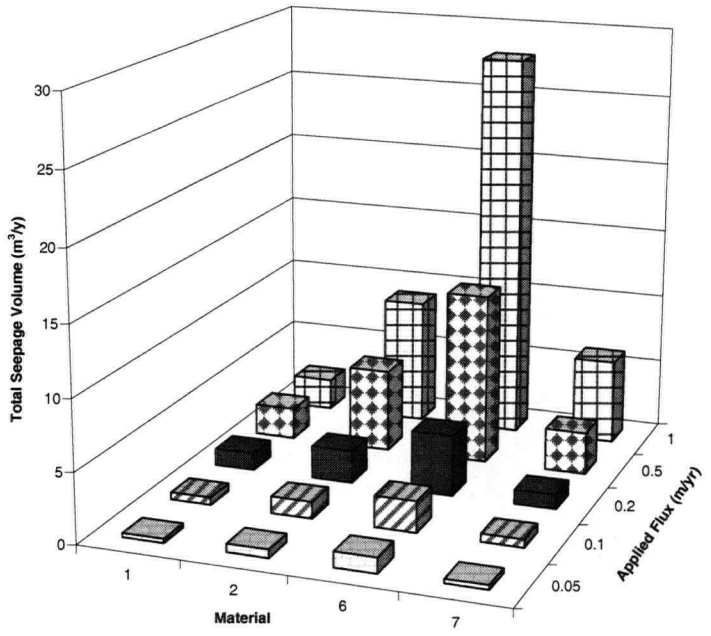

Figure 5.16 Total Seepage Volume Summary Plot for SEEP/W Section 3

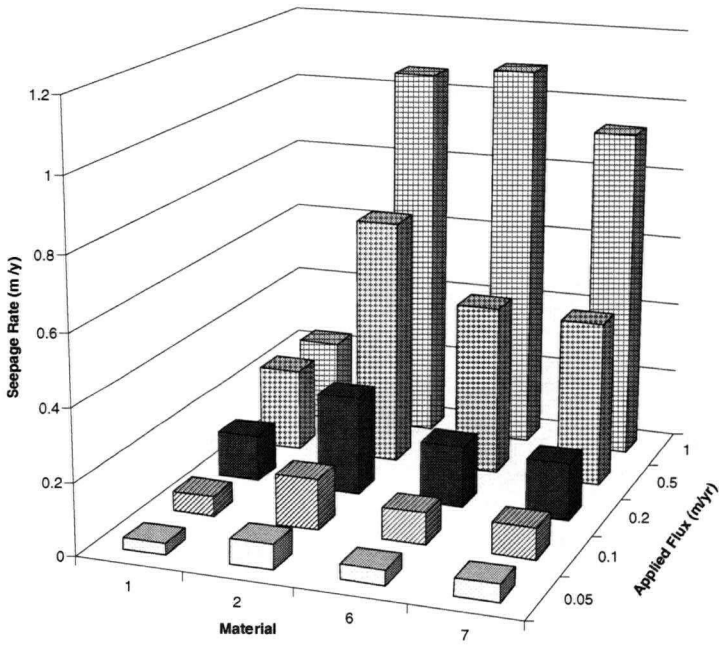

Figure 5.17 Seepage Rate Summary Plot for SEEP/W Section 3

Figure 5.17 shows that there is little difference between Material 2, 6 and 7 in the section analyzed. Material 6 produces the largest volume of seepage (Figure 5.16) but this is due to the fact that 51 percent of the layer is composed of Material 6. Material 1 which has the smallest D_{50}, and greatest amount of material passing 4.75 mm has the lowest flux rate and will be the least leached material. The remainder of the materials have very similar characteristics. At the base of the waste dump the materials were extremely dense and very similar in particle size and structure. It appears reasonable that there is very little difference in predicted seepage rate for this section.

5.2.4 Discussion

The analysis completed in the preceding sections shows that there will be development of preferential flow throughout the waste dump. This preferential flow will affect everything from outflow seepage quality to weathering of in-situ materials. Geochemical testing conducted by Tran (INAP, 2004) show that most of the samples at Site 1 are at a relatively advanced state of weathering due to the lack of water soluble ions present on the surfaces of particles sampled.

Table 5.8 Summary of Geochemical Results (INAP, 2004)

MATERIAL	WATER SOLUBLE SULFATE (mg/kg)	NON-WATER SOLUBLE SULFATE (mg/kg)	PERCENT WATER SOLUBLE IONS
1	2378	7500	32
2	1208	6350	19
3	125	10300	1
4	1079	1900	57
6	387	1500	26
7	859	17350	5

Contaminant loadings associated with ARD can be estimated based on the flux rates determined by the seepage model for Sections 1, 2 and 3. The actual outflow geochemistry is

complex but this type of analysis could be used to establish which materials may be most likely to contribute to poor quality leachate. Geochemical analyses conducted by Tran (INAP, 2004) determined the metals present on the samples when they were collected. Leaching tests were also conducted to determine the water soluble fraction of metals present in the samples.

Extraction testing on the samples indicates that Material 3 and Material 7 had the lowest available percentage of water soluble metals. This indicates that the materials are heavily leached, leaving only non-water soluble metals on the surfaces of the particles. The testing also shows that Material 1 and Material 4 contained the highest fraction of water soluble metals.

Based on the analyses for Section 2, Material 4 has the highest seepage rate and total flux volume and therefore can be expected to contribute the greatest mass of sulfate and other metals because it also appears to contain a large fraction of water soluble metals. In addition, Material 2, for Section 1, has the highest seepage outflow rate and also contains a high fraction of water soluble metals. Material 3, in Section 1, will transport the greatest volume of flow but contains a much lower percentage of water soluble metals. The analysis for Section 3 shows that total volume of material is the dominant factor in determining poor quality leachate due to the fact that the hydraulic properties of the materials are very similar. Material 6 is the dominant material in terms of volume but Material 2 contains a higher fraction of water soluble metals and will therefore have the biggest impact on water quality of seepage leaving the stockpile.

5.3 Site 2 Conceptual Model

This section outlines the field observations and laboratory test results that were used in the development of a conceptual model for the waste rock dump at Site 2.

5.3.1 Representative Materials

The mineralized ore zone at Site 2 occurred within a host granitic zone that dominates throughout the region. The granite is extremely competent and contains little to no sulfide but does contain some buffering capacity in the form of carbonate minerals (Tran, 2003). The rock that was associated with the ore zone contains significant sulfide mineralization. These two materials represented the bulk of the rock sampled in the Site 2 waste rock pile.

The average particle size of the material sampled at Site 2 was greater than 500 mm and field observations indicate that there is less than 10% by weight material passing 75 mm (Devos, et. al., 1997). This range of particle size leads to a drained structure and materials with a high hydraulic conductivity (typically ranging from 10^{-1} m/s to 10^{-2} m/s) due to the pore size between the cobble and boulder sized particles. The physical strength of both materials present in the dump indicates that there would be little consolidation and no significant variation in the hydraulic conductivity vertically within the dump.

The hydraulic conductivity of the waste rock dump at Site 2 was determined by Klohn Crippen (Personal Communication, 2002), and suggested that water could not be supplied to the surface of the dump fast enough to generate ponding under the field conditions. The result indicates that under intense rainstorm events there will be significant infiltration and limited runoff. It also clearly shows that the dump is unsaturated and will remain unsaturated even under high rainfall events. The unsaturated nature of the waste rock dump and the extremely coarse nature of the waste rock itself will lead to complex flow paths that are governed by rainfall intensity and gravity.

5.3.2 Representative Structure

Structure similar to that observed at Site 1 discussed in the previous sections was also observed at Site 2. The larger particle size led to a less defined structure within much of the waste rock dump, and flow paths were not easily determined by visual observation. The alternate coarse and fine material is less evident at Site 2 because there are few fine particles

present throughout the matrix of the material in the dump. Close examination of exposed faces showed some internal layering within the dump but it was not continuous throughout a layer and the fine materials were still coarse sand particles that were desaturated.

The main difference between Site 1 and Site 2 is that at Site 2 there are not enough particles finer than 5 mm to retain significant water under tension. The development of preferential flow requires a fine material to maintain a higher degree of saturation under tension, and has hydraulic conductivity higher than the surrounding materials that desaturate under the same applied tension. The materials at Site 2 are drained to residual water content and have insufficient fines to retain water under suction. This means that the flow pathways through the waste rock pile are gravity dominated rather than by capillarity forces. Figure 5.15 shows the typical structure observed within the dump at Site 2.

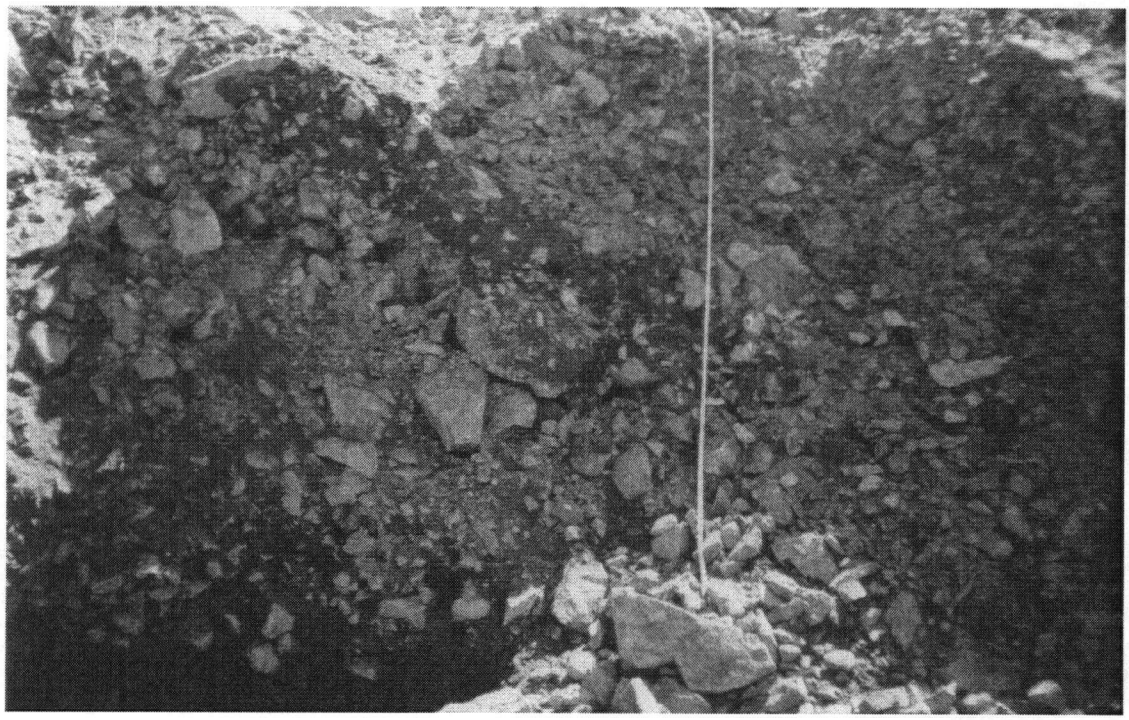

Figure 5.18 Typical Structure at Site 2 within Test Pit 15

5.3.3 Development of Model for Site 2

One of the objectives of the field program was to attempt to model idealized sections of waste rock to determine where the bulk of the flow is migrating through the dump. This could then be used to estimate potential loading rates based on the annual infiltration rate into the dump. The purpose of the analysis was to show on a comparative basis what the potential loading rates would be given a particular infiltration rate and assumed structure of the internal material.

Previous conceptual models that have been developed for flow within waste rock piles have been based on a preferential flow model that does not apply to Site 2. The field observations therefore have been used to develop a conceptual flow model applicable to coarse waste rock dumps that have not weathered to generate sand and clay sized particles.

Flow was observed in the field during rainfall events within the waste rock pile. The flow of water through the waste rock dump could be clearly heard trickling downward through the waste rock material. Visual observation also found many zones of material that had significant build up of oxidation products not being flushed away from the surface of the particles. The base of the waste rock dump contained large zones of frozen waste rock when sampled during the summer of 2001. The melt water from this region of the waste rock dump was pH 7. A short distance away (less than 500 m), there was an actively flowing seep from the toe of the dump that was orange in color and had a pH < 3. All of these observations indicated that there is a partitioning of flow within the waste rock dump that that is likely a result of any or all of: infiltration rate; gravity; particle size of the waste rock; temperature; or other factors that have not been identified.

5.4 Site 2 Numerical Model

The coarse texture of waste rock materials encountered at Site 2 made numerical simulation of the waste rock pile extremely difficult. This was due to the numerical instability inherent with the steep Soil-Water Characteristic Curves (see Figure 4.4). However, it was possible to describe a mechanistic conceptual model of the flow paths within

the waste rock pile to aid in defining the dominant flow paths and resulting outflow geochemistry.

As previously discussed the seepage paths appear to be spatially sporadic. Phenomenon observed by Belleheumer (2000) and Reinson (2000) showed that there could be ponding of water on the surface of a particle and then flow over the surface, but the path of that water would cover only a fraction of the available surface area of the particle. Bellehuemer (2002) conducted a tracer test that showed water quickly infiltrating a coarse rubble zone, flowing along the surfaces of large particles and then ponding on a compacted traffic surface. At Site 2 there were no identifiable compacted traffic layers encountered during the deconstruction. Fines (sand and gravel) were added at the top surface of each exposed to create a trafficable surface for the excavation equipment. The only obstruction to the downward migration of flow in the dump at Site 2 was ice lenses and entire lifts of frozen material. The field observations indicated that the infiltrating water is moving in a downward direction under gravity dominated flow paths.

The observations and trends outlined are generally supported by the results of the geochemical analysis. Tran (2003) observed that a large fraction of the water soluble oxidation products were stored on the surface of the waste rock particles. This suggested that if there had been adequate flushing, these constituents would have been removed from the particle surfaces, leaving only the insoluble fraction.

The geochemical analysis showed that there was a large volume of water soluble oxidation products present within the waste rock dump at Site 2. Figure 5.19 (from INAP, 2004) showed that materials with greater than 40% passing 4.75 mm or less than 20% passing 4.75 mm could store significant amounts of water soluble oxidation products. The field work together with the seepage modeling supports the observation presented in Figure 5.19.

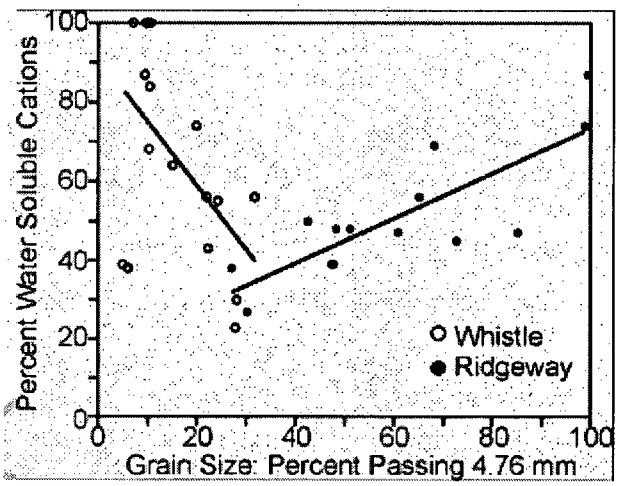

Figure 5.19 Summary of Geochemistry and Grain Size Results (INAP, 2004)

6.0 CHAPTER SIX CONCLUSIONS AND RECOMMENDATIONS

6.1 Summary

The research program conducted at two sites analyzed internal structure, in-situ conditions and hydraulic properties of the waste rock. The goal of the research program was to better understand the structure and flow within the waste rock dumps. The two sites contrasted both in climate, geology, weathering, and time since construction.

6.1.1 Site 1

The dump at Site 1 was composed mostly of saprolitic materials that were weathered from rock to predominantly silt and clay sized particles in the 10 years it had been stockpiled. The high rainfall and median air temperatures of 20°C resulted in extensive physical and chemical weathering; particles were close to an end-stage weathering point. Geochemical analyses (INAP, 2004) of the samples had shown that there was a small fraction of sulfide

present in the waste rock at Site 1. The waste rock at Site 1 contained very little carbonate buffer.

At Site 1, a consistent structure within the dump was evident in all of the test pits excavated. Interbeded layers oriented at approximately the angle of repose showed the end-dumped construction technique used for this dump. The materials were very dense, highly compacted and extremely weathered. The fine texture and high density of the waste rock resulted in most materials having a degree of saturation of between 30% and 50%. The finest layers maintained a higher degree of saturation but had extremely low values of hydraulic conductivity.

The numerical models indicated that there was preferential flushing occurring throughout the waste rock dump. The analysis showed that certain materials had a higher seepage rate while some materials dominated strictly due to the relative volume of material present. Detailed analysis showed that Material 4, as part of the analysis of SEEP/W Section 2 would have a high flux rate and would also likely contain a high fraction of water soluble metals.

6.1.2 Site 2

Site 2 was composed of a granitic rock that showed little evidence of particle size alteration due to chemical or physical weathering. The climate at Site 2 was affecting the weathering rate of the waste rock stockpiled in the dump as the dump was partially frozen all year round. Site 2 contained high percentages of sulfur and carbonate (INAP, 2004). The

acid generating capacity outstripped the neutralizing capacity of the buffer present in the waste rock. The waste rock pile contained large voids drained to residual water content.

The structure within the waste rock pile at Site 2 was less obvious due to the large size of the particles stockpiled in the dump. Test pit excavations exposed some evidence of dipping, interbedded layers but due to the low density and large void spaces between the large particles; the material separations were much less distinct. There was evidence of chemical oxidation of sulfides within the dump at Site 2. Elevated temperature in the winter, iron staining, and metal hydroxide deposits was all evidence of sulfide oxidation.

6.2 Conclusions

Specific conclusions resulting from the study are summarized in point form below:

- Structure and construction technique influence the development of seepage paths within a waste rock pile.
- The rate of both chemical and physical weathering, governs the development of layering (fine layers and coarse rubble zones) in waste rock dumps.
- Site 1 was characterized by highly weathered particles. The dump contained interbedded dipping layers close to the angle of repose. Overall the material had weathered to a soil-like particle size and was extremely dense. Geochemical testing (INAP, 2004) also showed that much of the particles are reaching an end-stage weathering point.
- Site 2 was characterized by large oversize particles, containing very little interstitial water. There was evidence of layering of particles, close to the angle of repose. Geochemical oxidation was evident in the iron staining present on much of the material sampled. Geochemical testing (INAP, 2004) indicates a large fraction of water soluble metals and a large fraction on non-reacted sulphides. This all indicates that the weathering state was not advanced either physically or geochemically.

- Materials with a median particle size significantly larger than 5 mm will tend to store oxidation products due to the drained nature of the waste rock. Median particle sizes significantly lower than 1 mm tend to store oxidation products due to low hydraulic conductivity.
- The hydraulic conductivity of the samples at Site 1 ranged from $1x10^{-4}$ m/s to $1x10^{-9}$ m/s. At Site 2 hydraulic conductivities were approximately $1x10^{-1}$ m/s.
- Spatial variability of flow paths within coarse-grained waste rock makes it difficult to accurately describe the outflow chemistry in space and time. The seepage analyses conducted for Site 1 show that a certain materials within the waste rock dump will likely be subjected to limited flushing and the result will be storage of oxidation products.
- The coarse grained nature of the Site 2 waste rock dump would show variability in flushing due to the nature of the downward seepage paths. The paths are not clearly defined and will be influenced by the presence of small lenses of fine material where water could pond or large connected zones of coarse material where water could bypass large sections of waste rock. The waste rock dump is almost completely drained resulting in most of the particle surfaces being dry. Under an infiltration event different surfaces will be flushed depending on the downward path the infiltrating water takes.
- The lack of uniform flushing within the dump at Site 2 results in the storage of oxidation products on particle surfaces within the waste rock pile.

6.3 Recommendations for Future Research

One of the main factors controlling the physical behavior of waste rock is the change in grain size distribution during the life of a waste rock pile. Physical stability, flow paths, or geochemistry, grain size distribution control the material behavior. All of the predictions and models are based on a known grain size distribution. However, both physical and chemical

weathering, result in a constantly changing grain size distribution. Prediction of changes in the grain size distribution would be valuable in designing structures for very long lifetimes.

A large lab scale experiment could be carried out to analyze the effects of physical and geochemical weathering on grain size distribution. The experiment would need to be a multi stage batch experiment allowing for measurement of changing soil properties during the life of the experiment. The results could be used to determine if the necessary particle size breakdown will occur to allow significant flushing of oxidation products or if the material will resist physical and chemical weathering and result in long term storage of water soluble oxidation products.

Further field trials along with better planning and monitoring of new waste dumps would be very beneficial in understanding the evolution of water quality, flow paths and material changes with time. Long term liability from ARD and poor quality drainage has a significant monetary impact for mining companies. Improved understanding of the physical processes within the waste rock dump would allow for improved construction designs to limit ARD generation during the life of the waste dump and would aid in the development of better construction closure strategies, resulting in significant cost savings.

REFERENCES

Belleheumer, T M, 2001. *Mechanisms and spatial variability of rainfall infiltration on the Claude waste rock pile.* M.A.Sc. thesis, University of British Columbia, Vancouver.

Craig, R F, 1987. *Soil Mechanics*, 4th Edition. T.J. Press, Cornwall England.

Devos, K J, Pettit, C, Martin, J, Knapp, R A and Jansons, K J, 1997. *Whistle Mine waste rock study*, Volume 1, Golder Associates Limited and SENES Consultants Limited.

Fines, P E, 2003. Hydrologic characterisation of two full scale waste rock piles, *Proceedings of the Sixth International Conference on Acid Rock Drainage.*

Fetter, C.W. 1993. *Applied Hydrogeology 3rd Edition.* Macmillan College Publishing Company, New York, USA.

Fredlund, D.G., and Xing, A., 1994. Equations for the soil-water characteristic curve. *Canadian Geotechnical Journal.*Vol.31 pp. 533-546.

Fredlund, D.G., and Rahardjo, H. 1993, *Soil Mechanics for Unsaturated Soils.* John Wiley and Sons, Inc., New York.

GeoSlope, 2000. SEEP/W Users Manual. GEO-SLOPE International Ltd, Calgary, Canada

Herasymuik, G M, 1996. *Hydrology of a sulphide waste rock dump.* M.Sc. thesis, University of Saskatchewan, Saskatoon.

INAP, 2004. *Waste Rock Characterization Study.* Joint project with University of British Columbia, University of Queensland and the International Network for Acid Prevention. Final Report.

Newman, L, 1999. *A mechanism for preferential flow in vertically layered, unsaturated systems.* M.Sc. thesis, University of Saskatchewan, Saskatoon.

Nichol, R S, 1986. Rock Segregation in Waste Dumps. *Proceedings of the International Conference on Flow-Through Rock Drains.* pp.105-120.

Nichol, C., 2002. *Transient Flow and Transport in Unsaturated Heterogeneous Media: Field Experiments in Mine Waste Rock.* Ph.D. thesis, University of British Columbia, Vancouver, British Columbia.

Nichol, C, 2003. Water Flow in Uncovered Waste Rock – A Multi-Year Large Lysimeter Study. *Proceeding of the Sixth International Conference on Acid Rock Drainage.* pp.919-926

Personal Communication with Greg Noack 2002. Discussed results of field experiments at Site 2, confidential client report.

Reinson, J R, Fredlund D G, and Wilson G W 2005. Unsaturated Flow in Coarse Porous Media, *Canadian Geotechnical Journal* Vol. 42. pp 252-262.

SoilVision Systems Ltd. 2001. SoilVision User's Manual. SoilVision Systems Ltd. Saskatoon, Saskatchewan.

Stockwell, J, Beckie, R, and L Smith, 2003. The hydrogeochemical characterization of an unsaturated waste rock pile, Key Lake, Saskatchewan, Canada. *Proceeding of the Sixth International Conference on Acid Rock Drainage.* pp.927-938

Tran, A B, Millar, S, Williams, D J, Fines, P, and Wilson G W, 2003. Geochemical characterisation of two full scale waste rock dumps – The INAP Waste Rock Dump Characterization Project, *Proceedings of the Sixth International Conference on Acid Rock Drainage.* pp.939-948

van Genuchten,, M. Th., 1980. A closed form equation for predicting the hydraulic conductivity of unsaturated soils. *Soil Science Society of America Journal.* Vol. 44 pp 892-898

Yazdani, J., Barbour, L., and Wilson, W. 2000. Soil Water Characteristic Curve for Mine Waste Rock Containing Coarse Material. *Proceedings of the 6th Environmental Specialty CSCE and 2nd Spring Conference of the Geoenviromental Division of the CGS*, London, Ontario, pp. 198-202.

Wilson, J A, Wilson, G W, and Fredlund D G, 2000. Numerical modelling of vertical and inclined waste rock layers, *Proceedings of the Fifth International Conference on Acid Rock Drainage* pp.257-266.

APPENDIX I

Site 1 Test Pit Logs

TEST PIT 11

Test pit 11 was excavated June 21, 2000 to a depth of 4 m below the surface of the top bench. Seven internal layers were observed in the profile of the test pit. Table 11.1 summarizes the materials and corresponding depth for each layer encountered. Photograph 11.1 shows a typical exposure of the excavated test pit.

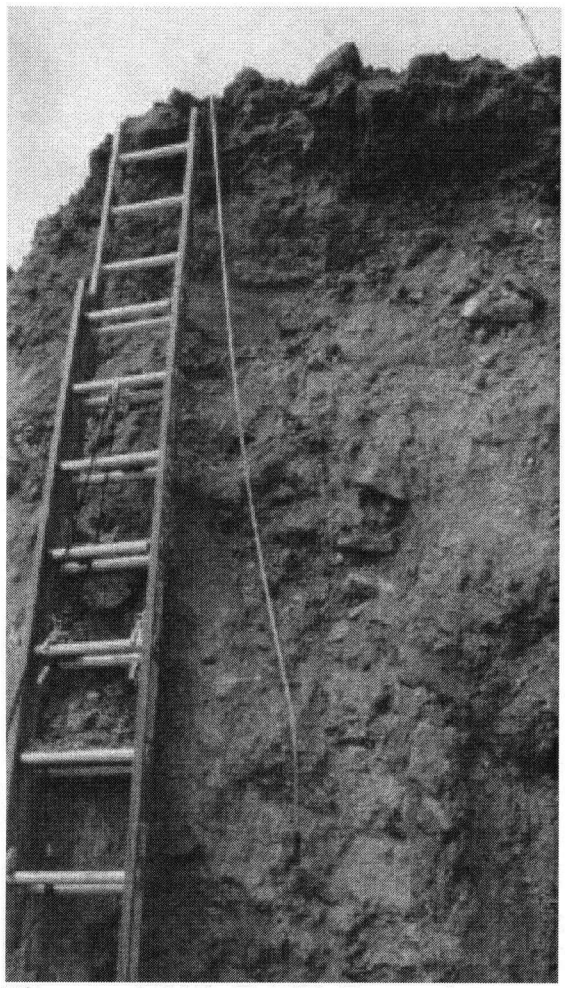

Photograph 11.1: Test Pit Excavation.

Table 11.1

Depth (m)	Layer inclination	Description
0.00		clay- with sand and gravel
0.17	horizontal	brown, no evidence of sulfide oxidation
0.33		moist, stiff
0.33		clay- well graded with silt
0.50	horizontal	red, no evidence of sulfide oxidation
0.67		moist, soft
0.67		silt with high clay content
0.75	horizontal	olive yellow
0.83		damp, friable
0.83		clay fill- red
1.17	horizontal	no obvious sulfide oxidation
1.50		damp, highly plastic
1.5		clay- with silt and gravel
	dipping	light brown, no obvious
1.92	30°	sulfide oxidation
2.33		damp, soft
2.33		clay-silt with soft rock fragments
	dipping	yellowish brown
2.67	45°	low paste pH
3.00		damp, stiff
3.00		clay- silt with large rock fragments
	dipping	light brown
3.50	45°	low paste pH
4.00		dry, stiff

Figure 11.1 shows the water content, dry density, matric suction and paste pH profiles measured at selected depths in test pit 11. Figure 11.2 shows the particle size distribution for the materials sampled within test pit 11.

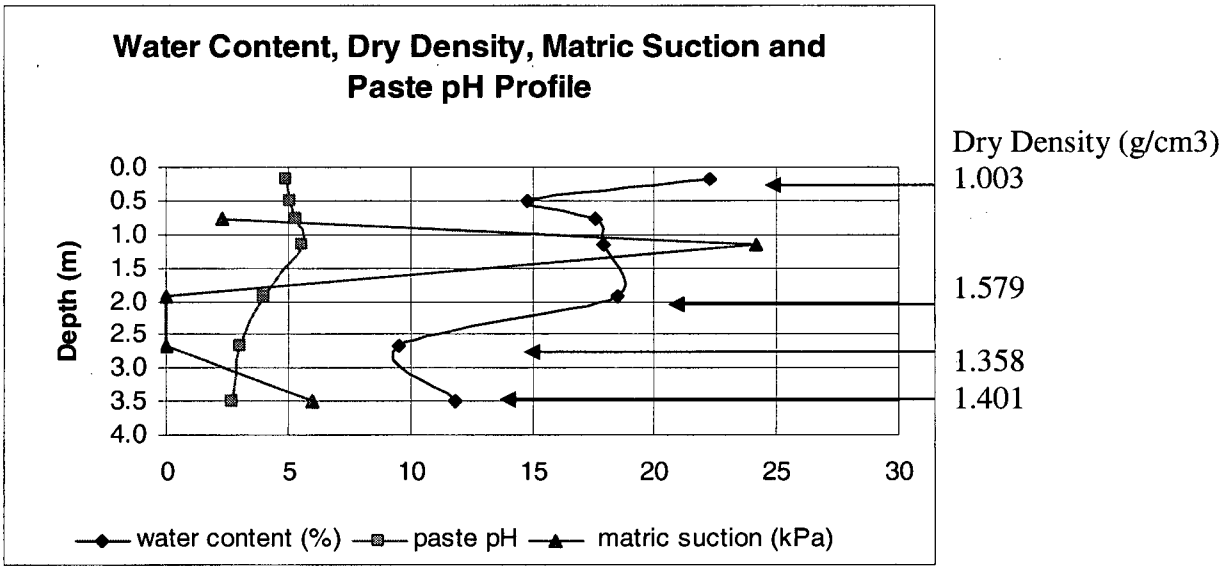

Fig. 11.1: Water Content, Dry Density, Matric Suction and Paste pH Values Measured Versus Depth in Test Pit 11.

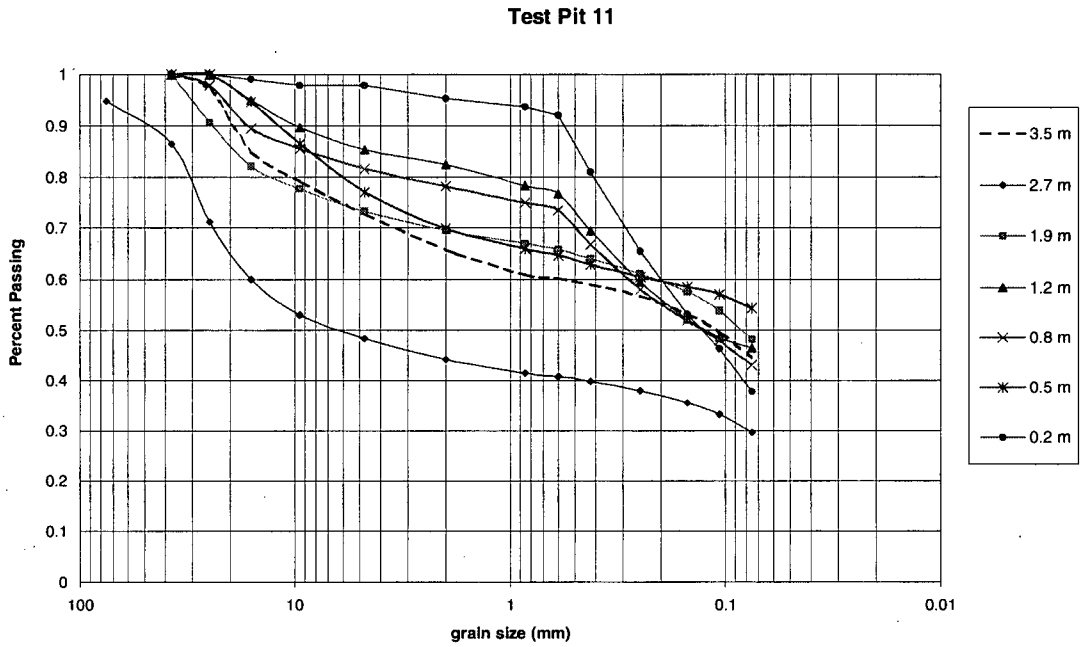

Fig. 11.2: Particle Size Distribution for Samples Encountered at Selected Depths.

TEST PIT 12

Test pit 12 was excavated June 21, 2000 to a depth of 3 m below the bottom of test pit 11. Four internal layers were observed in the profile of the test pit. Table 12.1 summarizes the materials and corresponding depth for each layer encountered. Photograph 12.1 shows a typical exposure of the excavated test pit.

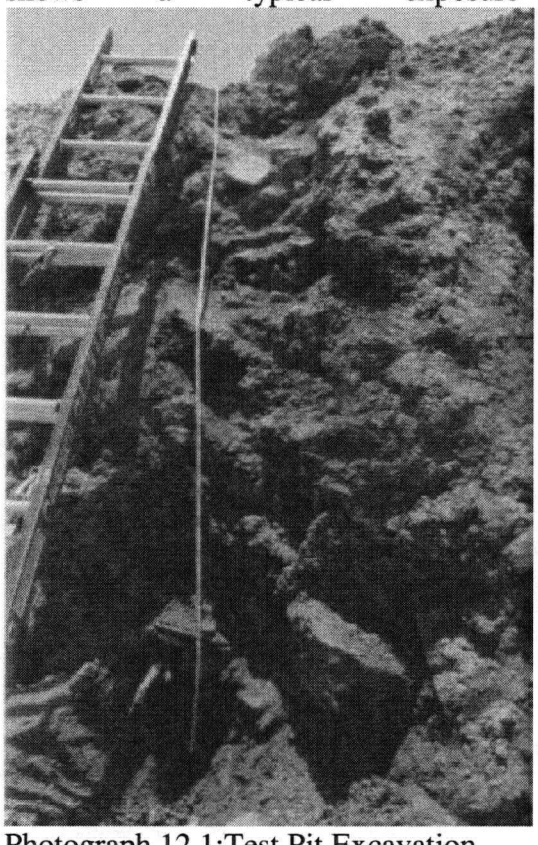

Photograph 12.1:Test Pit Excavation.

Table 12.1

Depth (m)	Layer Inclination	Description
0.00		clay, well graded with silt and gravel
0.42	dipping 30°	light brown, obvious sulfide oxidation
0.83		moist, stiff
0.83		clay with sand, gravel and soft rock particles
1.61	dipping 30°	red, obvious sulfide oxidation
2.39		moist, soft
2.39		soft rock, contains gravel
2.60	dipping 30°	red, obvious sulfide oxidation
2.81		dry, stiff
2.81		clay with silt and gravel
2.90	dipping 30°	pale yellow with obvious sulfide oxidation
3.00		wet, soft

Figure 12.1 shows the water content, dry density, matric suction and paste pH profiles measured at selected depths in test pit 12. Figure 12.2 shows the particle size distribution for the materials sampled within test pit 12.

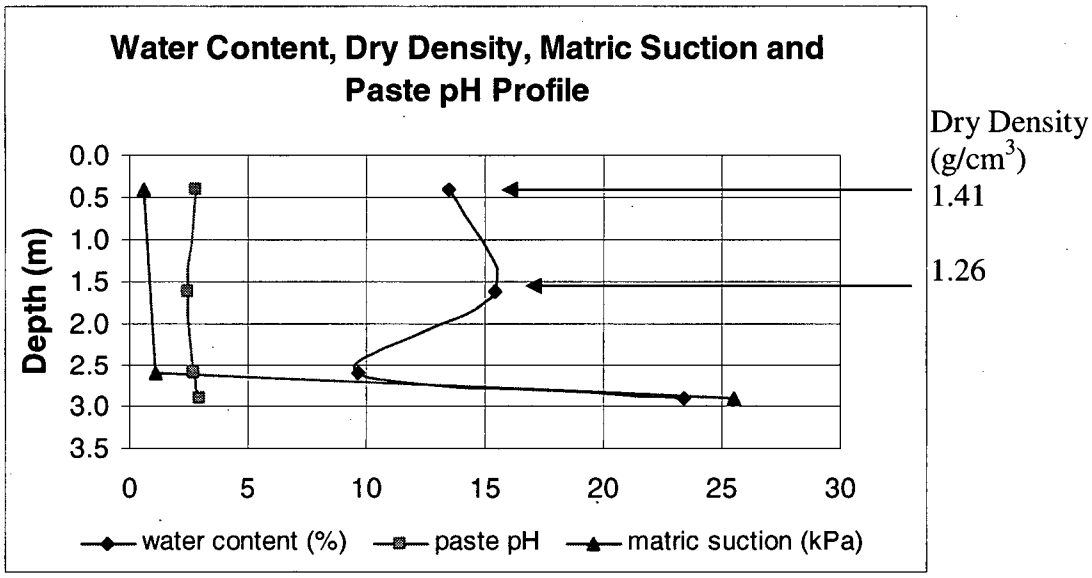

Fig. 12.1: Water Content, Dry Density, Matric Suction and Paste pH Values Measured Versus Depth in Test Pit 12.

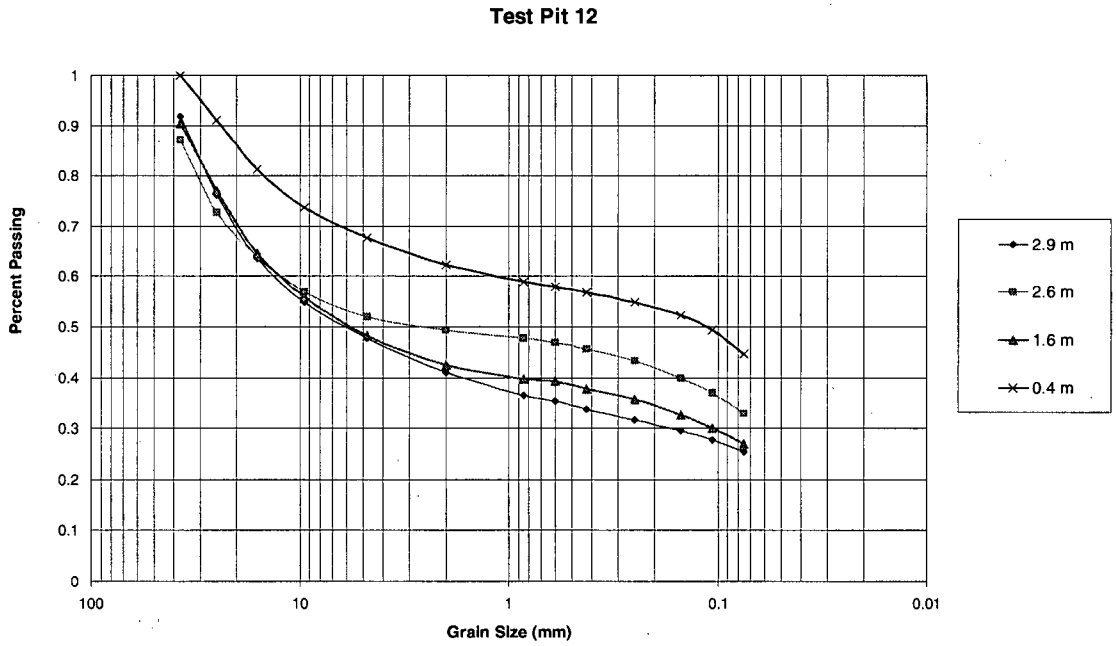

Fig. 12.2: Particle Size Distribution for Samples Encountered at Selected Depths.

TEST PIT 13

Test pit 13 was excavated June 21, 2000 to a depth of 4.5 m below the surface of the top bench. Six internal layers were observed in the profile of the test pit. Table 13.1 summarizes the materials and corresponding depth for each layer encountered. Photograph 13.1 shows a typical exposure of the excavated test pit.

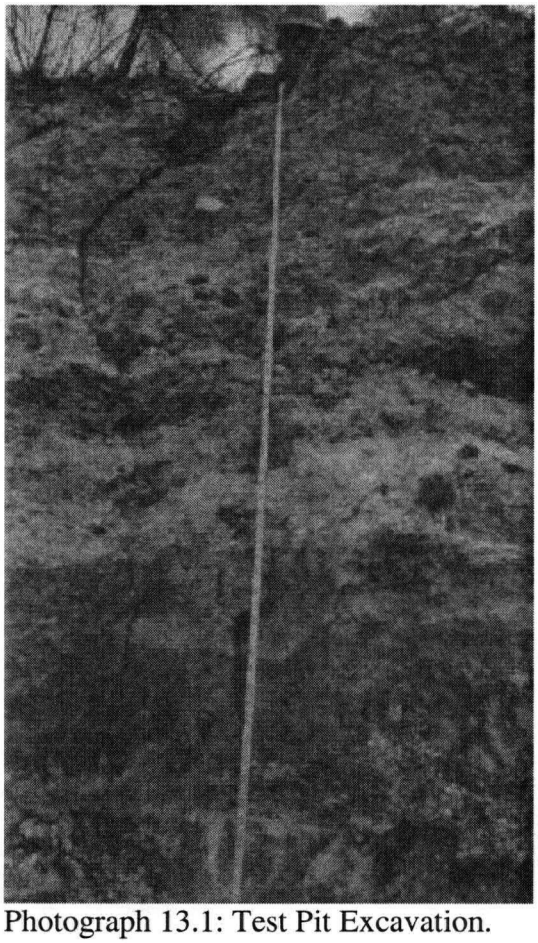

Photograph 13.1: Test Pit Excavation.

Table 13.1: Material Description Summary

Depth (m)	Layer Inclination	Description
0.00		organic, presence of tree roots
0.50	horizontal	pale yellow, no obvious sign of sulfide oxidation
1.00		damp, stiff
1.00		clay with silt and sand
1.42	horizontal	green grey, no obvious signs of sulfide oxidation
1.83		moist, stiff
1.83		clay with silt and hard rock particles
1.89	horizontal	dark brown, possible lime layer
1.94		moist, stiff
1.94		waste rock, 1m min. diameter material
2.47	horizontal	grey, no obvious signs of sulfide oxidation
3.00		dry, hard
3.00		clay, very silty
3.17	horizontal	red, no obvious signs of sulfide oxidation
3.33		moist, soft
3.33		gravel, well graded with silt and clay
4.00	horizontal	light grey, possible sulfide oxidation
4.67		dry, hard

Figure 13.1 shows the water content, dry density, matric suction and paste pH profiles measured at selected depths in test pit 13. Figure 13.2 shows the particle size distribution for the materials sampled within test pit 13.

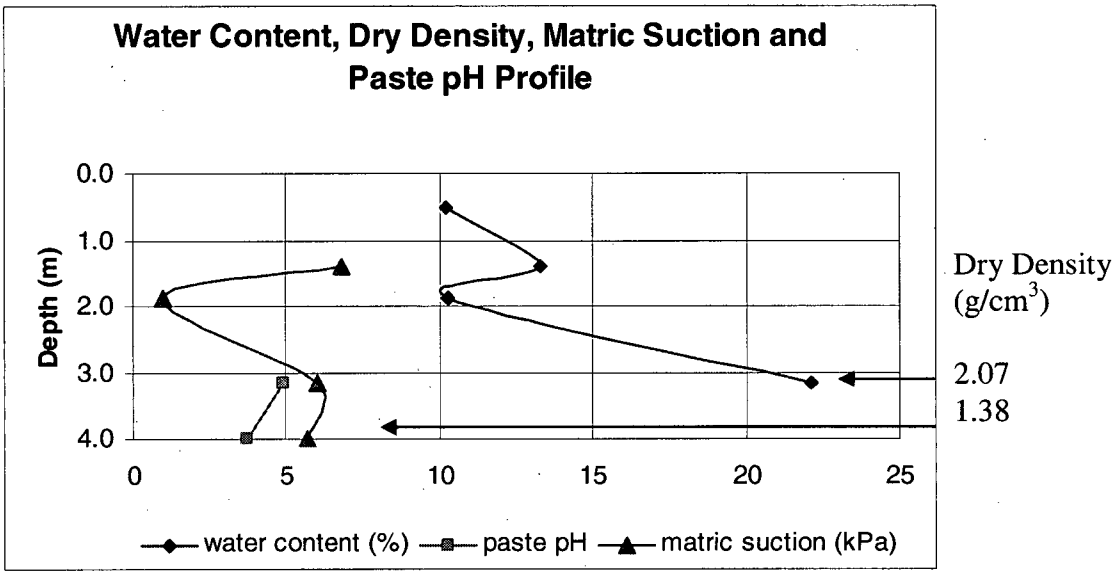

Fig. 13.1: Water Content, Dry Density, Matric Suction and Paste pH Values Measured Versus Depth in Test Pit 13.

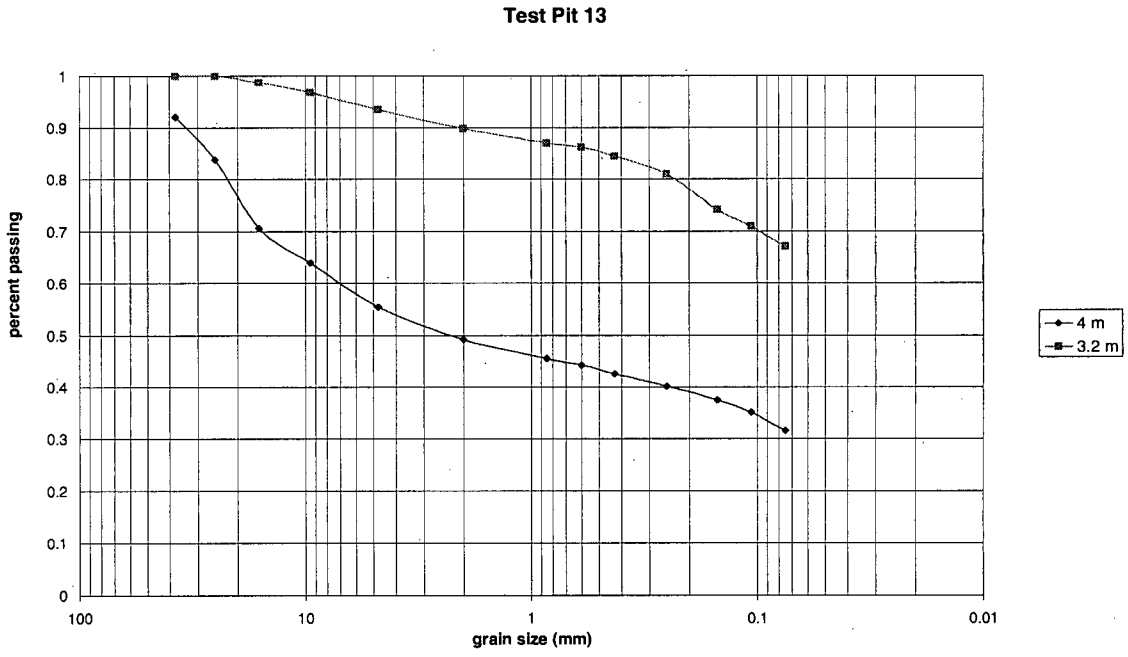

Fig. 13.2: Particle Size Distribution for Samples Encountered at Selected Depths.

TEST PIT 14

Test pit 14 was excavated June 29, 2000 to a depth of 4.5 m below the surface of the second bench. Seven internal layers were observed in the profile of the test pit. The measurement of the profile was done at the angle of the layers within the test pit. Table 14.1 summarizes the materials and corresponding depth for each layer encountered. Photograph 14.1 shows a typical exposure of the excavated test pit.

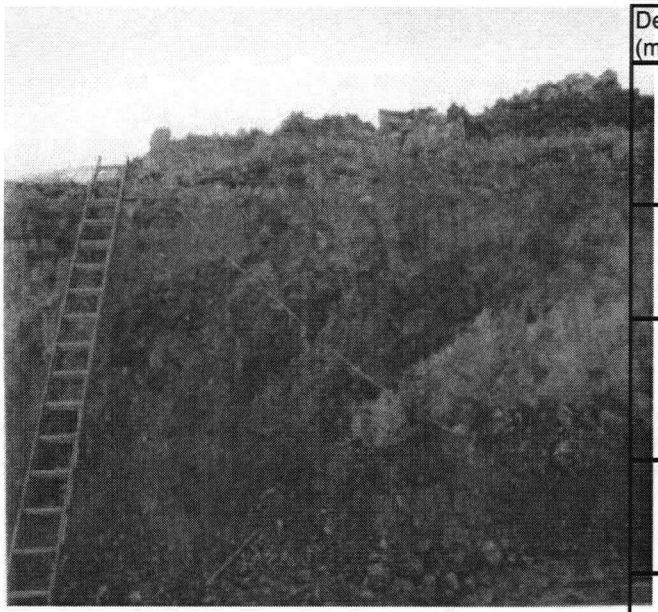

Photograph: 14.1: Test Pit Excavation.

Table 14.1: Material Description Summary

Depth (m)	Layer Inclination	Description
0.00		gravel, well graded with silt
		pale yellow, no obvious
0.17	horizontal	signs of sulfide oxidation
0.33		dry, stiff
0.33		clay, with silt
		red, no obvious signs of
0.83	dipping 30°	sulfide oxidation
1.33		moist, stiff
1.33		gravel with silt and rock
		brownish yellow, no
		obvious signs of sulfide
1.43	dipping 30°	oxidation
1.53		moist, stiff
1.53		clay, with silt and gravel
		olive brown, no obvious
2.18	dipping 30°	signs of sulfide oxidation
2.83		dry, hard
		clay with silt and soft rock
2.83		fragments
		red, no obvious signs of
3.47	dipping 30°	sulfide oxidation
4.11		moist, stiff
4.11		clay with silt and gravel
		grey to brown, no obvious
4.64	dipping 30°	signs of sulfide oxidation
5.17		moist, stiff
5.17		clay with silt
		pale yellow
6.08	dipping 30°	low pH
7.00		damp, stiff

Figure 14.1 shows the water content, dry density, matric suction and paste pH profiles measured at selected depths in test pit 14. Figure 14.2 shows the particle size distribution for the materials sampled within test pit 14.

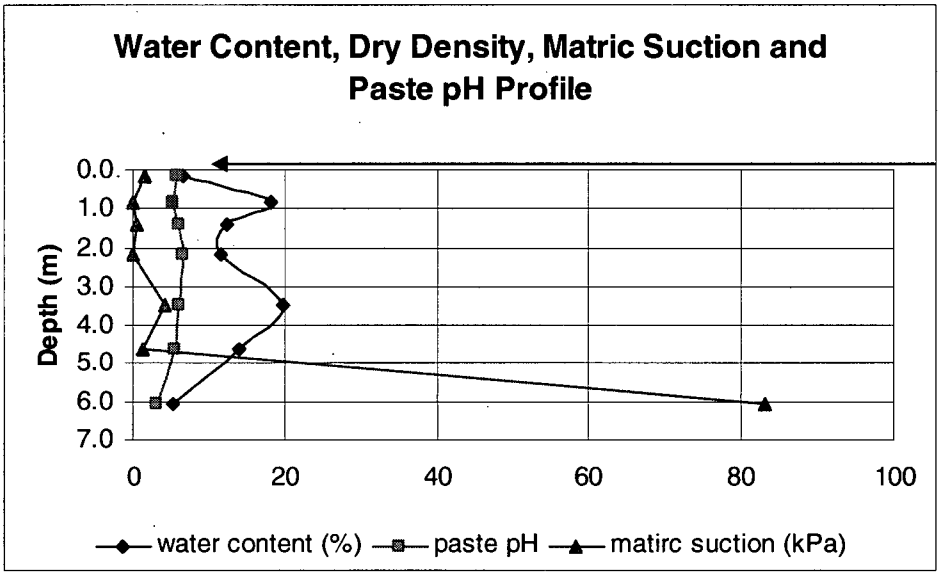

Fig 14.1: Water Content, Dry Density, Matric Suction and Paste pH Values Measured Versus Depth in Test Pit 14.

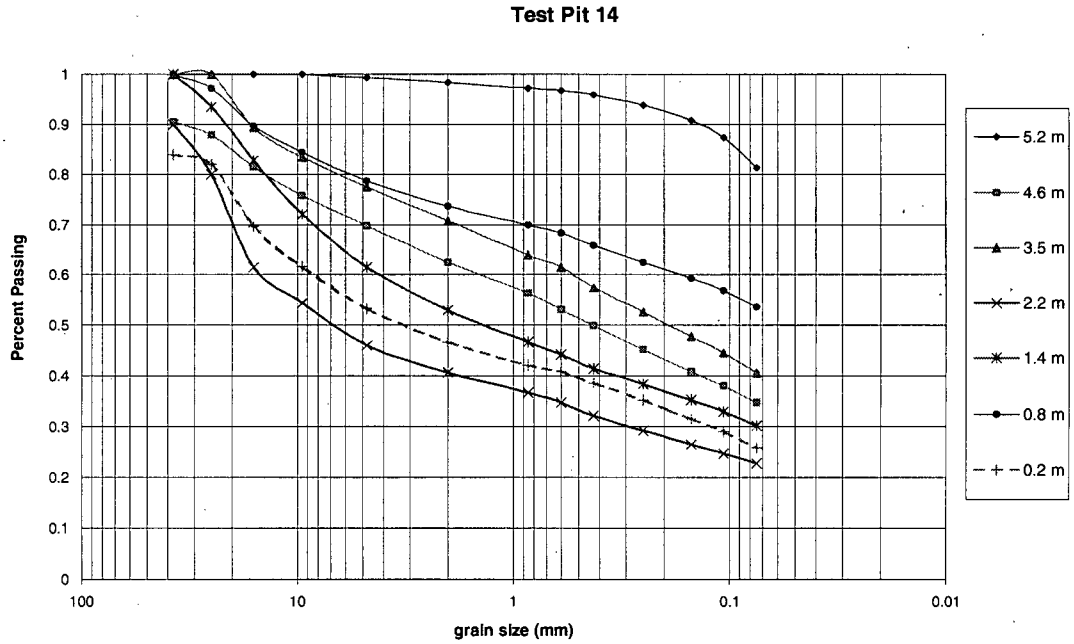

Fig. 14.2: Particle Size Distribution for Samples Encountered at Selected Depths.

TEST PIT 15

Test pit 15 was excavated June 29, 2000 to a depth of 3.5 m below the surface of the second bench. Ten internal layers were observed in the profile of the test pit. Table 15.1 summarizes the materials and corresponding depth for each layer encountered. Photograph 15.1 shows a typical exposure of the excavated test pit.

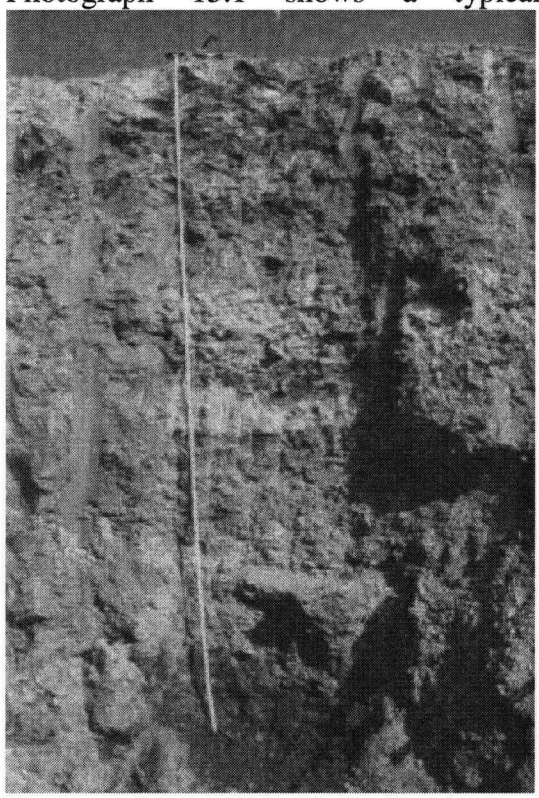

Photograph 15.1: Test Pit Excavation.

Table 15.1: Material Description Summary.

0.00	clay
	red, no obvious signs of
0.50 horizontal	sulfide oxidation
1.00	wet, plastic
1.00	gravel with silt and clay
	brown
1.17 horizontal	low pH
1.33	dry, stiff
1.33	clay with silt
	red
1.58 horizontal	low pH
1.83	wet, plastic
1.83	clay with silt and gravel
	brown
1.92 horizontal	low pH
2.00	damp, stiff
	clay with sand, silt and
2.00	gravel
	pale yellow
2.04 horizontal	low pH
2.08	dry, stiff
2.08	clay
2.24 horizontal	red
2.39	damp, soft
2.39	silt
	pale yellow
2.58 horizontal	low pH
2.78	moist, stiff
2.78	well graded clay to gravel
	pink
2.81 horizontal	low pH
2.83	moist, stiff
2.83	rock with silt and clay
3.00 horizontal	yellow to red
3.17	damp, stiff
3.17	clay
	red
3.33 horizontal	low pH
3.50	wet, plastic

Figure 15.1 shows the water content, dry density, matric suction and paste pH profiles measured at selected depths in test pit 15. Figure 15.2 shows the particle size distribution for the materials sampled within test pit 15.

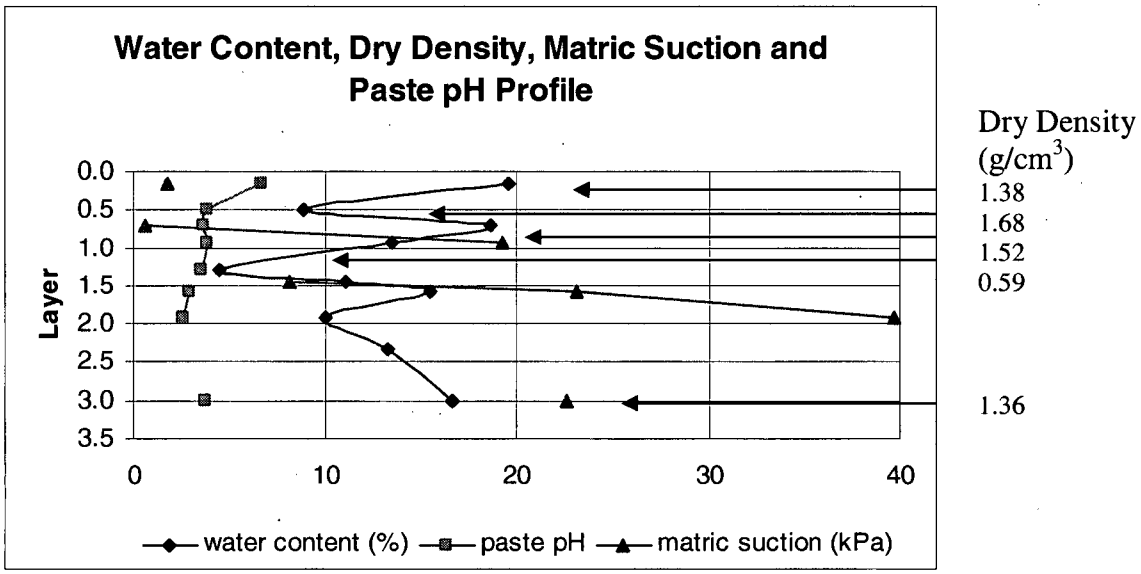

Fig. 15.1: Water Content, Dry Density, Matric Suction and Paste pH Values Measured Versus Depth in Test Pit 15.

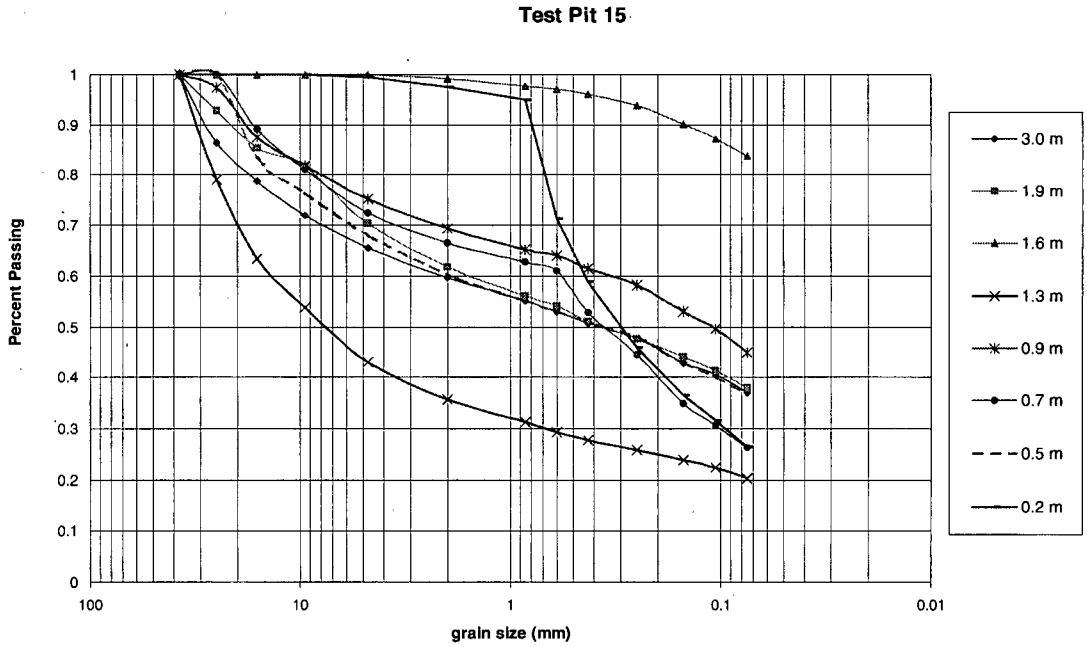

Fig. 15.2: Particle Size Distribution for Samples Encountered at Selected Depths.

TEST PIT 16

Test pit 16 was excavated June 29, 2000 to a depth of 4 m below the surface of the second bench. Four internal layers were observed in the profile of the test pit. Table 16.1 summarizes the materials and corresponding depth for each layer encountered. Photograph 16.1 shows a typical exposure of the excavated test pit.

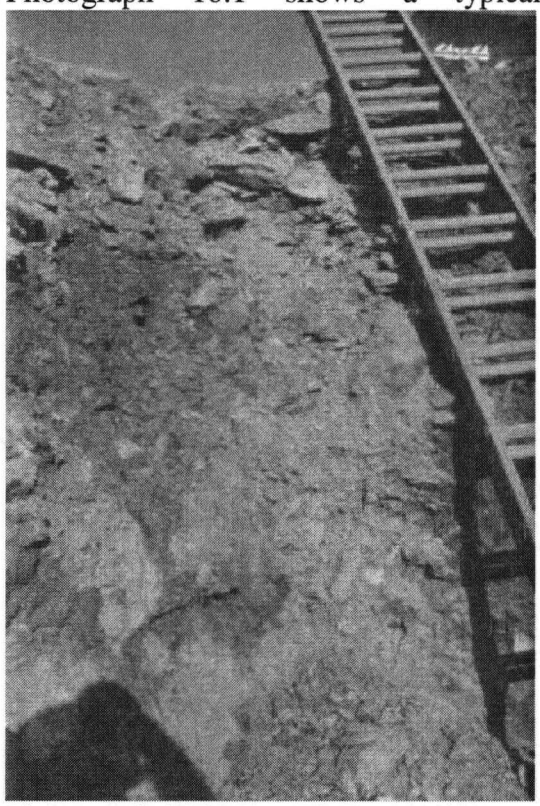

Photograph 16.1: Test Pit Excavation.

Table 16.1: Material Description Summary.

Depth (m)	Layer Inclination	Description
0.00		sand with silt and gravel
0.50	Dipping 30°	low pH
1.00		damp, stiff
1.00		gravel with silt, clay and sand brownish yellow
1.33	Dipping 30°	low pH
1.67		dry, stiff
1.67		gravel with silt and clay olive grey
2.50	Dipping 30°	low pH
3.33		moist, stiff
3.33		silt with clay and sand pale yellow
3.67	Dipping 30°	low pH
4.00		wet, stiff

Figure 16.1 shows the water content, dry density, matric suction and paste pH profiles measured at selected depths in test pit 16. Figure 16.2 shows the particle size distribution for the materials sampled within test pit 16.

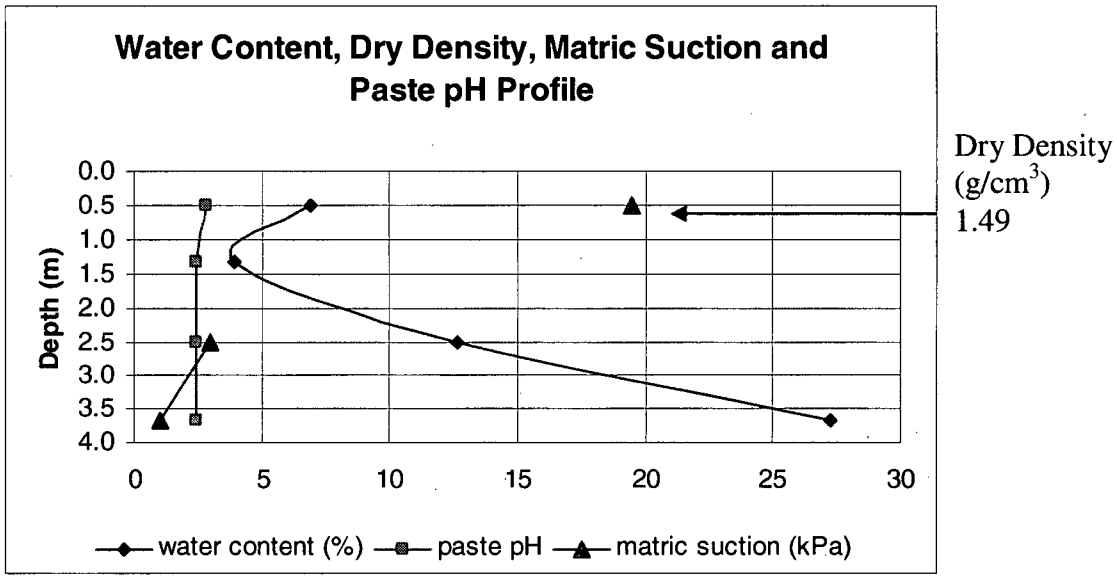

Fig. 16.1: Water Content, Dry Density, Matric Suction and Paste pH Values Measured Versus Depth in Test Pit 16.

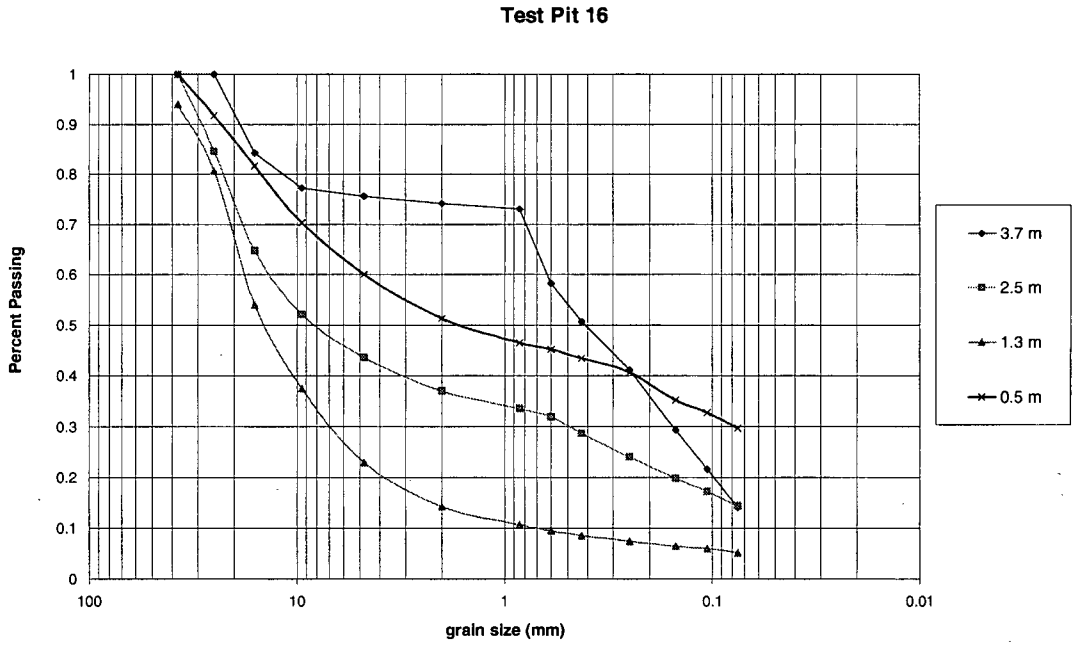

Fig. 16.2: Particle Size Distribution for Samples Encountered at Selected Depths.

TEST PIT 17

Test pit 17 was excavated June 29, 2000 to a depth of 2 m below the surface of the second bench. Two internal layers were observed in the profile of the test pit. Table 17.1 summarizes the materials and corresponding depth for each layer encountered. Photograph 17.1 shows a typical exposure of the excavated test pit.

Photograph 17.1: Test Pit Excavation.

Table 17.1: Material Description Summary.

Depth (m)	Layer inclination	Description
0.00		waste rock
	dipping	grey, no evidence of
0.67	20°	sulfide oxidation
1.33		dry, stiff
		silt with clay and
1.33		gravel
	inclined	yellowish brown
1.67	20°	low pH
2.00		moist, stiff

Figure 17.1 shows the water content and paste pH profiles measured at selected depths in test pit 17. Tensiometers were not installed in this test pit and no density data was collected. Figure 17.2 shows the particle size distribution for the materials sampled within test pit 17.

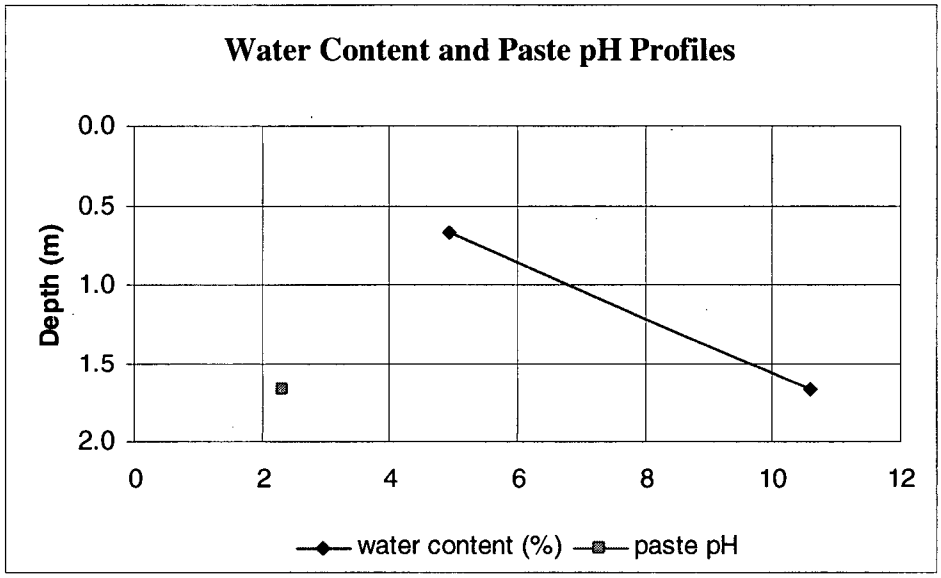

Fig. 17.1: Water Content and Paste pH Values Measured Versus Depth in Test Pit 17.

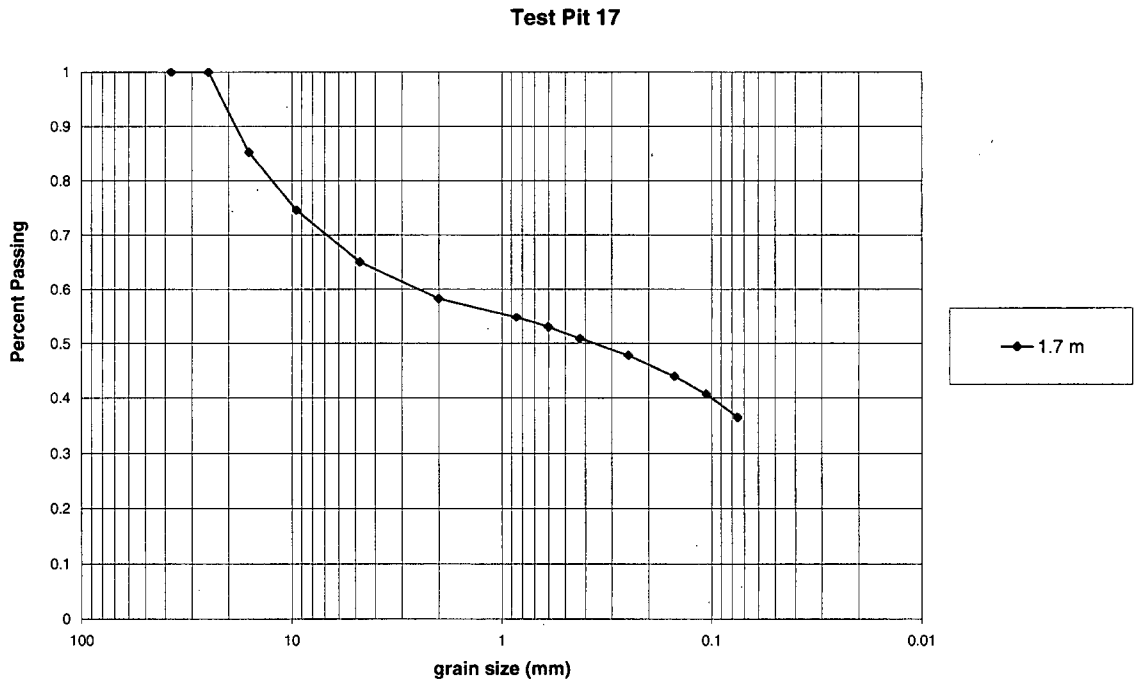

Fig. 17.2: Particle Size Distribution for Samples Encountered at Selected Depths.

TEST PIT 23

Test pit 23 was excavated August 1, 2000 to a depth of 3 m below the surface of the second bench. Five internal layers were observed in the profile of the test pit. Table 23.1 summarizes the materials and corresponding depth for each layer encountered. Photograph 23.1 shows a typical exposure of the excavated test pit.

Photograph 23.1: Test Pit Excavation

Table 23.1: Material Description Summary.

Depth (m)	Layer Inclination	Description
0.00		waste rock
		greenish yellow
0.83	horizontal	low pH
1.67		dry, stiff
		clay with silt and
1.67		sand
1.75	horizontal	red
1.83		damp, friable
		well graded
		gravel with silt,
1.83		clay and sand
		olive grey
2.25	horizontal	low pH
2.67		dry, stiff
		clay with silt and
2.67		sand
		red
2.75	horizontal	low pH
2.83		wet, soft
		clay with silt and
2.83		sand
		yellowish brown
2.92	horizontal	low pH
3.00		moist, stiff

Figure 23.1 shows the water content, dry density, matric suction and paste pH profiles measured at selected depths in test pit 23. Figure 23.2 shows the particle size distribution for the materials sampled within test pit 23.

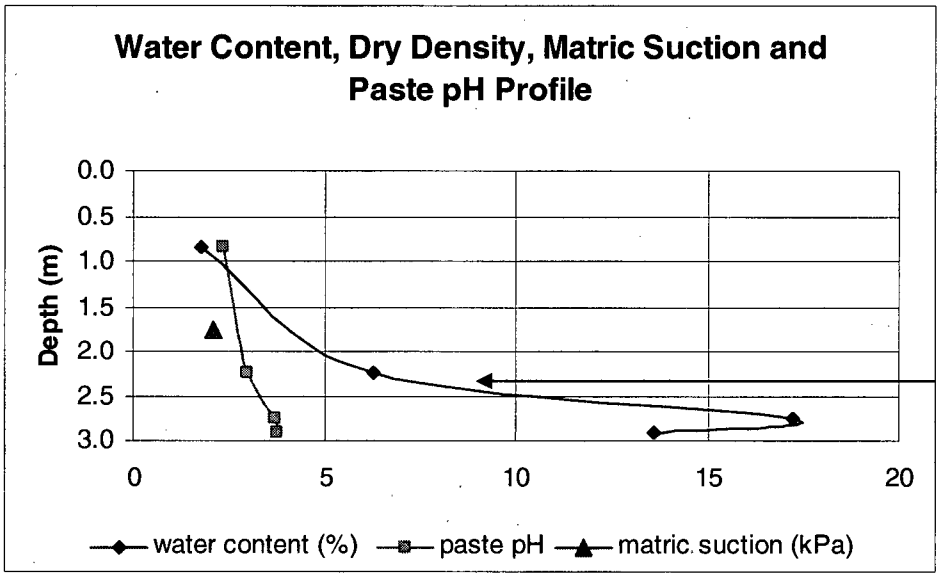

Fig. 23.1: Water Content, Dry Density, Matric Suction and Paste pH Values Measured Versus Depth in Test Pit 23.

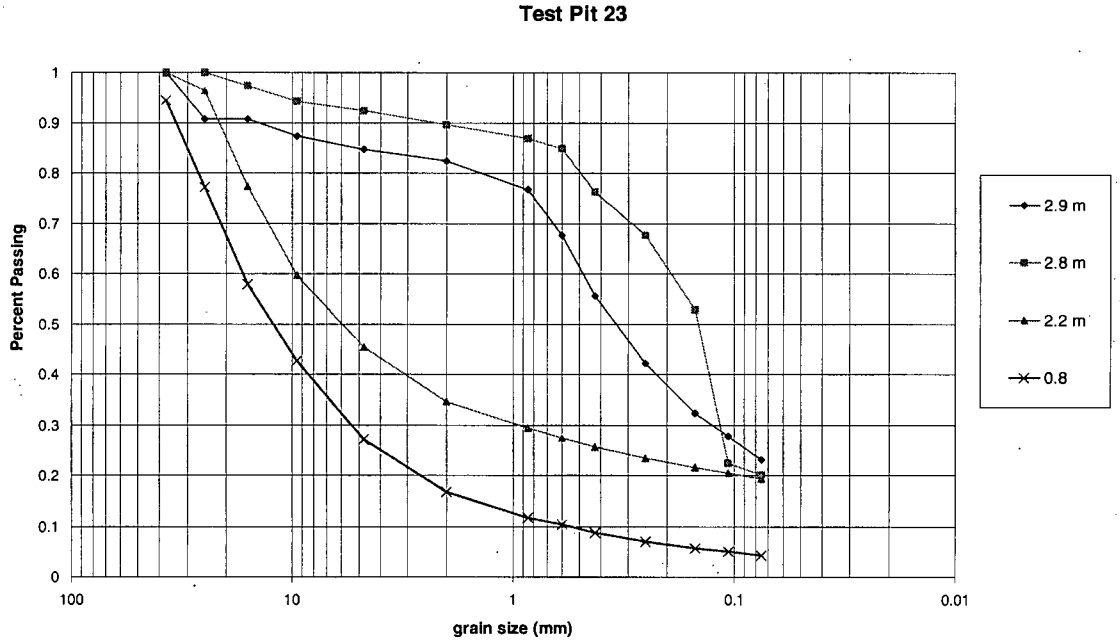

Fig. 23.2: Particle Size Distribution for Samples Encountered at Selected Depths.

TEST PIT 18

Test pit 18 was excavated August 1, 2000 to a depth of 3.3 m below the surface of the third bench. Seven internal layers were observed in the profile of the test pit. Table 18.1 summarizes the materials and corresponding depth for each layer encountered. Photograph 18.1 shows a typical exposure of the excavated test pit.

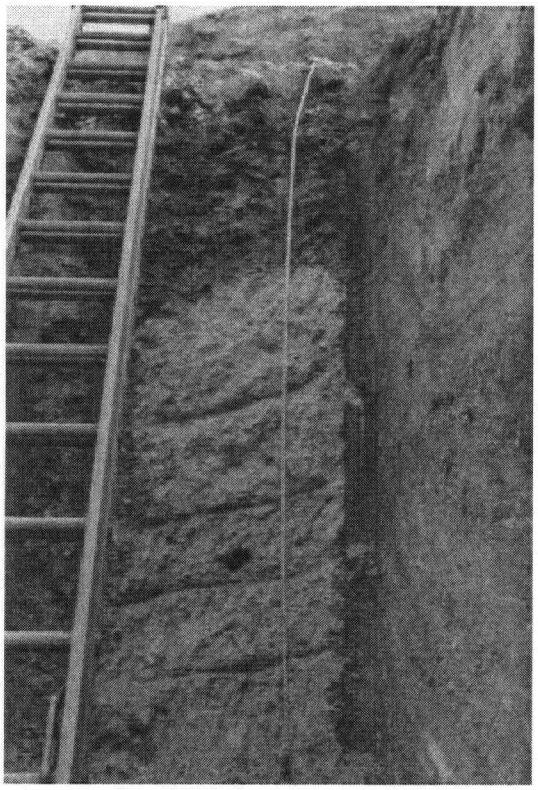

Photograph 18.1: Test Pit Excavation.

Table 18.1: Material Description Summary.

Depth (m)	Layer Inclination	Description
0.00		silt with sand and clay
0.33	dipping 10°	red, no obvious signs of sulfide oxidation
0.67		wet, soft
0.67		sand with clay, silt and gravel
0.97	dipping 10°	yellow brown, no obvious signs of sulfide oxidation
1.28		moist, soft
1.28		clay with silt
1.57	dipping 10°	grey, no obvious signs of sulfide oxidation
1.86		wet, friable
1.86		clay with silt
2.07	dipping 10°	pale yellow pH below 4.5
2.28		brittle
2.28		clay with silt
2.43	dipping 10°	pinkish grey with white low pH
2.58		wet, plastic
2.58		clay with silt
2.75	dipping 10°	pinkish grey with white low pH
2.92		wet, plastic
2.92		clay with silt
3.13	dipping 10°	pinkish grey with white low pH
3.33		wet, plastic

Figure 18.1 shows the water content, dry density, matric suction and paste pH profiles measured at selected depths in test pit 18. Figure 18.2 shows the particle size distribution for the materials sampled within test pit 18.

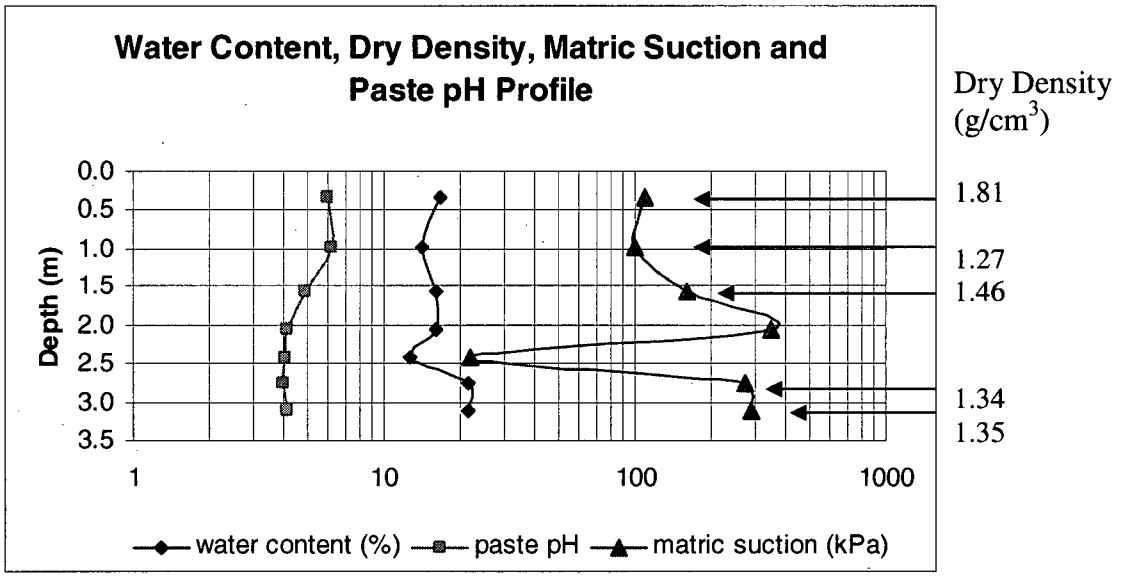

Fig. 18.1: Water Content, Dry Density, Matric Suction and Paste pH Values Measured Versus Depth in Test Pit 18.

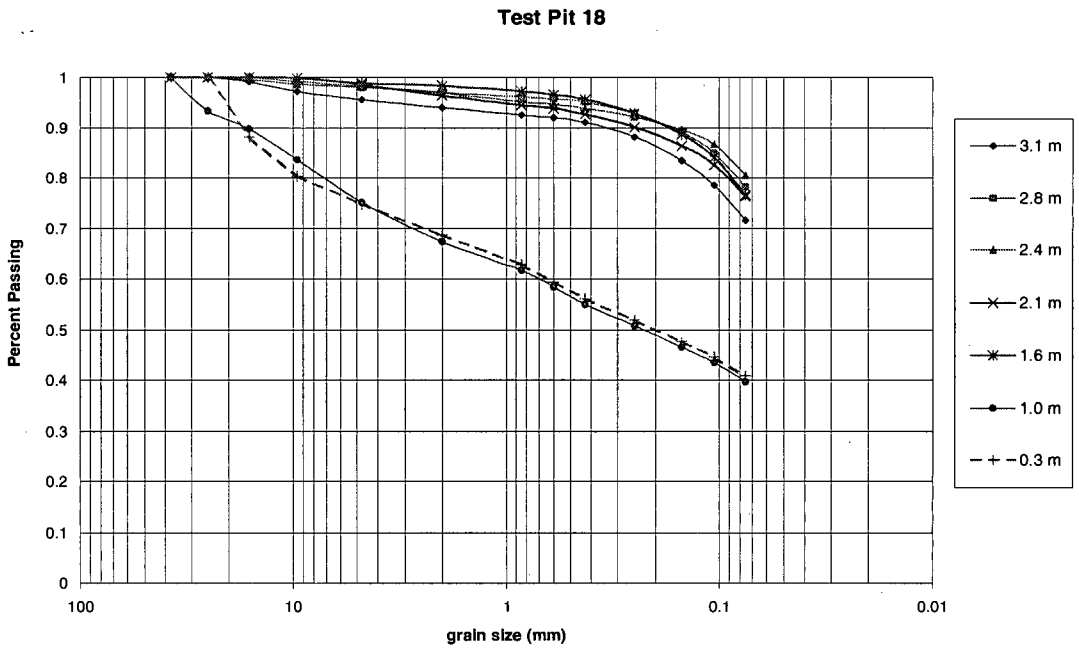

Fig. 18.2: Particle Size Distribution for Samples Encountered at Selected Depths.

TEST PIT 19

Test pit 19 was excavated July 17, 2000 to a depth of 3.3 m below the surface of the third bench. Four internal layers were observed in the profile of the test pit. Table 19.1 summarizes the materials and corresponding depth for each layer encountered. Photograph 19.1 shows a typical exposure of the excavated test pit.

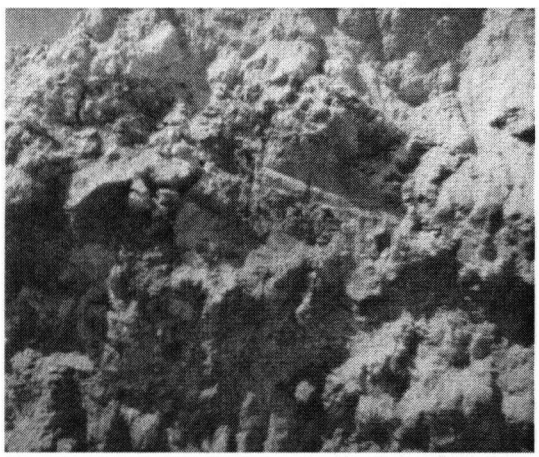

Photograph 19.1: Test Pit Excavation.

Table 19.1: Material Description Summary.

Depth (m)	Layer Inclination	Description
0.00		silt with clay
		red low
0.08	horizontal	pH
0.17		moist, plastic
0.17		clay with silt
		grey low
0.58	dipping 25°	pH
1.00		moist, stiff
		silt with clay and
1.00		sand
		light brown
1.67	dipping 25°	low pH
2.33		dry, stiff
		rock with silty
2.33		fines
2.83	dipping 20°	grey
3.33		dry, stiff

Figure 19.1 shows the water content, dry density, matric suction and paste pH profiles measured at selected depths in test pit 19. Figure 19.2 shows the particle size distribution for the materials sampled within test pit 19.

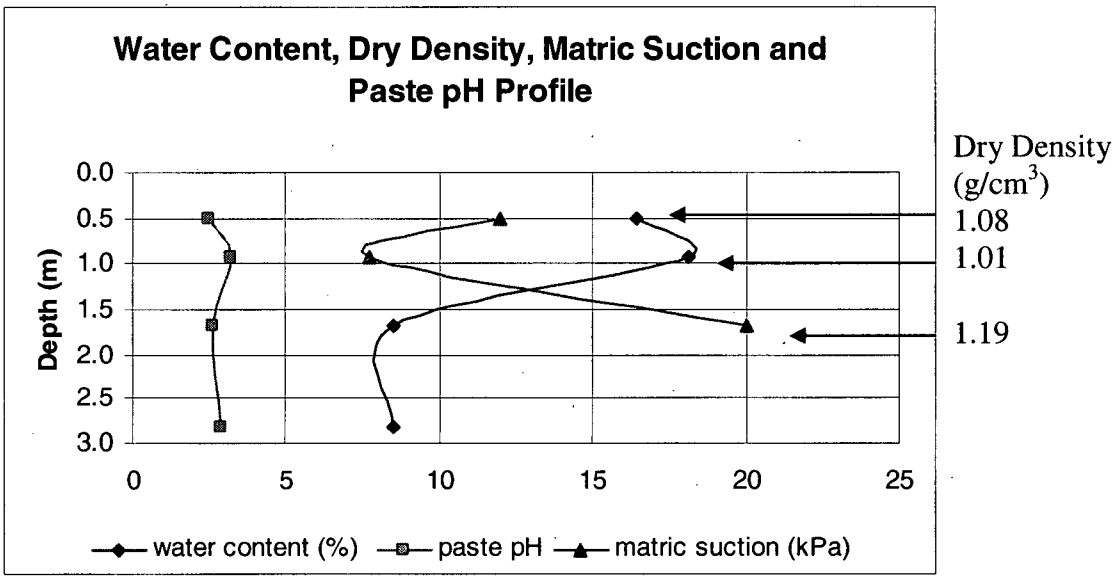

Fig. 19.1: Water Content, Dry Density, Matric Suction and Paste pH Values Measured Versus Depth in Test Pit 19.

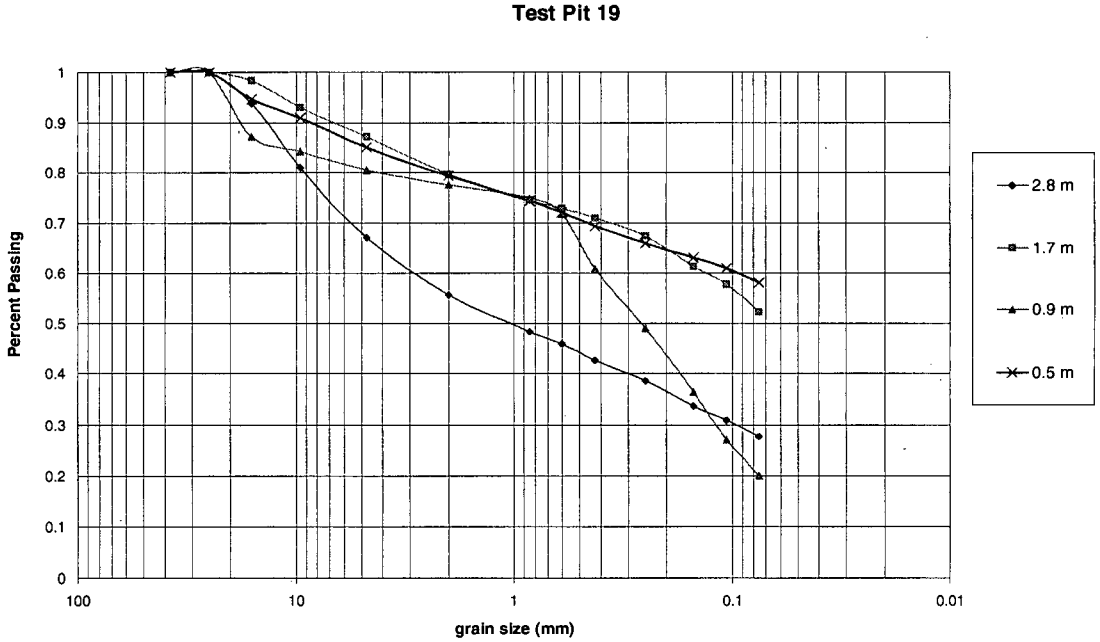

Fig. 19.2: Particle Size Distribution for Samples Encountered at Selected Depths.

TEST PIT 20

Test pit 20 was excavated July 18, 2000 to a depth of 2.83 m below the surface of the third bench. Five internal layers were observed in the profile of the test pit. Table 20.1 summarizes the materials and corresponding depth for each layer encountered. Photograph 20.1 shows a typical exposure of the excavated test pit.

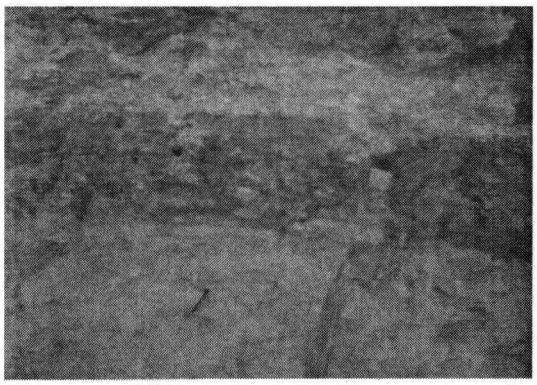

Photograph 20.1: Test Pit Excavation.

Table 20.1: Material Description Summary.

Depth (m)	Layer Inclination	Description
0.00		silt with clay brownish yellow
0.15	horizontal	low pH
0.31		wet, stiff
0.31		clay brownish yellow
0.32	horizontal	low pH
0.33		moist, friable
0.33		clay with silt dark red
0.42	horizontal	low pH
0.50		moist, stiff
0.50		gravel with silt and sand light grey low
1.17	dipping 30°	pH
1.83		dry, hard
1.83		silt with gravel, sand and clay olive grey low
2.33	dipping 30°	pH
2.83		damp, firm

Figure 20.1 shows the water content, dry density, matric suction and paste pH profiles measured at selected depths in test pit 20. Figure 20.2 shows the particle size distribution for the materials sampled within test pit 20.

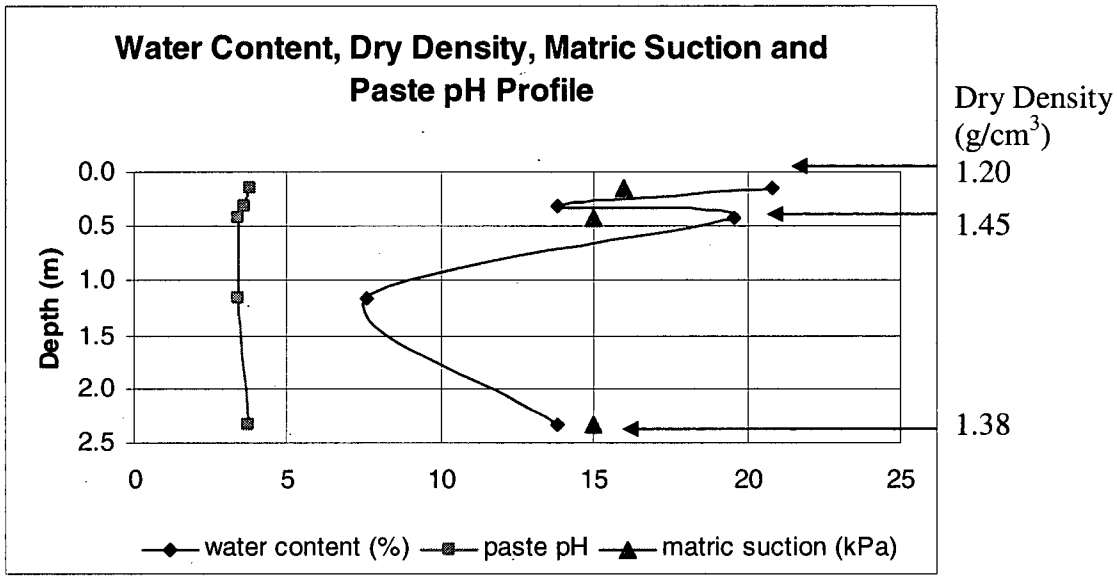

Fig. 20.1: Water Content, Dry Density, Matric Suction and Paste pH Values Measured Versus Depth in Test Pit 20.

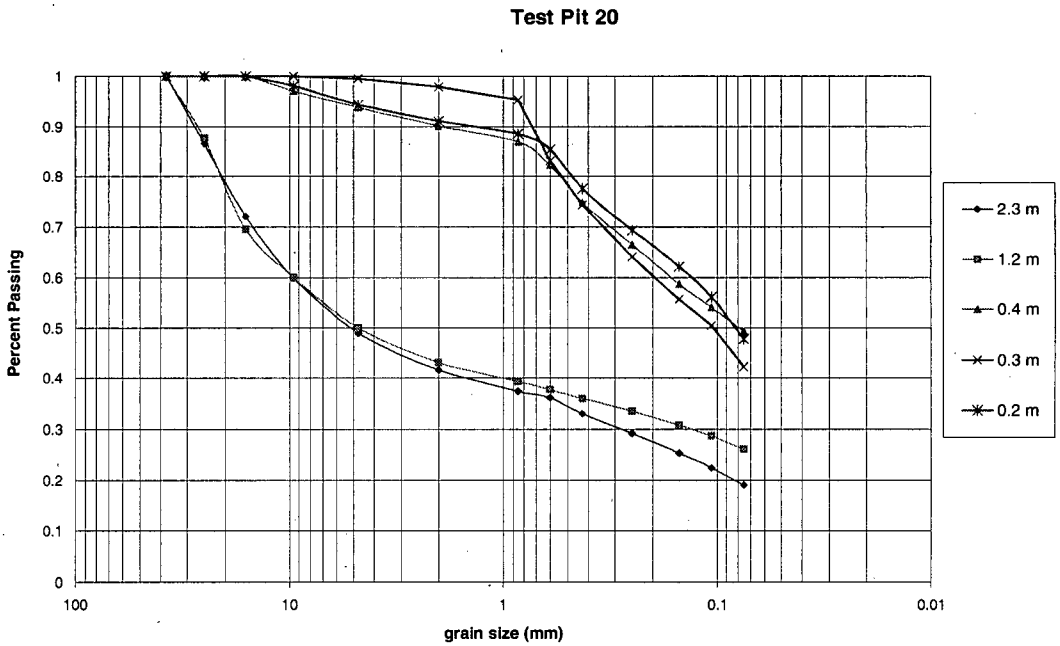

Fig. 20.2: Particle Size Distribution for Samples Encountered at Selected Depths.

TEST PIT 21

Test pit 21 was excavated July 24, 2000 to a depth of 3.3 m below the surface of the third bench. Three internal layers were observed in the profile of the test pit. Table 21.1 summarizes the materials and corresponding depth for each layer encountered. Photograph 21.1 shows a typical exposure of the excavated test pit.

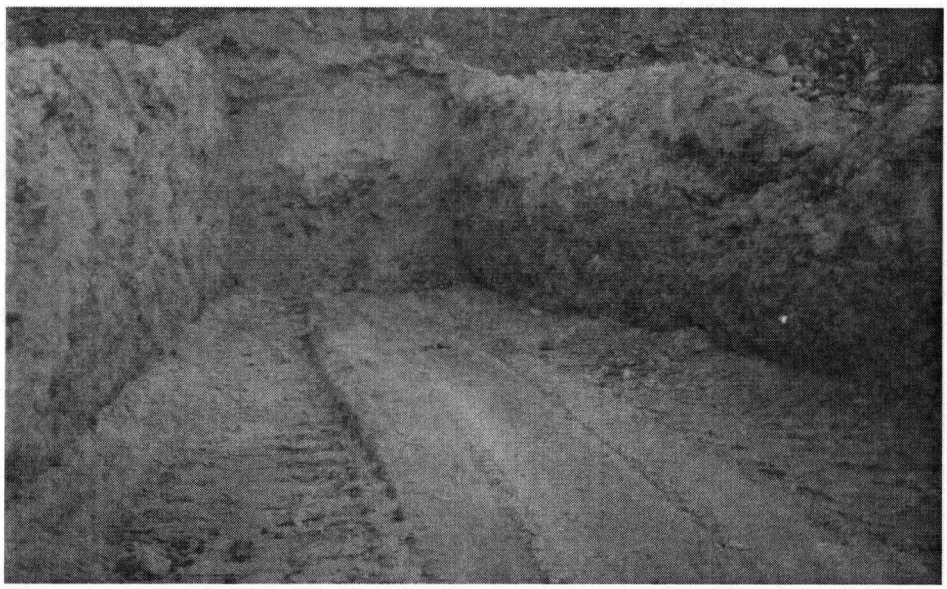

Photograph 21.1: Test Pit Excavation.

Table 21.1: Material Description Summary.

Depth (m)	Layer Inclination	Description
0.00		silt with clay and sand
0.67	dipping 10°	brownish yellow pH under 4.5
1.33		moist, friable
1.33		silt with clay pale yellow
1.67	dipping 10°	low pH
2.00		damp, friable
2.00		silt with clay reddish brown
2.67	dipping 10°	pH under 4.5
3.33		damp, friable

Figure 21.1 shows the water content, dry density, matric suction and paste pH profiles measured at selected depths in test pit 21. Figure 21.2 shows the particle size distribution for the materials sampled within test pit 21.

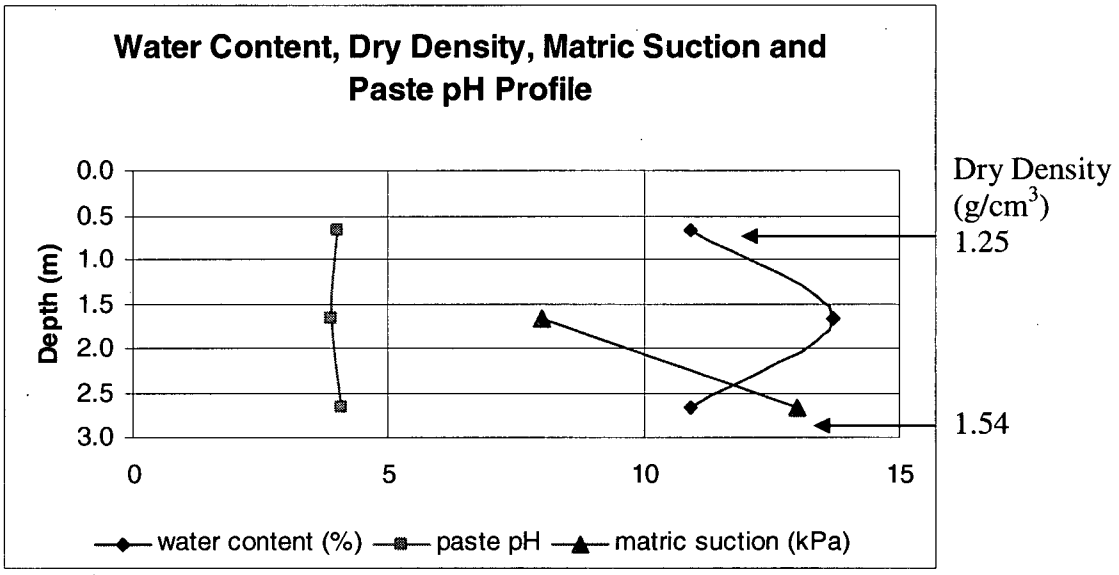

Fig. 21.1: Water Content, Dry Density, Matric Suction and Paste pH Values Measured Versus Depth in Test Pit 21.

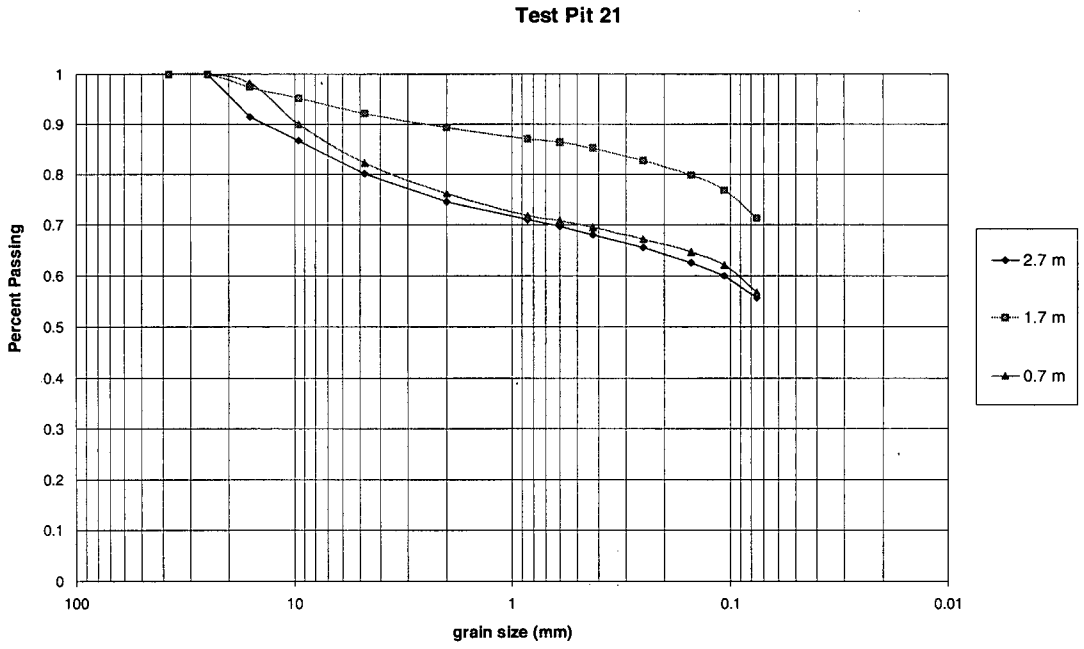

Fig. 21.2: Particle Size Distribution for Samples Encountered at Selected Depths.

TEST PIT 22

Test pit 22 was excavated July 24, 2000 to a depth of 2 m below the surface of the third bench. Three internal layers were observed in the profile of the test pit. The measurement of the profile was done at the angle of the layers within the test pit. Table 22.1 summarizes the materials and corresponding depth for each layer encountered. Photograph 22.1 shows a typical exposure of the excavated test pit.

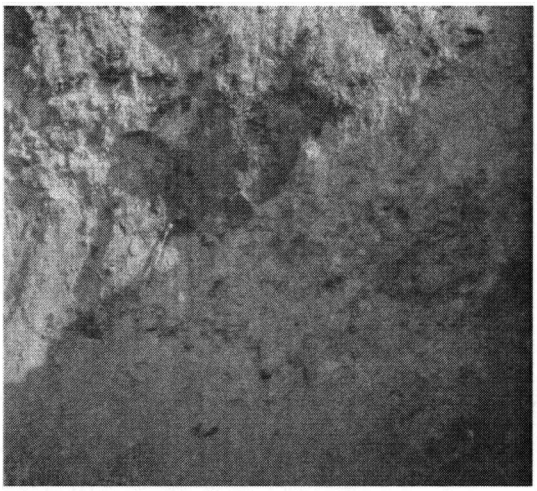

Photograph 22.1: Test Pit Excavation.

Table 22.1: Material Description Summary.

Depth (m)	Layer Inclination	Description
0.00		clay with silt red
0.17	dipping 60°	low pH
0.33		wet, stiff
0.33		rock and soil, gap graded brownish yellow
0.83	dipping 60°	low pH
1.33		moist, friable
1.33		rock and soil, gap graded light grey
1.50	dipping 60°	low pH
1.67		dry, friable

Figure 22.1 shows the water content and paste pH profiles measured at selected depths in test pit 22.Matric suction and density data was not collected for this test pit. Figure 22.2 shows the particle size distribution for the materials sampled within test pit 22.

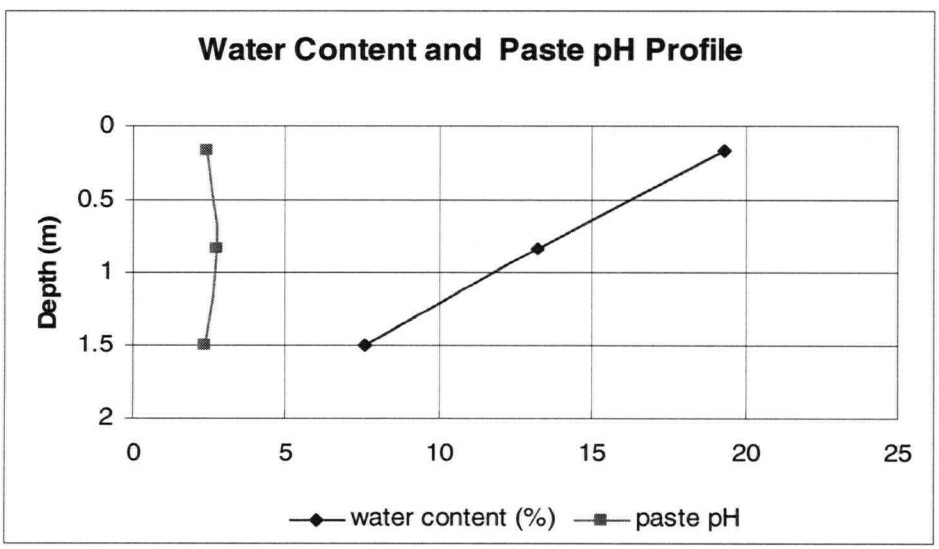

Fig. 22.1: Water Content and Paste pH Values Measured Versus Depth in Test Pit 22.

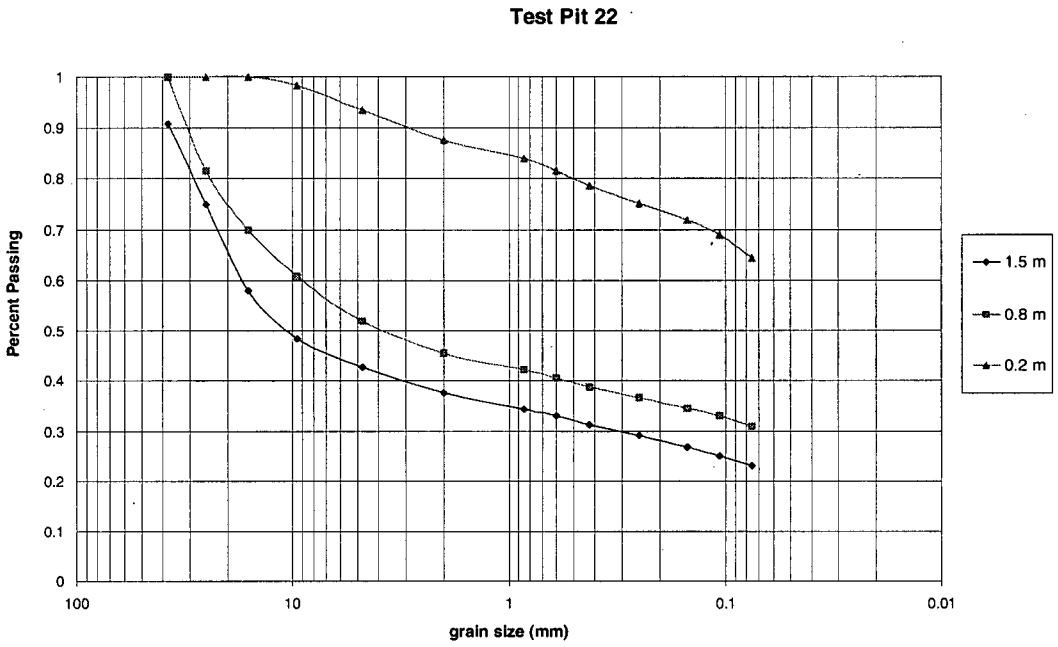

Fig. 22.2: Particle Size Distribution for Samples Encountered at Selected Depths.

TEST PIT 24

Test pit 24 was excavated August 10, 2000 to a depth of 1.33 m below the surface of the third bench. Six internal layers were observed in the profile of the test pit. Table 24.1 summarizes the materials and corresponding depth for each layer encountered. Photograph 24.1 shows a typical exposure of the excavated test pit.

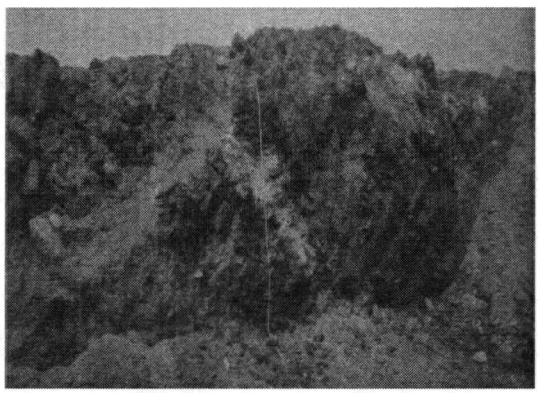

Photograph 24.1: Test Pit Excavation.

Table 24.1: Material Description Summary.

Depth (m)	Layer Inclination	Description
0.00		clay with silt and friable soil clumps
0.07	dipping 35°	dark green, no obvious signs of sulfide oxidation
0.15		wet, friable
0.15		sand with silt and rock particles
0.32	dipping 35°	pale yellow pH below 4.5
0.49		dry, rocky
0.49		clay
0.53	dipping 35°	red, no obvious signs of sulfide oxidation
0.57		moist, medium plasticity
0.57		clay
0.86	dipping 10°	red, green, yellow, no obvious signs of sulfide oxidation
1.15		moist, hardened, low plasticity
1.15		sand with clay and silt
1.19	dipping 10°	olive green
1.22		damp, cohesive
1.22		clay
1.28	dipping 20°	red
1.33		moist, friable

Figure 24.1 shows the water content, dry density and paste pH profiles measured at selected depths in test pit 24.Matric suction data was not collected for this test pit because the material was too rocky to allow for the installation of the tensiometers. Figure 24.2 shows the particle size distribution for the materials sampled within test pit 24.

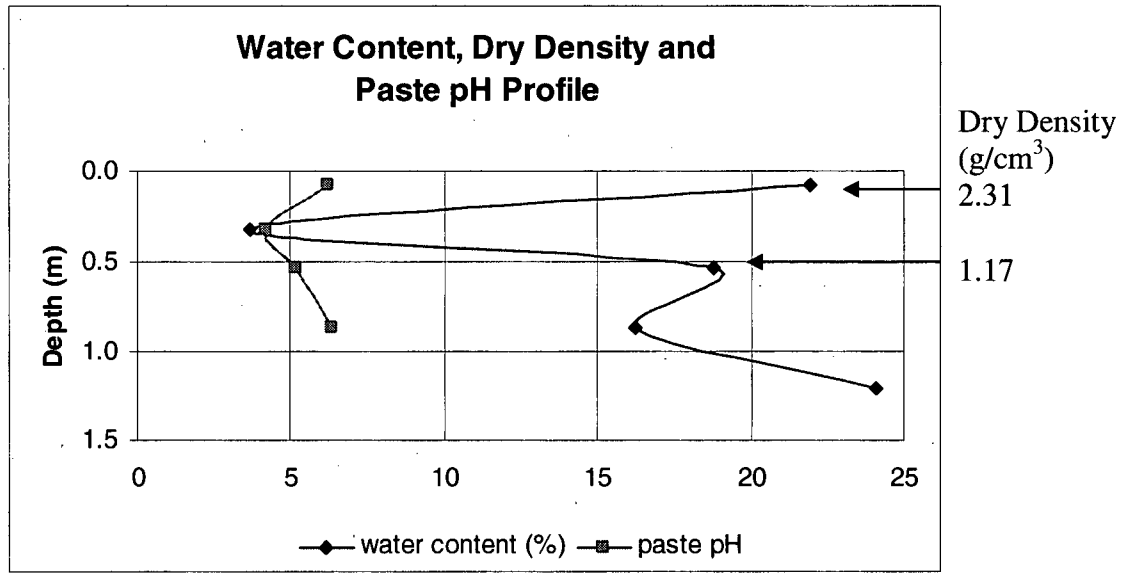

Fig. 24.1: Water Content, Dry Density and Paste pH Values Measured Versus Depth in Test Pit 24.

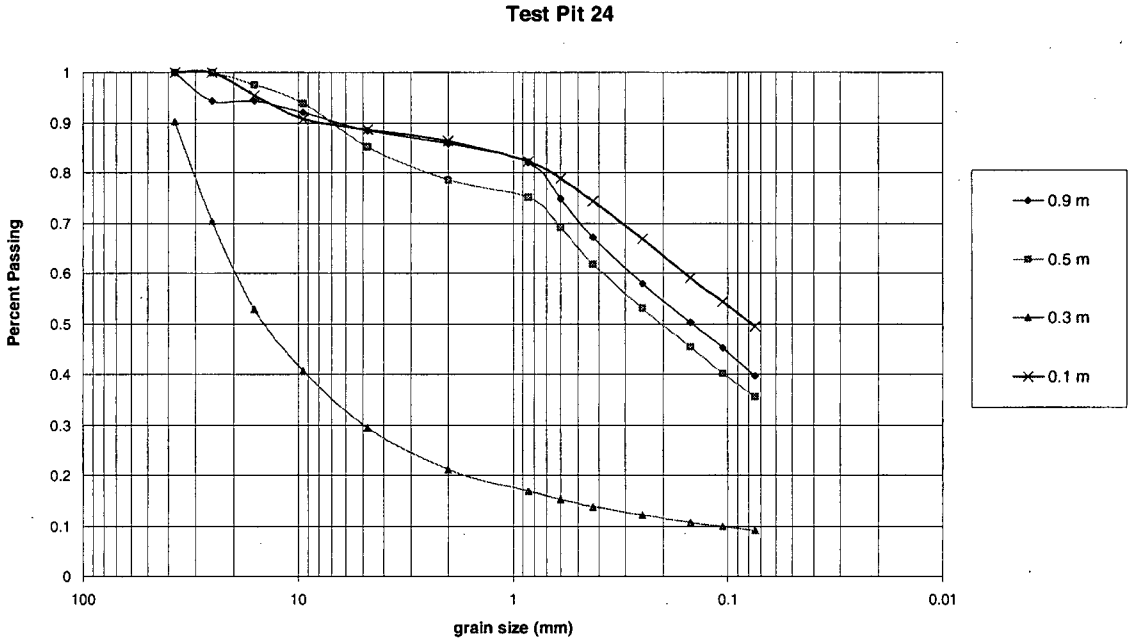

Fig. 24.2: Particle Size Distribution for Samples Encountered at Selected Depths.

TEST PIT 25

Test pit 25 was excavated August 15, 2000 to a depth of 1.66 m below the surface of the fourth bench. Four internal layers were observed in the profile of the test pit. Table 25.1 summarizes the materials and corresponding depth for each layer encountered. Photograph 25.1 shows a typical exposure of the excavated test pit.

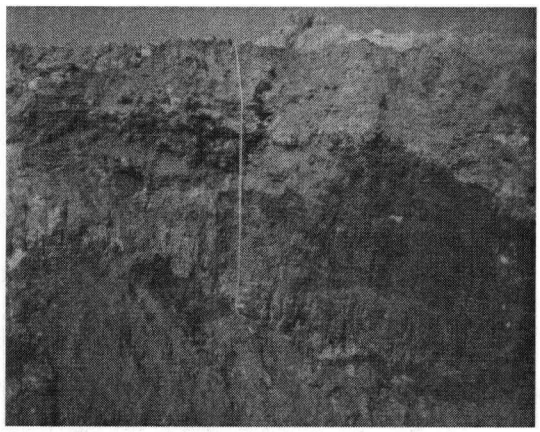

Photograph 25.1: Test Pit Excavation.

Table 25.1: Material Description Summary.

Depth (m)	Layer Inclination	Description
0.00		clay with silt and gravel light brown
0.28	dipping 20°	pH of 4.5
0.56		damp, soft
0.56		clay with silt pale yellow, no evidence of sulfide
0.61	dipping 20°	oxidation
0.67		moist, soft
0.67		clay with silt red, no evidence of
1.08	dipping 20°	sulfide oxidation
1.50		damp, friable
1.50		clay with silt pale yellow, no evidence of sulfide
1.58	dipping 20°	oxidation
1.67		moist, friable

Figure 25.1 shows the water content, dry density, matric suction and paste pH profiles measured at selected depths in test pit 25. Figure 25.2 shows the particle size distribution for the materials sampled within test pit 25.

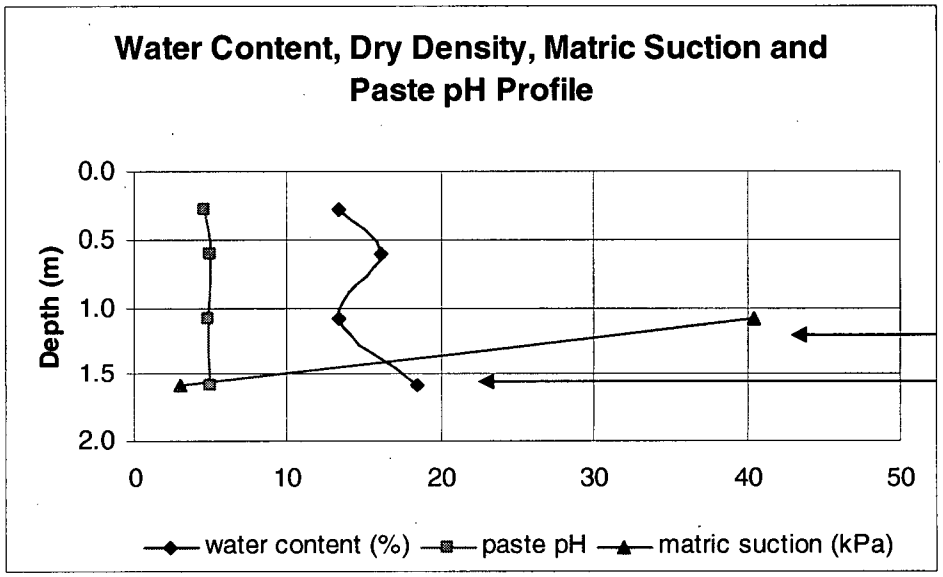

Fig. 25.1: Water Content, Dry Density, Matric Suction and Paste pH Values Measured Versus Depth in Test Pit 25.

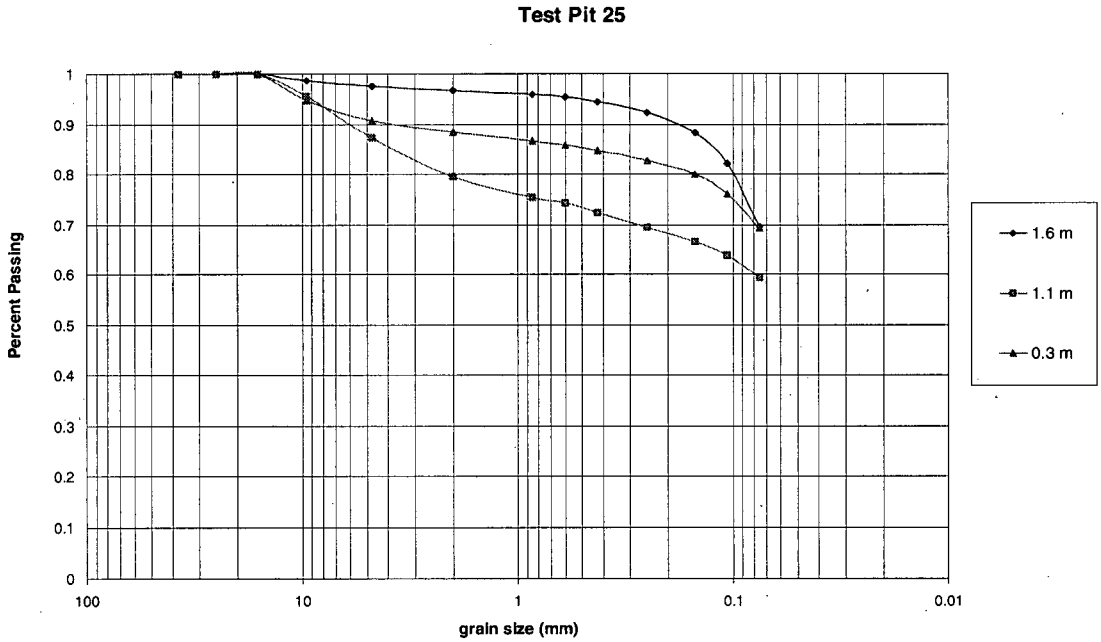

Fig. 25.2: Particle Size Distribution for Samples Encountered at Selected Depths.

TEST PIT 26

Test pit 26 was excavated August 21, 2000 to a depth of 1.83 m below the surface of the fourth bench. Two internal layers were observed in the profile of the test pit. Table 26.1 summarizes the materials and corresponding depth for each layer encountered. Photograph 26.1 shows a typical exposure of the excavated test pit.

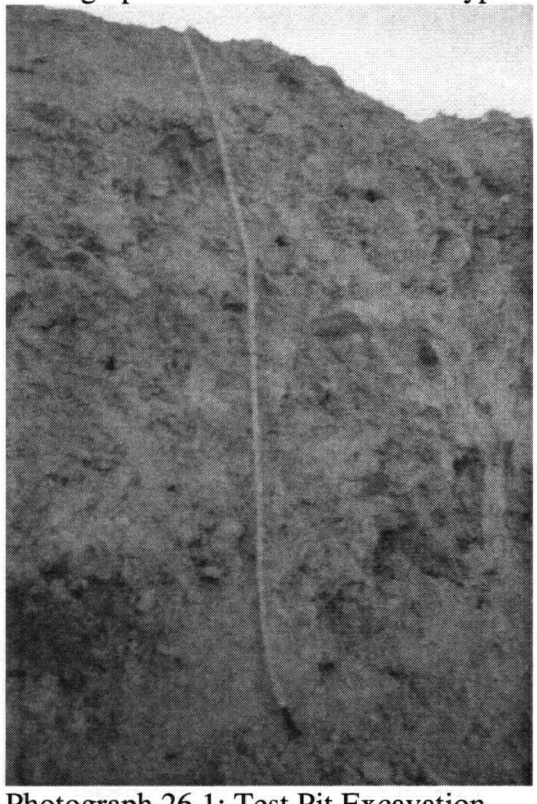

Photograph 26.1: Test Pit Excavation.

Table 26.1: Material Description Summary.

Depth (m)	Layer Inclination	Description
0.00		sand with silt and hard rock particles
0.54	dipping 15°	light grey pH below 4.5
1.08		moist, weathered
1.08		clay with silt and small hard rock particles
1.46	dipping 15°	light grey low pH
1.83		damp weathered

Figure 26.1 shows the water content, dry density and paste pH profiles measured at selected depths in test pit 26. The material in test pit 26 did not allow for the installation of tensiometers. Figure 26.2 shows the particle size distribution for the materials sampled within test pit 26.

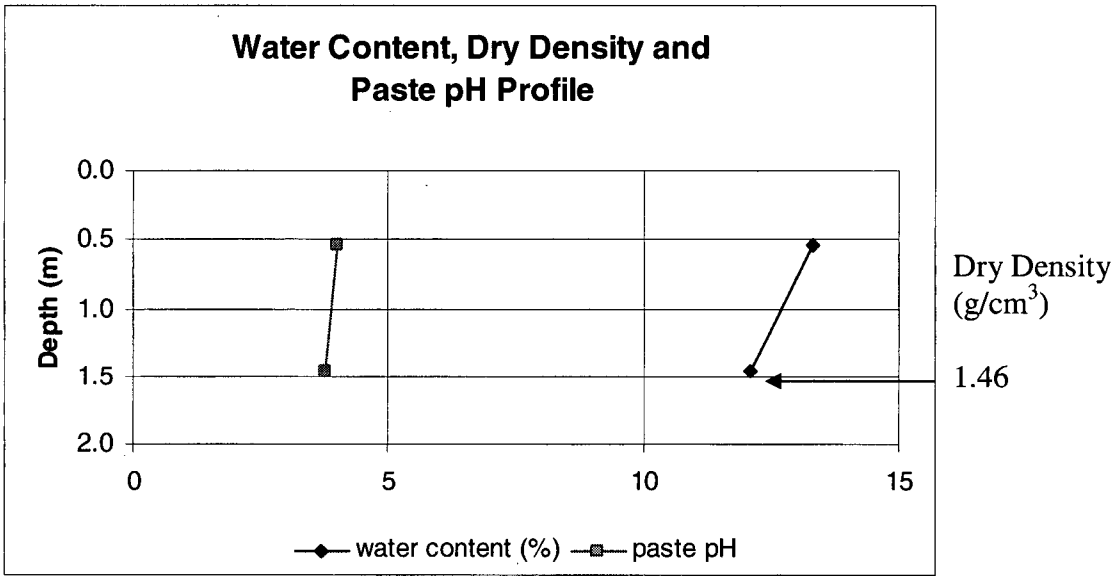

Fig. 26.1: Water Content, Dry Density and Paste pH Values Measured Versus Depth in Test Pit 26.

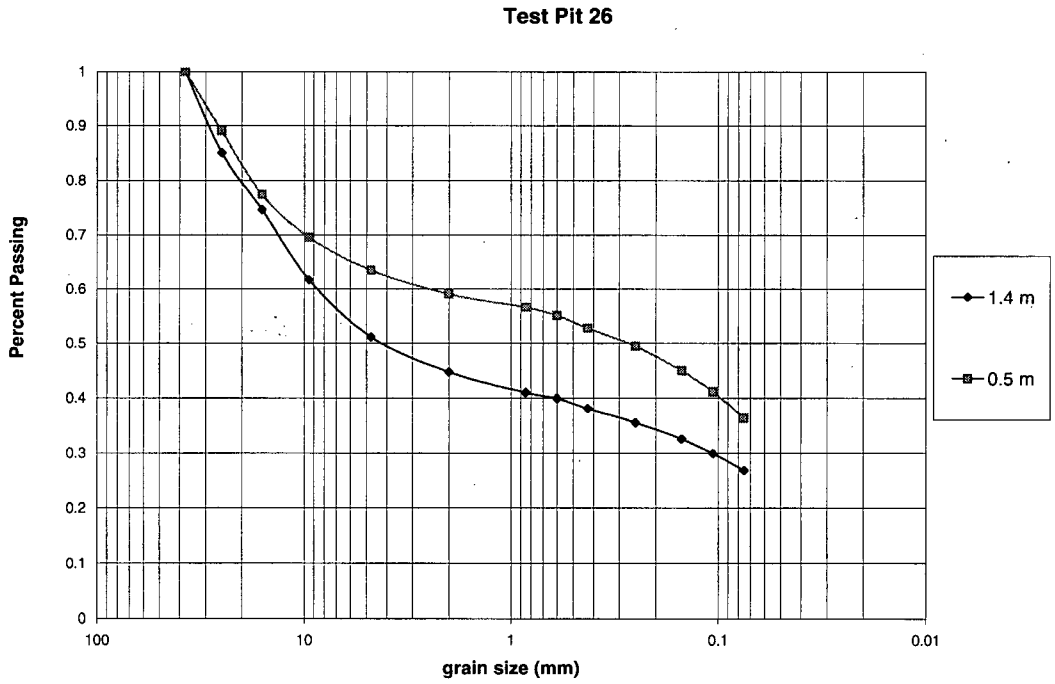

Fig. 26.2: Particle Size Distribution for Samples Encountered at Selected Depths.

TEST PIT 27

Test pit 27 was excavated August 28, 2000 to a depth of 1.83 m below the surface of the fourth bench. Four internal layers were observed in the profile of the test pit. Table 27.1 summarizes the materials and corresponding depth for each layer encountered. Photograph 27.1 shows a typical exposure of the excavated test pit.

Photograph 27.1: Test Pit Excavation.

Table 27.1: Material Description Summary.

Depth (m)	Layer Inclination	Description
0.00		clay with silt, sand and gravel
0.08	dipping 20°	brownish yellow low pH
0.17		damp, friable
0.17		sand with silt and large angular rock
0.50	dipping 25°	brown low pH
0.83		dry, weathered
0.83		clay with silt and small rock fragments
1.00	dipping 25°	pink low pH
1.17		damp, soft
1.17		clay with silt and 3" rock particles
1.33	horizontal	grey low pH
1.50		dry, weathered

Figure 27.1 shows the water content, dry density, matric suction and paste pH profiles measured at selected depths in test pit 27. Figure 27.2 shows the particle size distribution for the materials sampled within test pit 27.

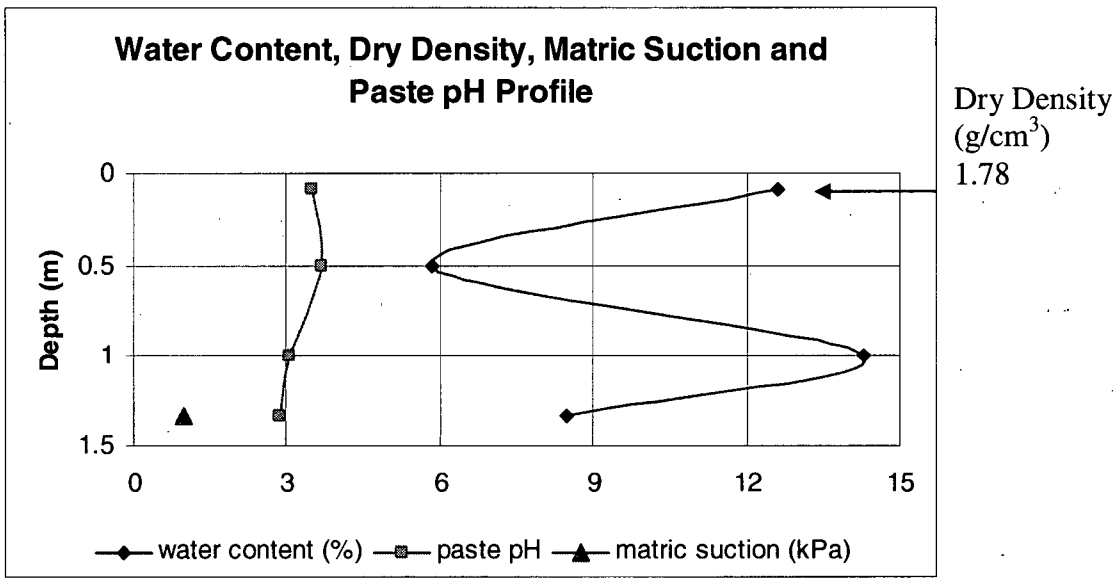

Fig. 27.1: Water Content, Dry Density and Paste pH Values Measured Versus Depth in Test Pit 27.

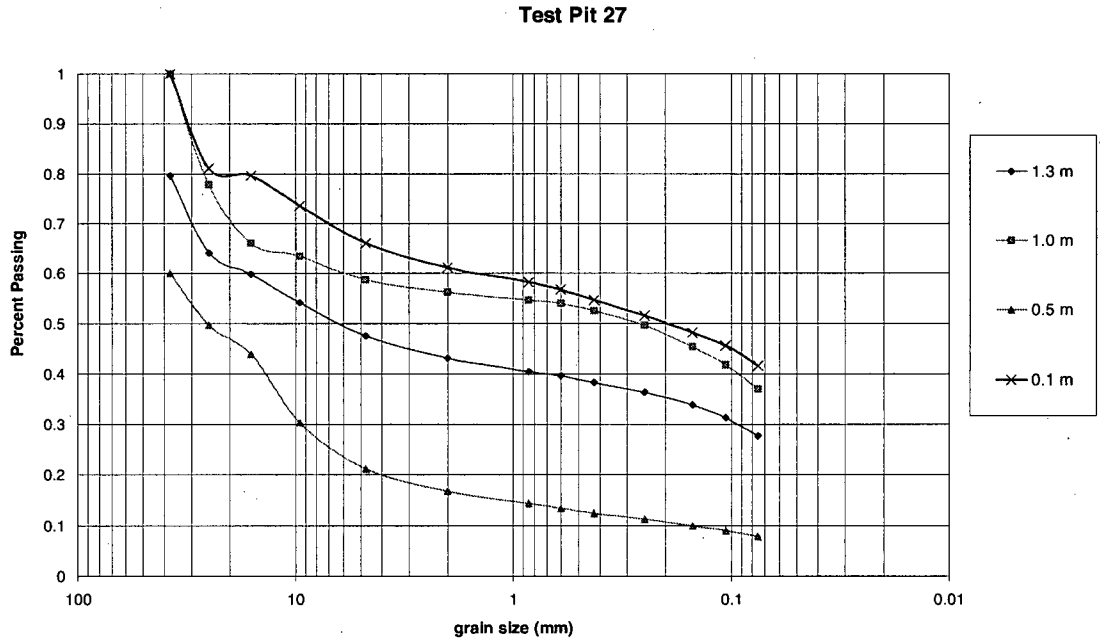

Fig. 27.2: Particle Size Distribution for Samples Encountered at Selected Depths.

TEST PIT 28

Test pit 28 was excavated October 20, 2000 to a depth of 1.89 m below the surface of the fifth bench. Five internal layers were observed in the profile of the test pit. Table 28.1 summarizes the materials and corresponding depth for each layer encountered. Photograph 28.1 shows a typical exposure of the excavated test pit.

Photograph 28.1: Test Pit Excavation.

Table 28.1: Material Description Summary.

Depth (m)	Layer Inclination	Description
0.00		sand with silt and rock particles
0.28	dipping 15°	reddish brown
0.56		dry, weathered
0.56		sand with silt and rock particles
0.79	dipping 15°	greyish green pH under 5
1.03		dry, weathered
1.03		sand with silt and rock particles
1.12	dipping 15°	brown
1.22		moist, stiff
1.22		gravel with silt and clay
1.36	dipping 15°	greyish green pH under 4.5
1.50		damp, friable
1.50		silt with sand and hard rock particles
1.69	dipping 15°	brown pH under 4.5
1.89		dry, weathered

Figure 28.1 shows the water content, dry density and paste pH profiles measured at selected depths in test pit 28. The material in test pit 28 did not allow for the installation of tensiometers. Figure 28.2 shows the particle size distribution for the materials sampled within test pit 28.

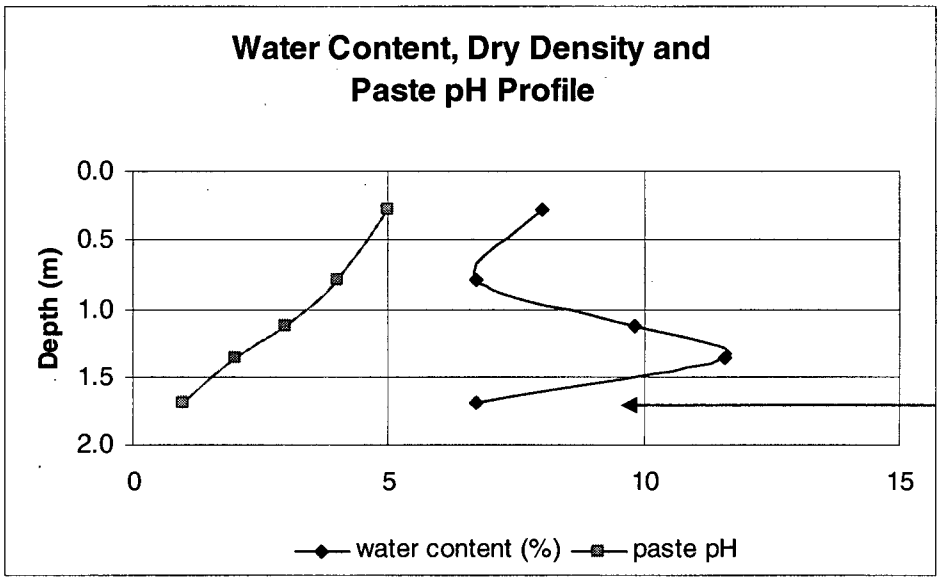

Fig. 28.1: Water Content, Dry Density and Paste pH Values Measured Versus Depth in Test Pit 28.

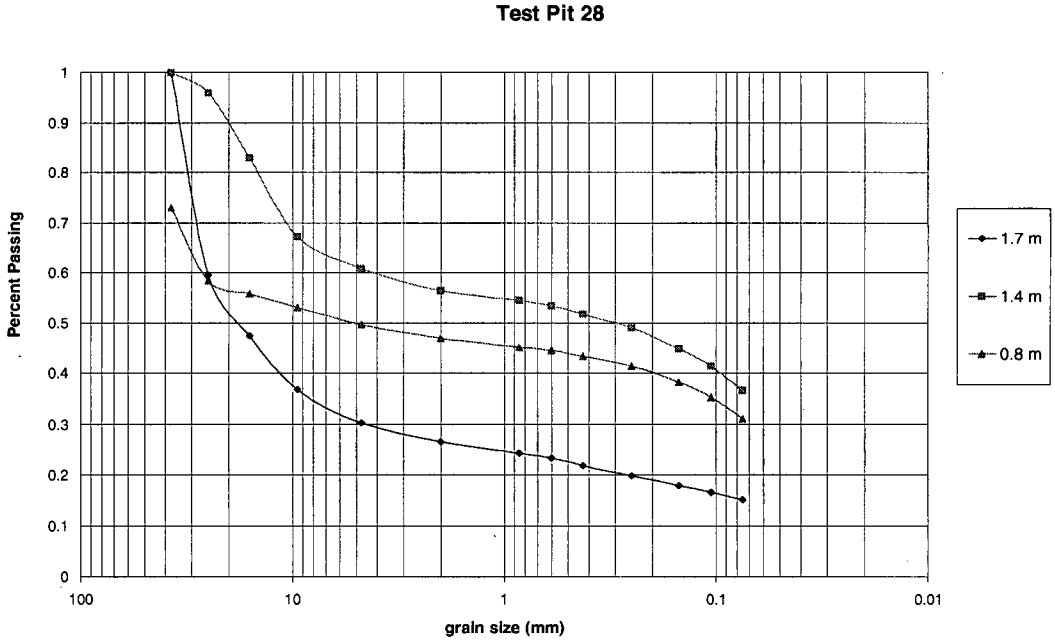

Fig. 28.2: Particle Size Distribution for Samples Encountered at Selected Depths.

TEST PIT 29

Test pit 29 was excavated October 20, 2000 to a depth of 1.33 m below the surface of the fifth bench. Three internal layers were observed in the profile of the test pit. Table 29.1 summarizes the materials and corresponding depth for each layer encountered. Photograph 29.1 shows a typical exposure of the excavated test pit.

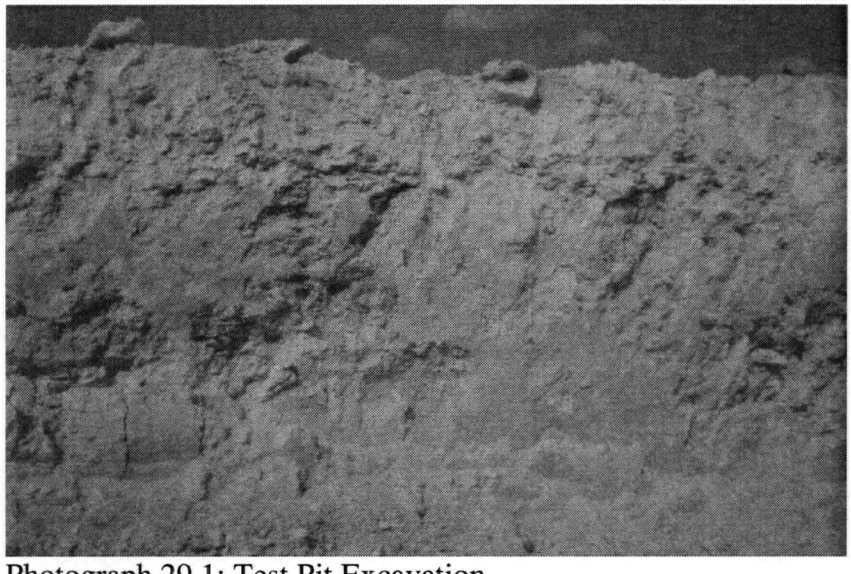

Photograph 29.1: Test Pit Excavation.

Table 29.1: Material Description Summary.

Depth (m)	Layer Inclination	Description
0.00		sand with silt and gravel
	inclinded	brown pH
0.33	10°	under 4.5
0.67		dry, weathered
0.67		gravel with silt and rock
	inclinded	greenish grey
0.86	10°	pH under 5
1.06		moist, friable
1.06		clay with silt and rock
		red pH
1.36	dipping 10°	under 5
1.67		dry, weathered

APPENDIX I

Figure 29.1 shows the water content, dry density, matric suction and paste pH profiles measured at selected depths in test pit 29. Figure 29.2 shows the particle size distribution for the materials sampled within test pit 29.

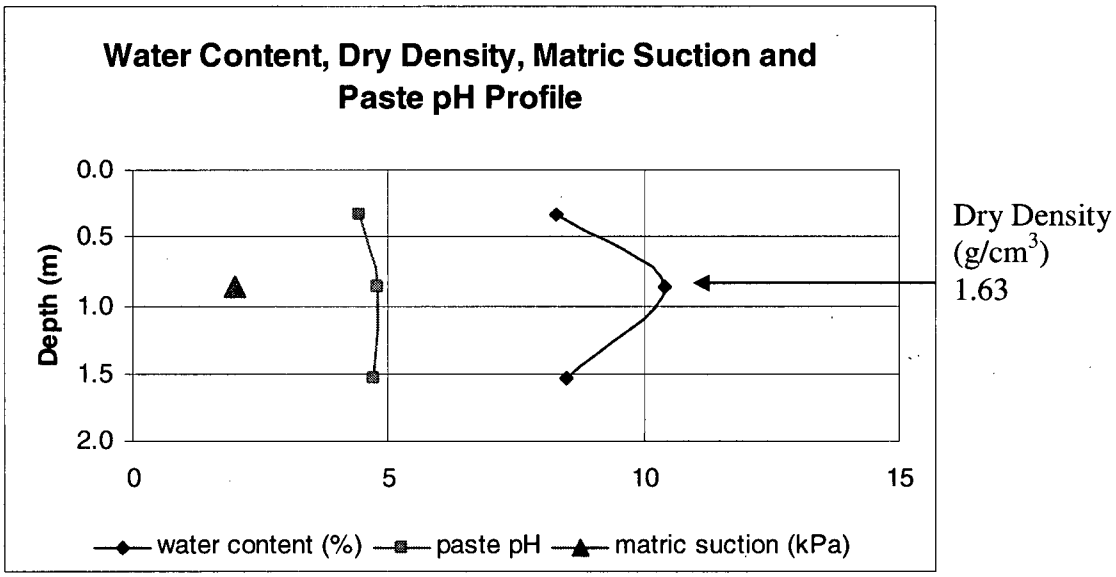

Fig. 29.1: Water Content, Dry Density and Paste pH Values Measured Versus Depth in Test Pit 29.

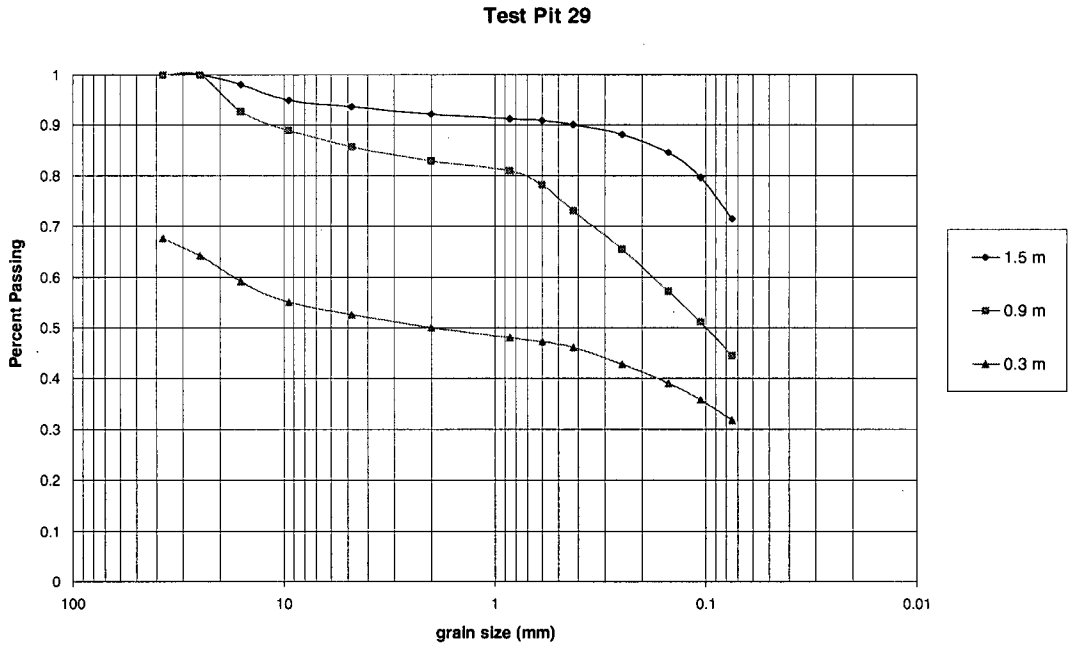

Fig. 29.2: Particle Size Distribution for Samples Encountered at Selected Depths.

APPENDIX II

Site 2 Test Pit Logs

TEST PIT 11

Test pit 11 was excavated November 10, 2000 to a depth of 1.2 m below the surface of the top bench. Three internal layers were observed in the profile of the test pit. Table 11.1 summarizes the materials and corresponding depth for each layer encountered. Photograph 11.1 shows a typical exposure of the excavated test pit

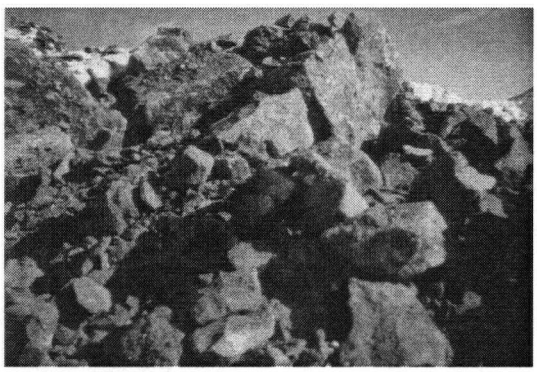

Photograph 11.1: Test Pit Excavation.

Table 11.1: Material Description Summary

Depth (m)	Layer inclination	Description
0.00		angular gravel with high silt content and no plasticity
0.08	dipping 15°	dark grey
0.17		damp, friable
0.17		coarse angular rock with gravel
0.33	dipping 15°	grey
0.50		dry, stiff
0.50		gap graded 2-6" rock with silt and clay matrix
0.83	dipping 15°	olive brown
1.17		damp, friable

Figure 11.1 shows the water content and paste pH profiles measured at selected depths in test pit 11.

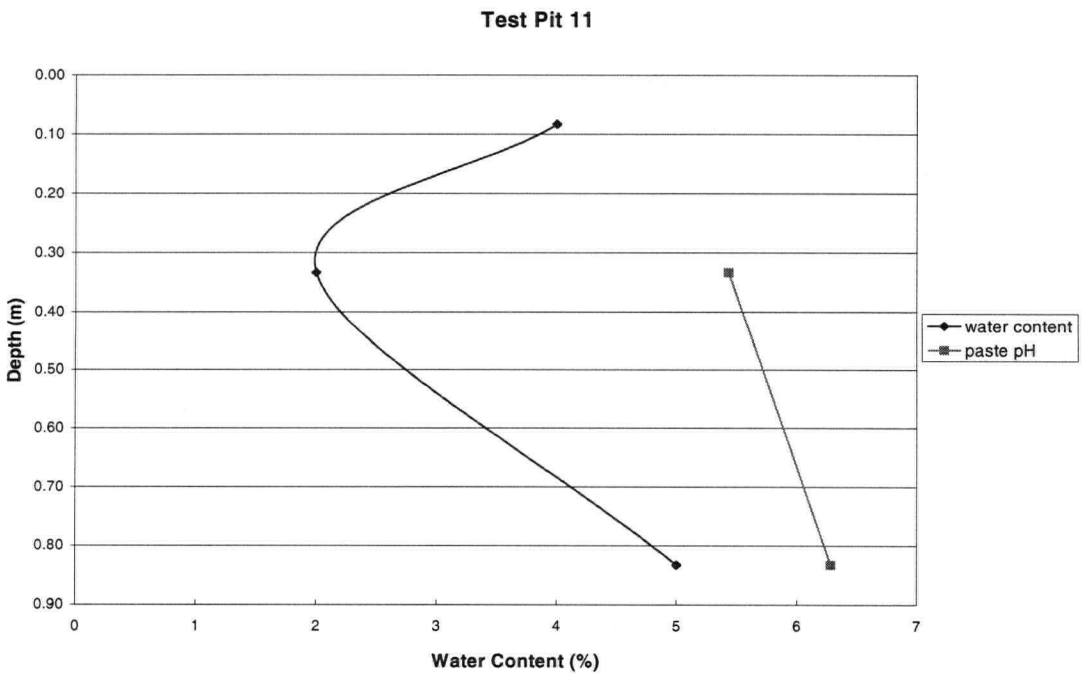

Fig. 11.1 Water Content and Paste pH Profiles Measured at selected Depths in Test Pit 11.

TEST PIT 12

Test pit 12 was excavated November 10, 2000 to a depth of 2.66 m below the surface of the second bench. Three internal layers were observed in the profile of the test pit. Table 12.1 summarizes the materials and corresponding depth for each layer encountered. Photograph 12.1 shows a typical exposure of the excavated test pit.

Table 12.1: Material Description Summary.

Depth (m)	Layer Inclination	Description
0.00		angular gravel with 4" max particle size
0.63	horizontal	grey
1.25		dry, stiff
1.25		angular gravel and rock and 5 to 10% clay sized particles
1.46	horizontal	yellowish brown
1.67		damp, friable
1.67		angular rock 2-6"
2.17	horizontal	grey to purple
2.67		dry, stiff

Figure 12.1 shows the water content and paste pH profiles measured at selected depths in test pit 12.

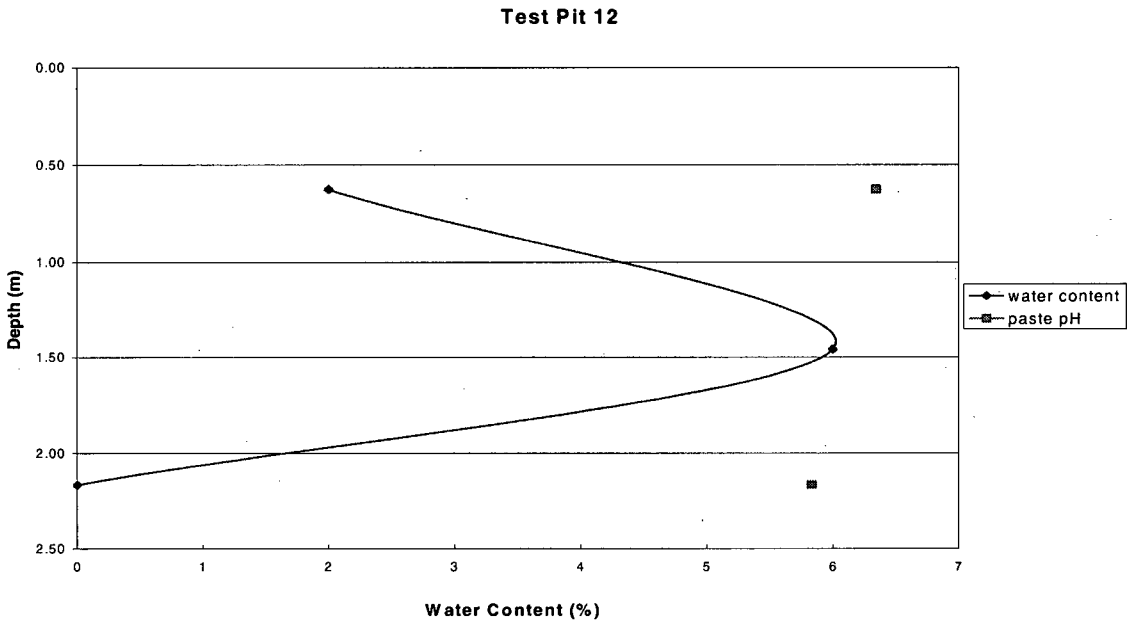

Fig. 12.1: Water Content and Paste pH Profiles Measured at Selected Depths in Test Pit 12.

TEST PIT 13

Test pit 13 was excavated February 23, 2001 to a depth of 3.33 m below the surface of the forth bench. Six internal layers were observed in the profile of the test pit. Table 13.1 summarizes the materials and corresponding depth for each layer encountered. Photograph 13.1 shows a typical exposure of the excavated test pit.

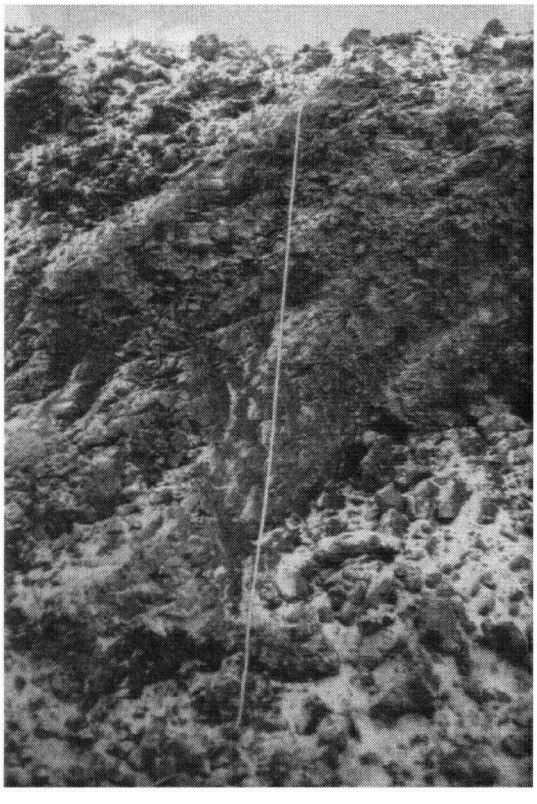

Photograph 13.1: Test Pit Excavation.

Table 13.1: Material Description Summary

Depth	Layer Inclination	Description
0.00		large rock and 50% sand and silt sized material
0.42	dipping 35°	yellowish brown
0.83		damp, stiff
0.83		unoxidized rock with fine matrix material
1.00	dipping 35°	olive grey
1.17		damp, soft
1.17		clay silt with gravel
1.25	dipping 35°	yellowish brown
1.33		dry, stiff
1.33		unoxidized rock, few fines
1.75	dipping 35°	olive grey
2.17		damp, soft
2.17		clayey silt with small rock particles
2.33	dipping 35°	brown
2.50		damp, friable
2.50		hard rock with sandy silt matrix material
2.92	dipping 35°	yellowish brown
3.33		dry, stiff

Figure 13.1 shows the water content and paste pH profile measured at selected depths in test pit 13. Figure 13.2 shows the grain size distributions for two materials sampled from within test pit 13.

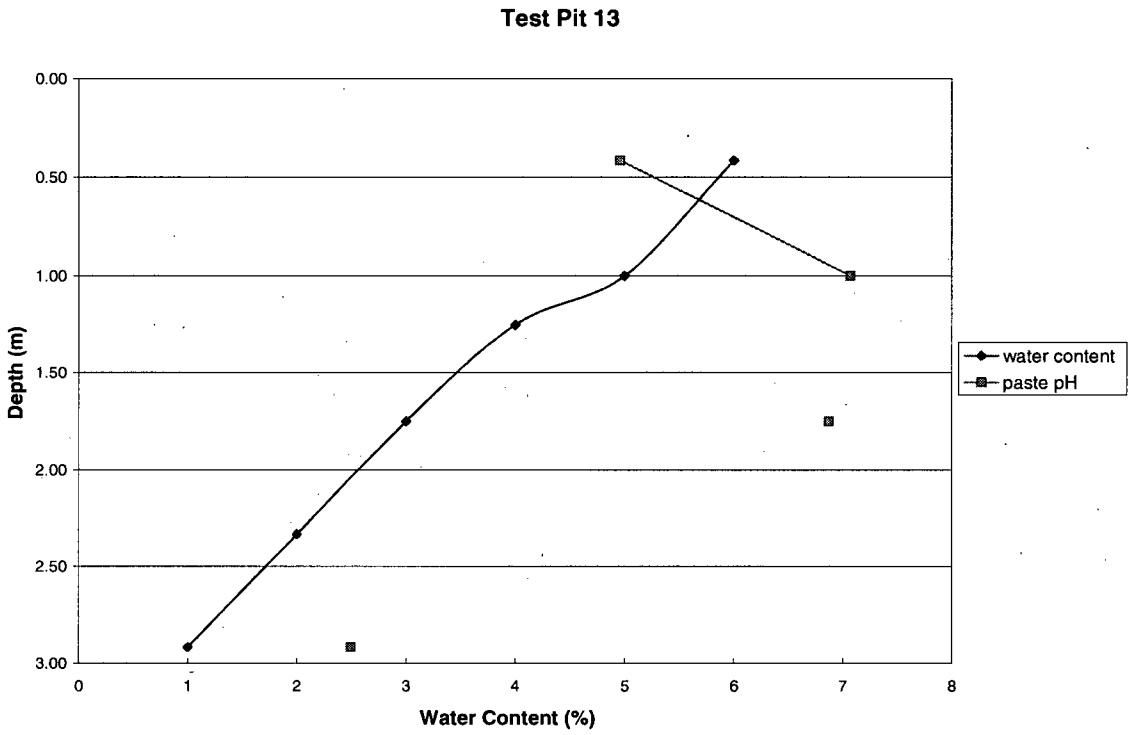

Fig. 13.1: Water Content Profile Measured at Selected Depths in Test Pit 13.

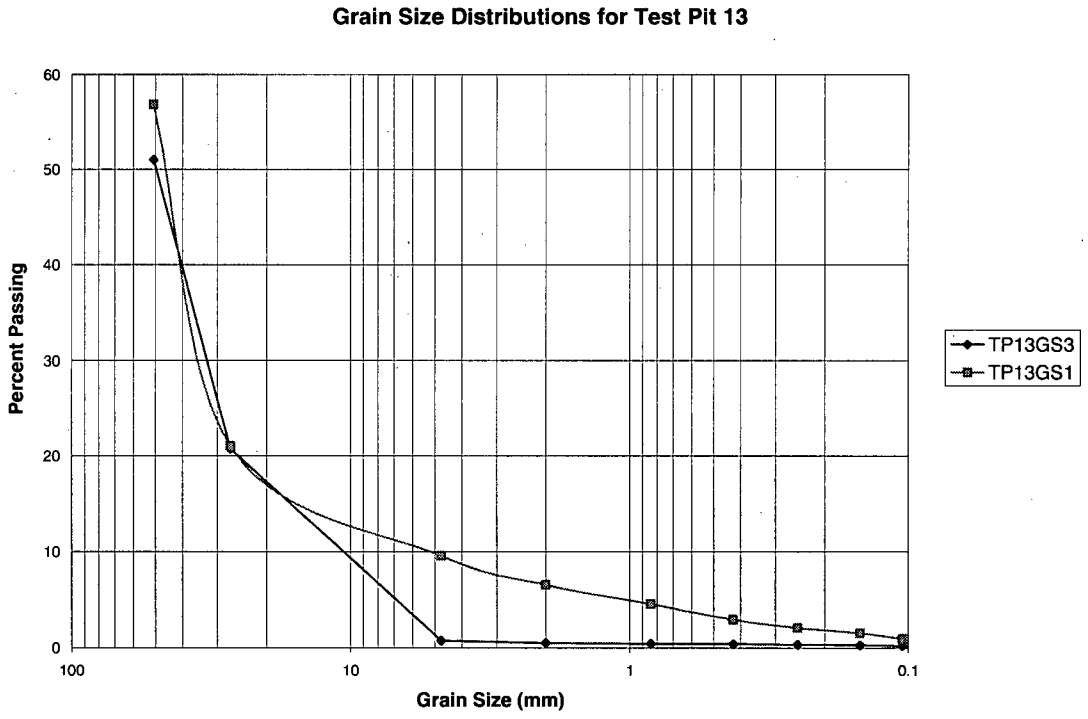

Fig. 13.2: Grain Size Distributions for Materials in Test Pit 13.

TEST PIT 14

Test pit 14 was excavated February 22, 2001 to a depth of 4.0 m below the surface of the forth bench. Two internal layers were observed in the profile of the test pit. Table 14.1 summarizes the materials and corresponding depth for each layer encountered. Photograph 14.1 shows a typical exposure of the excavated test pit.

Table 14.1: Material Description Summary.

Depth (m)	Layer Inclination	Description
0		large rock, few fines edge of layer shows migration of oxidation products
1	dipping 20°	olive grey
2		dry, hard
2		large rock and cobbles with silt and sand sized material
3	dipping 20°	yellowish brown
4		wet, stiff

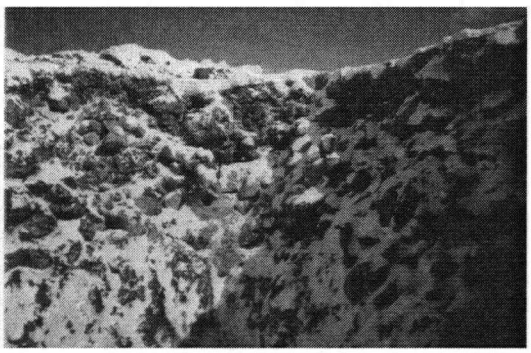

Photograph 14.1: Test Pit Excavation.

Figure 14.1 shows the water content profile measured at selected depths in test pit 14.

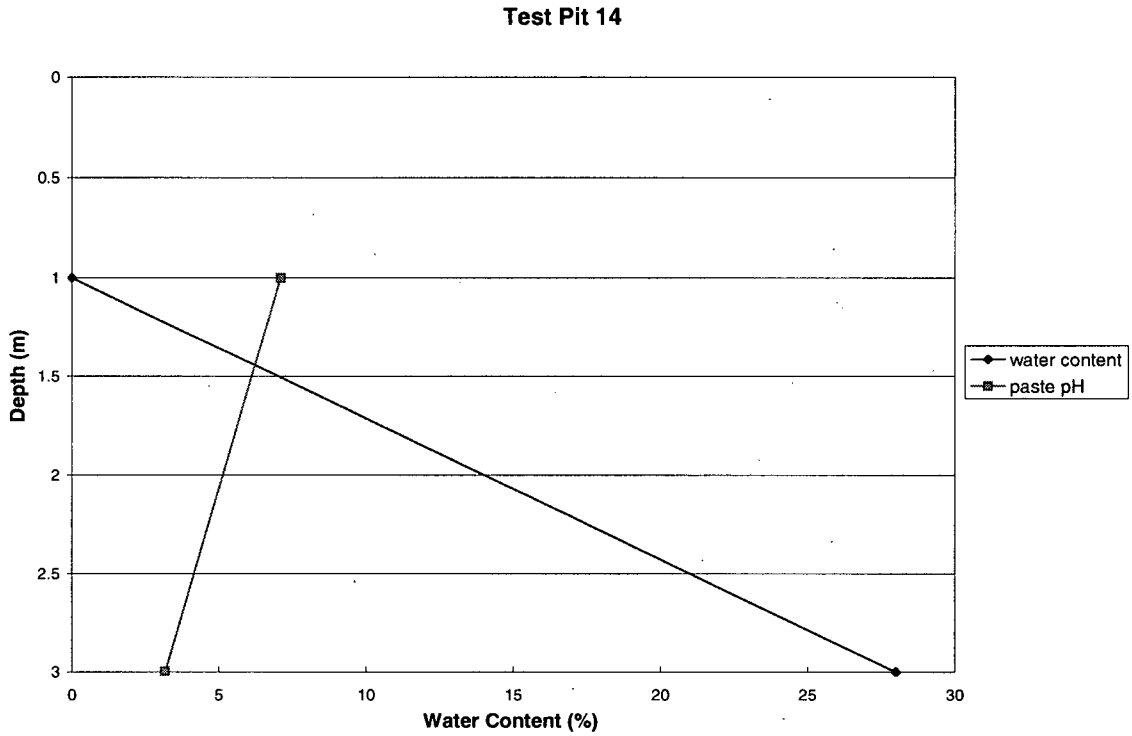

Fig. 14.1: Water Content Profile Measured at Selected Depths in Test Pit 14.

TEST PIT 15

Test pit 15 was excavated May 5, 2001 to a depth of 3.33 m below the surface of the fifth bench. Four internal layers were observed in the profile of the test pit. Table 15.1 summarizes the materials and corresponding depth for each layer encountered. Photograph 15.1 shows a typical exposure of the excavated test pit.

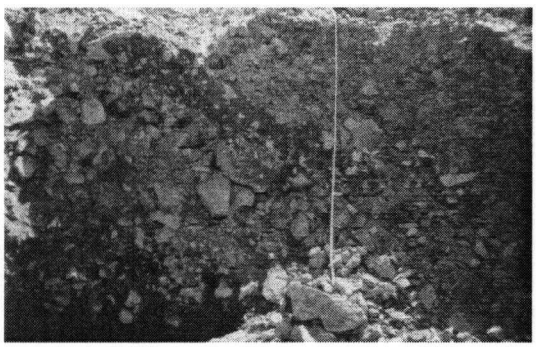

Photograph 15.1: Test Pit Excavation

Table 15.1: Material Description Summary.

Depth (m)	Layer Inclination	Description
0.00		sandy with small gravel and silt fraction
0.17	horizontal	brown
0.33		dry
0.33		large cobbles and boulders
0.96	dipping 25°	yellowish brown
1.58		dry
1.58		sandy silt with gravel and cobbles
1.79	dipping 25°	dark brown
2.00		dry
2.00		silty sand with gravel and cobbles
2.67	horizontal	brown
3.33		damp

Figure 15.1 shows the grain size distributions for the materials sampled within test pit 15.

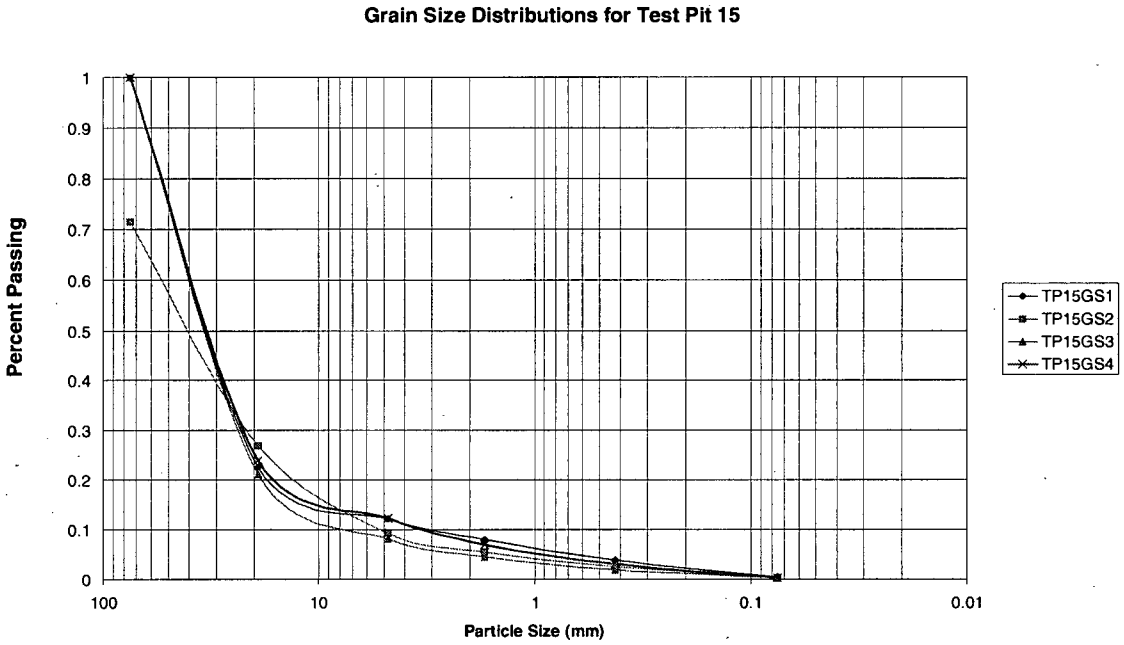

Fig. 15.1: Grain Size Distributions for Materials in Test Pit 15.

TEST PIT 16

Test pit 16 was excavated May 5, 2001 to a depth of 2.67 m below the surface of the fifth bench. Four internal layers were observed in the profile of the test pit. Table 16.1 summarizes the materials and corresponding depth for each layer encountered. Photograph 16.1 shows a typical exposure of the excavated test pit.

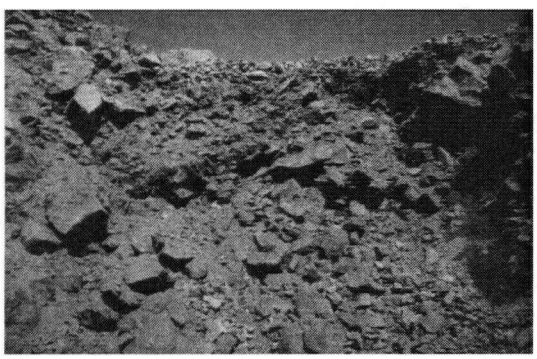

Photograph 16.1: Test Pit Excavation.

Table 16.1: Material Description Summary.

Depth (m)	Layer Inclination	Description
0.00		gravel and cobble with silty clay matrix
0.50	dipping 25°	yellowish brown
1.00		dry, stiff
1.00		silty clay and tree roots
1.33	dipping 25°	dark brown
1.67		moist, frozen
1.67		gravel and cobble with silty clay matrix
1.83	dipping 25°	yellowish brown
2.00		dry, stiff
2.00		silty sand with clay and gravel
2.33	dipping 25°	brown
2.67		wet, soft

Figure 16.1 shows the grain size distributions for the materials sampled in test pit 16.

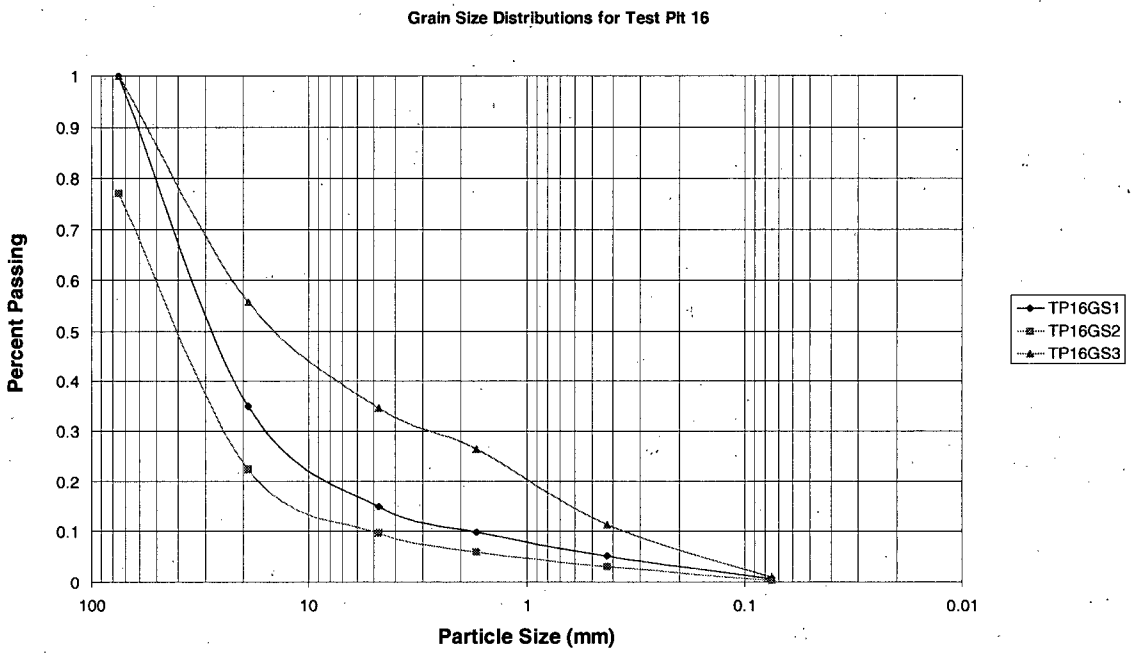

Fig. 16.1: Grain Size Distributions for Materials in Test Pit 16.

TEST PIT 17

Test pit 17 was excavated May 5, 2001 to a depth of 4.0 m below the surface of the fifth bench. Two internal layers were observed in the profile of the test pit. Table 17.1 summarizes the materials and corresponding depth for each layer encountered. Photograph 17.1 shows a typical exposure of the excavated test pit.

Table 17.1: Material Description Summary.

Depth (m)	Layer Inclination	Description
0.00		sandy silt matrix around gravel to boulder sized particles
0.67	horizontal	olive grey
1.33		dry, stiff
1.33		silt, sand, gravel, cobble angular and dry
2.67	horizontal	yellowish brown
4.00		dry, stiff

Photograph 17.1: Test Pit Excavation.

Figure 17.1 shows the grain size distributions for the materials sampled in test pit 17.

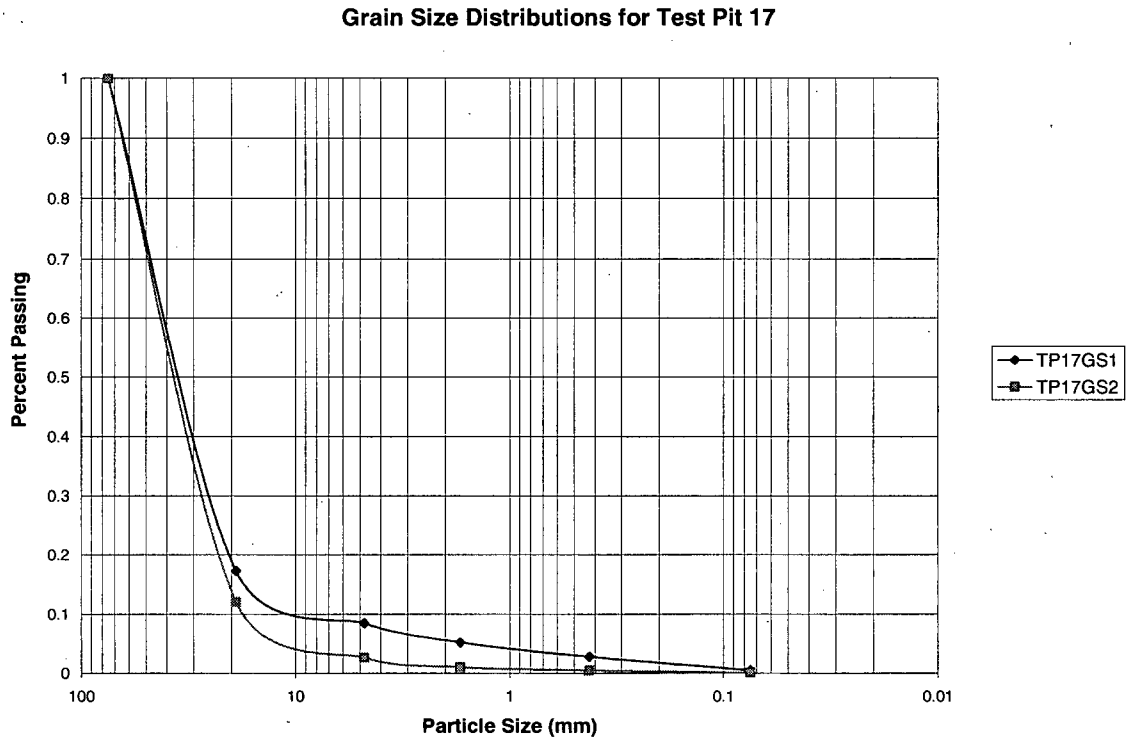

Fig. 17.1: Grain Size Distributions for Materials in Test Pit 17.

TEST PIT 18

Test pit 18 was excavated July 28, 2001 to a depth of 2.0 m below the surface of the sixth bench. Six internal layers were observed in the profile of the test pit. Table 18.1 summarizes the materials and corresponding depth for each layer encountered. All materials were sampled at the midpoint of the bench and the distance listed in table 18.1 is a linear distance from the extreme left of the test pit. Photograph 18.1 shows a typical exposure of the excavated test pit.

Photograph 18.1: Test Pit 18.

Table 18.1: Material Description Summary

Distance (m)	Layer Inclination	Material Description
0.00 2.00 4.00	15-20°	coarse rubble with maximum 2" particle size iron staining present
4.00 5.33 6.67	15-20°	coarse rock with 8" max particle size and 1" traffic surface present
6.67 7.83 9.00	15-20°	fine grained silty sand matrix in coarse gravel to cobble sized particles
9.00 10.67 12.33	15-20°	cobble sized matrix in boulder sized material
12.33 14.00 15.67	15-20°	fine rock and sand with 2" max particle size
15.67 17.33 19.00	15-20°	coarse rock (1' max particle size) with gravel matrix material
19.00 22.33 25.67	15-20°	coarse rock with 2' max particle size and fragmented gravel and sand matrix material
25.67 30.67 35.67	15-20°	1-4" cobble interbedded with 6"-2' boulders

Figure 18.1 shows a profile of water content and paste pH values measured at specific depths through test pit 18.

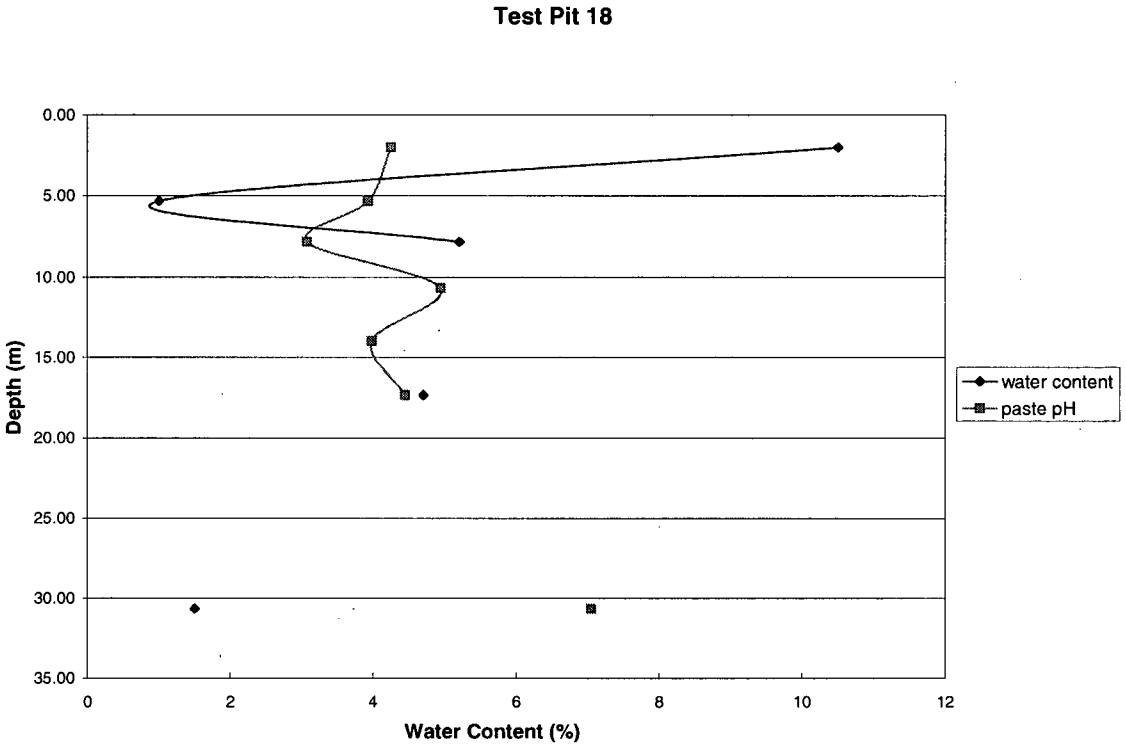

Fig. 18.1: Profile of Water Content and Paste pH within Test Pit 18.

TEST PIT 19

Test pit 19 was excavated July 28, 2001 to a depth of 3.0 m below the surface of the sixth bench. Three internal layers were observed in the profile of the test pit. Table 19.1 summarizes the materials and corresponding depth for each layer encountered. Photograph 19.1 shows a typical exposure of the excavated test pit.

Photograph 19.1: Test Pit 19

Table 19.1: Material Description Summary

Depth (m)	Layer Inclination	Material Description
0.00		boulders (3') with gravel and sandy silt matrix material. Oxidation products present
1.67	30°	
3.33		
3.33		cobbles and boulders (4' max particle size) gravel to clay sized matrix material.
5.50	60°	
7.67		
7.67		cobble to gravel sized matrix material in boulder sized (7' max particle size)
9.17	30°	
10.67		

Figure 19.1 shows a profile of the water content and paste pH values that have been measured at specific depths in test pit 19.

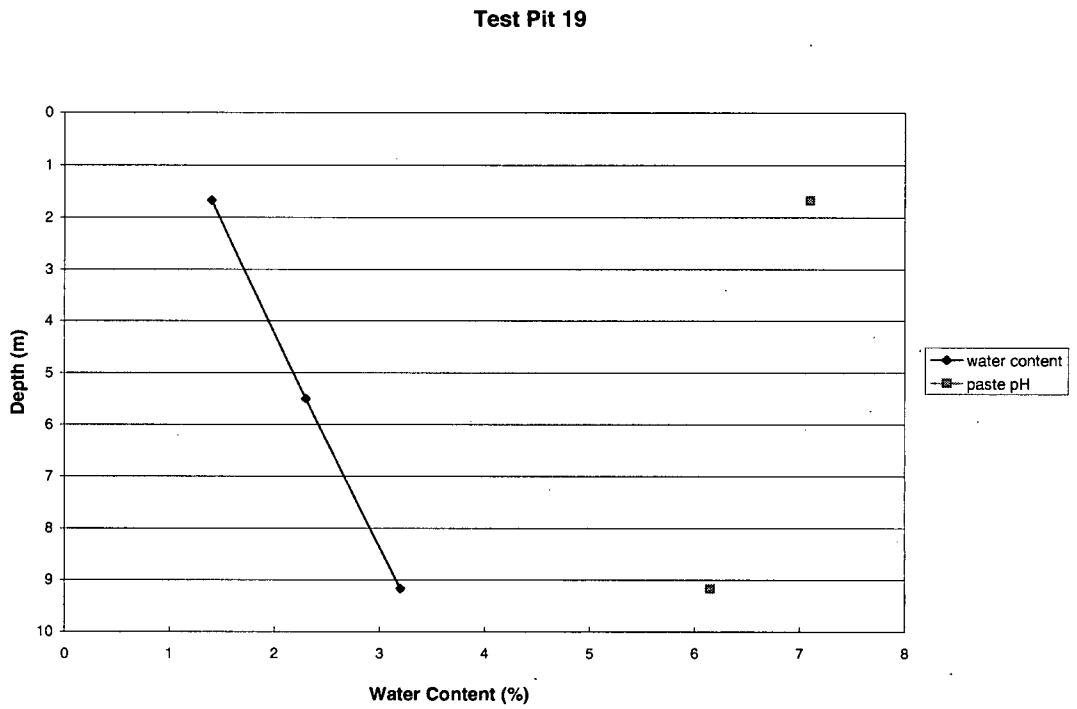

Fig. 19.1: Water Content and Paste pH profiles for Test Pit 19.

TEST PIT 20

Test pit 20 was excavated July 27, 2001 to a depth of 2.5 m below the surface of the sixth bench. Three internal layers were observed in the profile of the test pit. Table 20.1 summarizes the materials and corresponding depth for each layer encountered. Photograph 20.1 shows a typical exposure of the excavated test pit.

Photograph 20.1: Test Pit 20.

Table 20.1: Material Description Summary

Depth (m)	Layer Inclination	Material Description
0.00		coarse angular particles with
3.33	35°	sandy silty gravel matrix.
6.67		Oxidation products evident
6.67		pink granite and andisitic
9.50	35°	waste rock, angular cobble
12.33		and boulder sized particles
12.33		highly oxidized cobbles and
15.67	35°	boulders with a sandy, siltly
19.00		gravel matrix

Figure 20.1 shows a profile with depth of water content and paste pH values for the materials sampled in test pit 20.

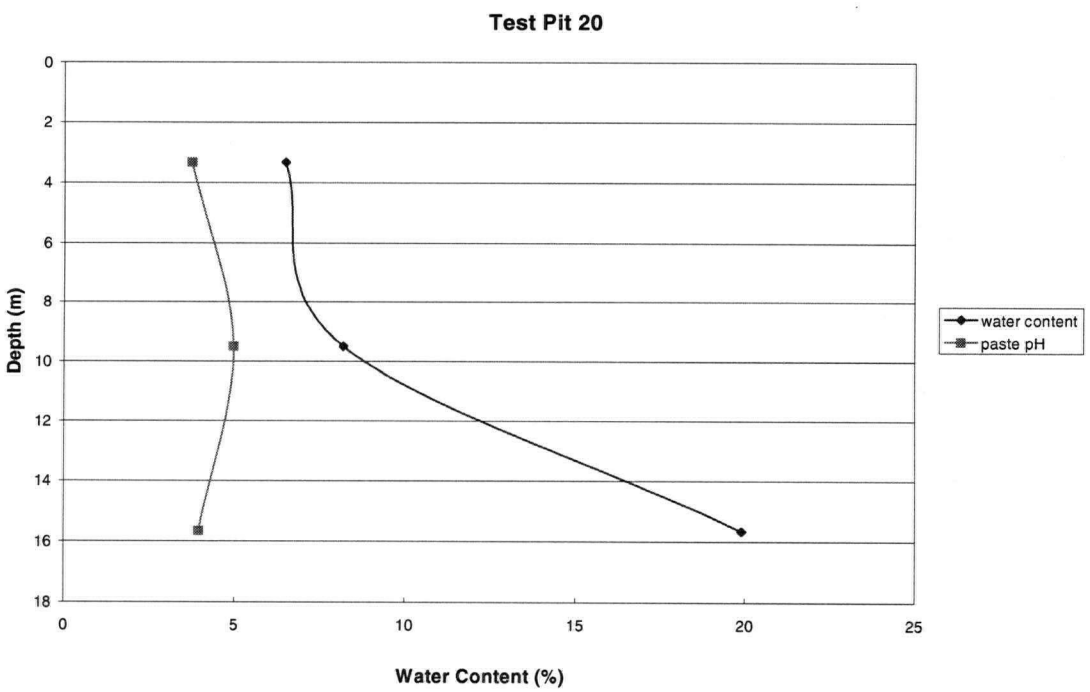

Fig. 20.1: Water Content Profile for Test Pit 20.

TEST PIT 21

Test pit 21 was excavated July 28, 2001 to a depth of 2.5 m below the surface of the sixth bench. Two internal layers were observed in the profile of the test pit. Table 21.1 summarizes the materials and corresponding depth for each layer encountered. Photograph 21.1 shows a typical exposure of the excavated test pit.

Photograph 21.1: Test Pit 21

Table 21.1: Material Description Summary

Depth (m)	Layer Inclination	Material Description
0.00		sandy silty gravel
3.00	35°	interbedded with
6.00		cobbles and boulders
6		sand and gravel with little fines interbedded
9.00	35°	with cobble and
12.00		boulders

TEST PIT 22

Test pit 22 was excavated July 31, 2001 to a depth of 4 m below the surface of the sixth bench. An almost homogeneous blended material was observed in the profile of the test pit. Table 22.1 summarizes the materials and corresponding depth for each layer encountered. Photograph 22.1 shows a typical exposure of the excavated test pit.

Photograph 22.1: Test Pit 22

Table 22.1: Material Description Summary

With the exception of a small zone of low grade ore the test pit was a homogeneous blend of andesitic and granitiod waste rock. There was no discernable inclination of the waste rock within the test pit.

The material is a sandy gravel with cobble and boulder sized material and a maximum particle size of 2 meters.

Figure 22.1 shows the water content and paste pH for the material that was sampled in test pit 22.

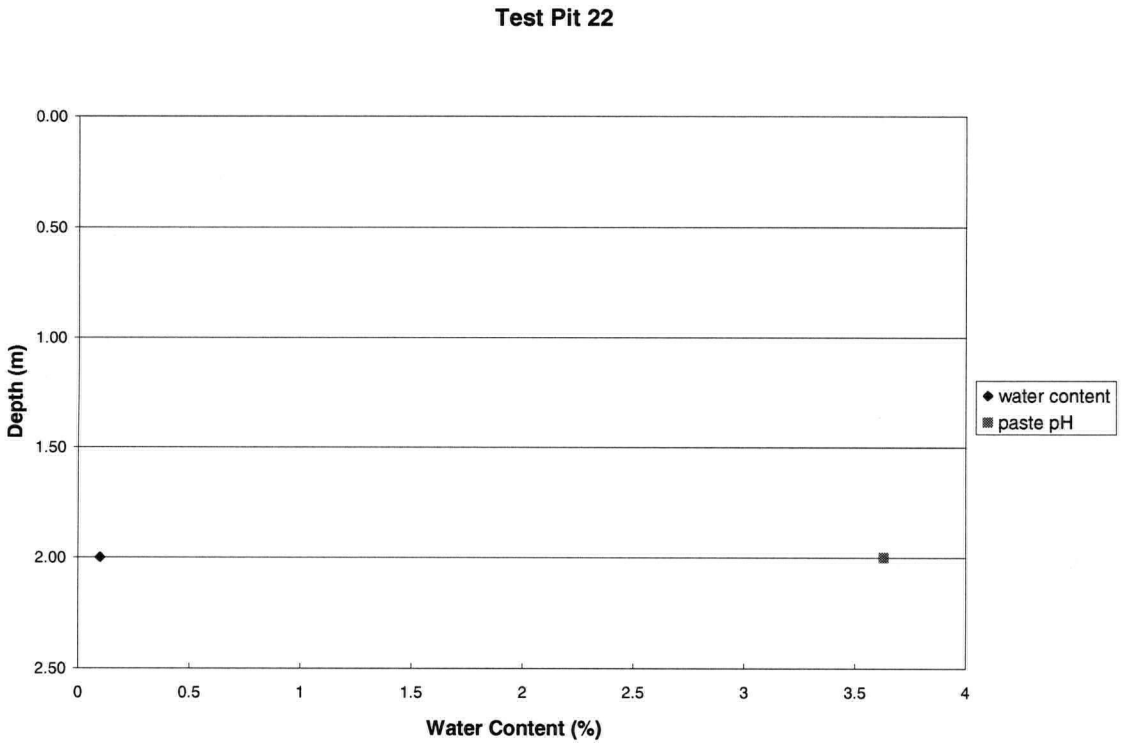

Fig. 22.1: Water Content and Paste pH Profile for Test Pit 22

TEST PIT 23

Test pit 23 was excavated September 11, 2001 to a depth of 1 m below the surface of the seventh bench. Three internal layers were observed in the profile of the test pit. Table 23.1 summarizes the materials and corresponding depth for each layer encountered. Photograph 23.1 shows a typical exposure of the excavated test pit.

Photograph 23.1: Test Pit 23

Table 23.1: Material Description Summary

Depth (m)	Layer Inclination	Material Description
0.00		
0.83	20°	gravel sized particles with some cobbles and little
1.67		fines. Some iron staining
1.67		
2.50	20°	large cobbles and boulders with silt to gravel
3.33		sized matrix material
3.33		gravelly silty sand with cobbles and boulders.
4.17	20°	Evidence of oxidation
5.00		products

TEST PIT 24

Test pit 24 was excavated the week of September 11, 2001 to a depth of 5 m below the surface of the seventh bench. Two internal layers were observed in the profile of the test pit. Table 24.1 summarizes the materials and corresponding depth for each layer encountered. Photograph 24.1 shows a typical exposure of the excavated test pit.

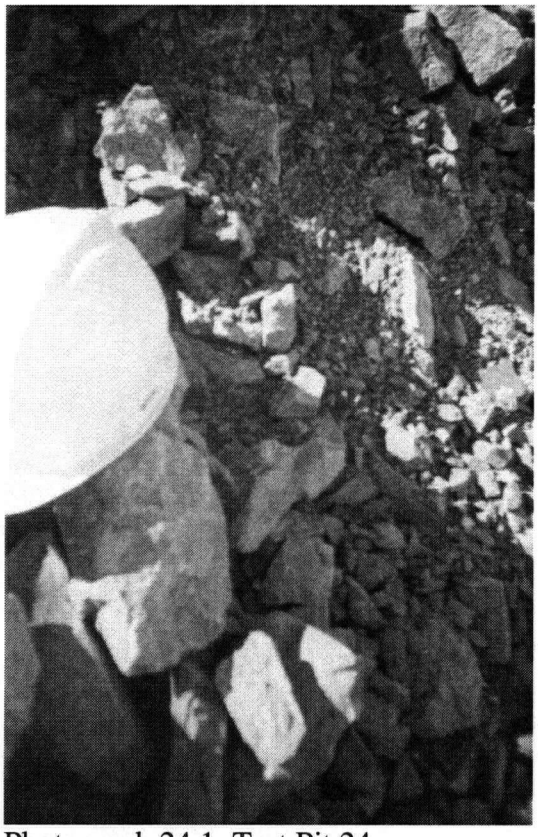

Photograph 24.1: Test Pit 24

Table 24.1: Material Description Summary

Depth (m)	Layer Inclination	Material Description
0.00		cobbles and boulders to fine
1.67	15°	sand and silt. Heavily
3.33		oxidized and damp in-situ
3.33		pink unoxodized granite,
5.00	15°	cobbles to fine shards of
6.67		sand and silt size